6-12-2018

Spatial Trends and Variability of Marsh Accretion Rates in Barataria Basin, Louisiana, USA Using 210Pb and 137Cs Radiochemistry

Samuel Bryant Shrull
Louisiana State University and Agricultural and Mechanical College

SPATIAL TRENDS AND VARIABILITY OF MARSH ACCRETION RATES IN BARATARIA BASIN, LOUISIANA, USA USING ^{210}PB AND ^{137}CS RADIOCHEMISTRY

A Thesis

Submitted to the Graduate Faculty of the
Louisiana State University and
Agricultural and Mechanical College
In partial fulfillment of the
Requirements for the degree of
Master of Science

in

The Department of Geology and Geophysics

by
Samuel Bryant Shrull
B.S., University of Texas at Austin, 2016
August 2018

Acknowledgements

I would like to sincerely thank my advisor Dr. Carol Wilson for her patience, helpfulness, and endless support throughout this whole process. I would also like to thank my committee members, Dr. Sam Bentley for allowing me to use his equipment, lab space, and assistance in framing the project and Dr. Gregg Snedden for acquiring the data used for this project and providing funding through the USGS. The organic matter and bulk density testing was conducted by Tommy Blanchard and the in LSU's Department of Oceanography. Thanks is also due to LSU undergrads Jonathan Camelo and Briana Crenshaw who were integral parts of the sampling and data processing. I want to thank the College of Science for my funding supported by the Board of Regents Fellowship. Lastly, special thanks to my parents and friends who supported me along the way to make it to this point.

Table of Contents

List of Abbreviations

BD = Bulk Density

CFCS = Constant Flux-Constant Sedimentation

CPRA = Coastal Protection and Restoration Authority

CRMS = Coastwide Reference Monitoring System

CRS = Constant Rate of Supply

CWPPRA = Coastal Wetlands Planning, Protection and Restoration Act

FW = freshwater

MAR = mass accumulation rate

MMA = mineral mass accumulation rate

MMPA = mineral mass per area

NAVD 88 = North American Vertical Datum of 1988

OM = Organic Matter

RSLR = relative seal-level rise

RSET = Rod Surface Elevation Table

VAR = vertical accretion rate

Abstract

Coastal Louisiana is presently experiencing large amounts of coastal land loss with estimated rates exceeding 50 km^2 lost per year. In an attempt to mitigate or reverse land loss, billions of dollars are earmarked for restoration projects that promote land reclamation, habitat stabilization, and defending against saline intrusion. This study was performed in an effort to better understand spatial trends of accretion rates in Barataria Basin in coastal Louisiana. Data for this project came from twenty-five shallow cores extracted over a broad span of the entire basin, from freshwater to saline environments. Cores were processed for ^{137}Cs and ^{210}Pb radiochemistry, bulk density, grain size, and organic matter measurements. The average vertical accretion rate (VAR) for the basin is 0.67 ± 0.14 cm/year and the average mass accumulation rate (MAR) is 1.58 ± 0.77 $kg \cdot m^{-2} year^{-1}$. Vertical accretion rates from this study's radiochemistry analysis agree with previous work in the basin (0.5-1.5 cm/year). Vertical accretion rates do not show a clear spatial trend but the mass accumulation rates shows sites south of Lake Salvador have larger values compared to those to the north. This dichotomy of trends suggests that paucity of mineral sediments does not inhibit marsh accretion in the northern area of the basin but that instead it is more reliant on the accumulation of organic material. Elevated mass accumulation rates in this study seem to overlap with the areas that historically have experienced the most land loss. It is hypothesized that material formerly comprising eroded marsh edges may be the source of this material, advected onto the marsh platforms during storm or inundation events. It was found here that hurricane sedimentation consists of 17.2 % of the mineral sediment inventory found across the basin. Fully contextualizing hurricane driven sedimentation requires more spatial data and analysis, however initial results presented here suggest that their presence is likely not the major source sustaining marsh elevations in Barataria Basin.

Introduction

1.1. Study Area/Background

Barataria Basin is a modern-day shallow water interdistributary basin on the south coast of Louisiana within the Mississippi River Delta. Basin boundaries are the modern day Mississippi River to the north and east, an abandoned distributary channel of the Mississippi, Bayou Lafourche, to the west, and barrier islands, like Grand Isle, to the south (see Figure 1). It is a part of the modern Mississippi River Delta plain consisting of the former St. Bernard (3.6-2 ka) and Lafourche (1.5-0.5 ka) deltas and the modern Plaquemine-Balize delta (1.3 ka-present) (Tornqvist, 1996, Blum & Roberts, 2009). The basin currently occupies approximately 6,300 km^2 south/west of the Mississippi River and south of New Orleans. In total, there is over 600 km^2 of swamplands, 680 km^2 of freshwater marsh, 240 km^2 of intermediate marsh, 400 km^2 of brackish marsh, and 530 km^2 of saline marsh within the basin boundaries with the remaining area being open water, unclassified, or inhabited (Penland & Ramsey 1990, CWPPRA 2017).

One of the areas of greatest coastal wetland loss in the US and the world, Barataria Basin land loss is estimated to be near or exceeding 30-70 km^2 lost per year with rates higher than other basins in the area (Walker et al. 1987, Boesch et al. 1994, Day et al 2005, Twilley et al. 2016, CWPPRA 2017). Rates of loss have slowed in recent decades from 80-100 km^2/year (Boesch et al. 1994) but studies estimate that over 2,500 km^2 of wetlands have already disappeared since the mid-20^{th} century with future projections exceeding that (Boesch 1994, Turner 1997, Stone & McBride 1998, Blum & Roberts 2009, Twilley et al. 2016, Couvillion et al. 2017). Estimated net land loss from 1932-2016 for all of coastal Louisiana is 4,833 km^2 which results in a roughly 25% loss since 1932 (Couvillion et al. 2017). The estimate for land loss in Barataria Basin alone

is 1,120 km^2 (Couvillion et al. 2017). With that amount of loss, the coast wide annual rate of loss has fluctuated between 28.01 to 83.5 km^2 per year (Couvillion et al. 2017). Land loss is occurring throughout Barataria Basin but the majority of land loss has been focused in the lake shores, barrier islands, and coastal areas near the Bird's Foot Delta (Couvillion et al. 2017).

Land loss naturally occurs as delta lobes are abandoned because of channel avulsion, as subsidence and sediment compaction begin to exceed the sediment deposition when the river avulses (Roberts 1997). Under this delta cycle, net loss of coastal areas can occur without human modification to the system (Roberts 1997, Bentley et al. 2014). However, delta deterioration and coastal retreat have been accelerated due to human alteration of the natural system (Boesch et al. 1994, Bentley et al. 2014, Condrey et al. 2014, Twilley et al. 2016). One of the largest examples of anthropogenic modification is the extensive levee system emplaced along the banks of the Mississippi River. Levees, dams, and channels have existed on or along the Mississippi River in some form as far back the 18^{th} century (Kesel 2003) and potentially earlier (Condrey et al. 2014). Distributaries of the Mississippi were cut off earlier (Bentley et al. 2016), but under the Flood Control Act of 1928, levees in Louisiana were expanded and raised, effectively eliminating the connection between the Mississippi River and the surrounding wetlands. Over 3000 km of levees have been constructed or otherwise emplaced along the Mississippi throughout the US, which has resulted in reducing approximately 90% of the natural overbank sedimentation (Kesel 2003). In addition to altering the sediment supply of wetlands, dams upstream and levee channelization have also drastically diminished the suspended sediment load the river carries (Kesel 1989, Boesch et al. 1994, Meade & Moody 2010, Bentley et al. 2014, Bentley et al. 2016). In natural unaltered systems, overbank sedimentation and hydrologic connection between a fluvial source and adjacent wetlands is the main sustaining input for wetland preservation (Kesel 1989, Wright

& Nittrouer 1995, Coleman et al. 1998, Kesel 2003, Shen at al. 2015, Twilley et al. 2016). Bayou Lafourche was formerly an outlet of the Mississippi and sediment source to Barataria until construction of the Donaldsonville dam in 1904 (Bentley et al. 2016). With the emplaced levee system, fluvial input to Barataria via overbank sedimentation has been non-existent with the exception of infrequent releases at engineered diversions or siphons (CWPPRA 2017, Day et al. 2018). There are three small scale (~100s to 1000s cubic feet per second) hydrologic restoration and diversion projects into Barataria Basin (Jonathan Davis Pond Freshwater Diversion Structure, Naomi Freshwater Diversion, and West Pointe a la Hache, seen in Figure 2) with another (Restoration in the Des Allemands Swamp) currently under construction (Neupane 2010, CPRA of Louisiana 2017). Two larger scale (~50,000 cubic feet per second) sediment diversions are planned for the basin (Mid-Barataria and Lower-Barataria Sediment Diversions) with a number of other restoration projects either planned or delayed due to funding or resource prioritization (see Figure 2 for locations). The restoration and diversion projects are designed to reintroduce riverine input and attempt to restore hydrologic conditions of wetlands disrupted by levees and navigation channels (CWPPRA 2017).

Erosion of the protective barrier islands is also a major factor contributing to land loss in coastal Louisiana. Due to storm erosion, sea-level rise, and a diminished sediment supply, the deterioration of barrier islands has contributed to erosion in the basin by increasing the volume of tidal influx that the bay receives (Boesch et al. 1994, Penland & Ramsey 1990, Coleman et al. 1998, Stone & McBride 1998). In addition to increased tidal influx, a reduction of land to water ratio has increased wind fetch and strengthened local wave activity (Stone & McBride 1998, Twilley et al. 2016). This not only facilitates sediment erosion, but has increased the salinity of the bays and marshes. Salinity regime change can disturb flora patterns and force relocation of

important freshwater species in the region (Gagliano et al. 1981, Walker et al. 1987, Nyman et al. 1993, Coleman et al. 1998).

Another threat to coastal marshes is high rates of Relative Sea Level Rise (RSLR), ranging range from 1-2 cm/year (Baumann et al. 1984, Penland & Ramsey 1990, Boesch et al. 1994, Blum & Roberts 2009). Some studies suggests that RSLR and associated flooding with adequate suspended sediment can initiate processes that can elevate marsh platforms (Wilson & Allison 2008, Jankowski et al. 2017) or is of no effect (Callaway & DeLaune 1997), but RSLR is generally regarded as a net contributor to land loss (Boesch et al. 1994, Shinkle & Dokka 2004). Subsidence, can account for up to 70% of the total RSLR observed (Dokka 2006). Large amounts of subsidence can be attributed to natural loading and compaction of unconsolidated sediments, fault displacement, tectonic subsidence, and salt migration (Penland & Ramsey 1990, Boesch et al. 1994, Shinkle & Dokka 2004, Dokka 2006, Kim et al. 2009). Hydrocarbon and subsurface fluid production, construction of navigational corridors, draining of wetlands, and agricultural land use are a few additional direct anthropogenic impacts on subsidence (Gagliano et al. 1981, Walker et al. 1987, Boesch et al. 1994, Morton et al. 2002, Jankowski et al. 2017). Many authors argue rapid subsidence coupled with an almost complete lack of supplied sediment to the basin are the main causes of wetland deterioration (Roberts 1997, Morton et al. 2002, Dokka 2006, Gonzalez & Tornqvist 2006, Tornqvist et al. 2006, Kolker et al. 2011).

Parsing mineral sedimentation and organic accumulation and what roles they play in the maintenance of marsh platforms is complex (Craft et al. 1993, Nyman et al. 1993, Reed 1995, Neubauer 2008). It is heavily debated whether mineral sediments or organic accumulation play a larger role in marsh elevation sustainability and is likely a function of location within a given basin and where in the delta cycle that area is undergoing (Roberts 1997, Cahoon et al. 2011).

However, it is relatively agreed upon that salinity, sediment source proximity, hydroperiod, and vegetation type, among others, play a role in determining overall marsh accretion (Nyman et al. 1993, Nyman et al. 2006, Neubauer 2008). Their interactions are not mutually exclusive and feedback mechanisms are present connecting mineral accumulation and organic accumulation. Plant growth can be controlled by marsh flooding (Nyman et al. 2006, Baustian et al. 2012) , a function of elevation, which, in turn, is controlled by the accumulation of both mineral and organic material (Nyman et al. 1993). One example is plants helping to slow water velocities and reduce turbulence which allows for sediment settling (Leonard et al. 1995), while having more mineral sediment present helps to increase autochthonous organic production (Bricker-Urso et al. 1989). A complex web of interactions makes determining inputs and net effects to these processes difficult. Additionally, some physical processes, like hurricanes and winter storm events, can act to both build and deteriorate wetland soils (Nyman et al. 1995, Barras 2005, Baustian & Mendelssohn 2015, Smith et al. 2015). An optimal combination of both adequate mineral and organic contribution seems to be required to maintain marsh platform elevation. Disruption of either source is likely a major reason for increasing amounts of marsh submergence and deterioration seen in coastal Louisiana (Hatton et al. 1983, Kesel et al. 1989, Boesch et al. 1994, Turner et al. 1997, Coleman et al. 1998, Nyman et al. 2006, Neubauer 2008).

Figure 1. A map of Barataria and CRMS sampling sites used in this study, labeled with their CRMS site number. The red line represents the boundaries of Barataria Basin as considered in this study.

Since the construction of the levees, the main inputs of water and sediment are from regular precipitation and storm events, with minor riverine inputs coming from the small-scale river diversion structures (100s of ft^3/s) (Figure 2) (Chmura & Kosters 1994, Shen et al. 2015, Smith et al. 2015, CPRA 2017). As such, additional pathways for intrabasinal sediment distribution, like hurricanes and winter storms, have been investigated in coastal Louisiana. Reports have found some areas receive sediment from hurricanes orders of magnitude larger than background rates and that they are major components in sustaining the marsh vegetation and sediment supply (Nyman et al. 1995, Turner et al. 2006). In addition to potentially bringing in sediment from extra-basinal sources or from bay bottoms, some work suggests that sediments

deposited as a result of hurricanes work as a natural fertilizer that help to stimulate plant growth (Baustian & Mendelssohn 2015). Hurricanes also can act as erosive agents, especially on the barrier islands, and the interactions between hurricanes and coastal marshes are complex and vary greatly dependent on the morphology of the landscape over which a storm passes (Barras 2005). Quantifying their long-term contribution to marsh elevation has shown hurricanes too irregular and too infrequent to be a major constituent of elevation capital in comparison to other sources (Stone et al. 1997, Barras 2005, Smith et al. 2015). Winter storms, while much smaller in magnitude when compared to hurricanes, are much more frequent (Walker & Hammack 1989). Winter storms are similarly complex, having been shown to be a factor in both sediment accumulation and erosion in coastal Louisiana (Reed 1989, Mossa & Roberts 1990, Walker & Hammack 2000).

1.2. Motivation for Study

The competitive balance between natural processes, direct and indirect human landscape alteration, and resource production (e.g. petroleum, fishing industries) has ultimately created the unique challenges that have arisen in delta management today. Long-term imbalance between anthropogenic and natural processes has and will likely continue to have major geomorphological, environmental, and economic impacts for decades to come. In efforts to reach an equilibrium in Louisiana, the 2017 Coastal Master Plan has allotted $5 billion towards sediment diversion projects in Louisiana with two projects in Barataria Basin (Mid-Barataria Sediment Diversion and Lower Barataria Diversion, Figure 2) (CPRA of Louisiana 2017). Estimated costs of construction and future maintenance are upwards of $1B for both of the Barataria projects (CPRA 2017b). The intent of these structures is to re-open a delivery pathway to the wetlands adjacent to the Mississippi River to reintroduce riverine waters and sediment

back into the basin. The two Barataria sediment diversions will join existing, smaller structures (Figure 2) to inhibit land loss and prevent further saline invasion (CPRA of Louisiana 2017). The Mid-Barataria structure is planned to be located on the river's west bank near Mississippi River Mile 61. Its design, engineering, and construction are still ongoing with design completion scheduled for 2021. The Lower-Barataria Diversion is planned further downstream near Empire, LA and is on a similar timeline (CPRA 2017).

Diversions are meant to reintroduce fluvial input into the basin whereas dredging projects utilize sediment accumulations (e.g. sand from Ship Shoal or mud from dredged navigation channels) to redistribute sediments along coastal areas, raise elevation, and promote land growth. Dredging projects, in large part, are meant to complement diversions in the short term while diversions serve as a more long-term solution of sustaining and building land (Boesch et al. 1994, CPRA of Louisiana 2017). Diversion structures are also used as salinity and flood control devices, not just for land reclamation (Bentley et al. 2014). In total, $10+ billion will be spent on coastal projects in Louisiana in the coming decades on a wide range of coastal improvement, restoration, and rejuvenation projects (CPRA 2017b, CPRA of Louisiana 2017). Estimates put the combined economic value of resources extracted from the delta and surrounding waters in the neighborhood of $10B+ per year (Coleman et al.1998, Twilley et al. 2016, CPRA of Louisiana 2017). Since 1990, the Coastal Wetlands Planning Protection and Restoration Act (CWPPRA) have implemented 77 restoration projects of various magnitudes and locations throughout the coast (Steyer 2010). Without question, the Mississippi River and Mississippi River Delta have great economic, agricultural, environmental, and societal importance, which makes the success of ongoing restoration projects vitally important.

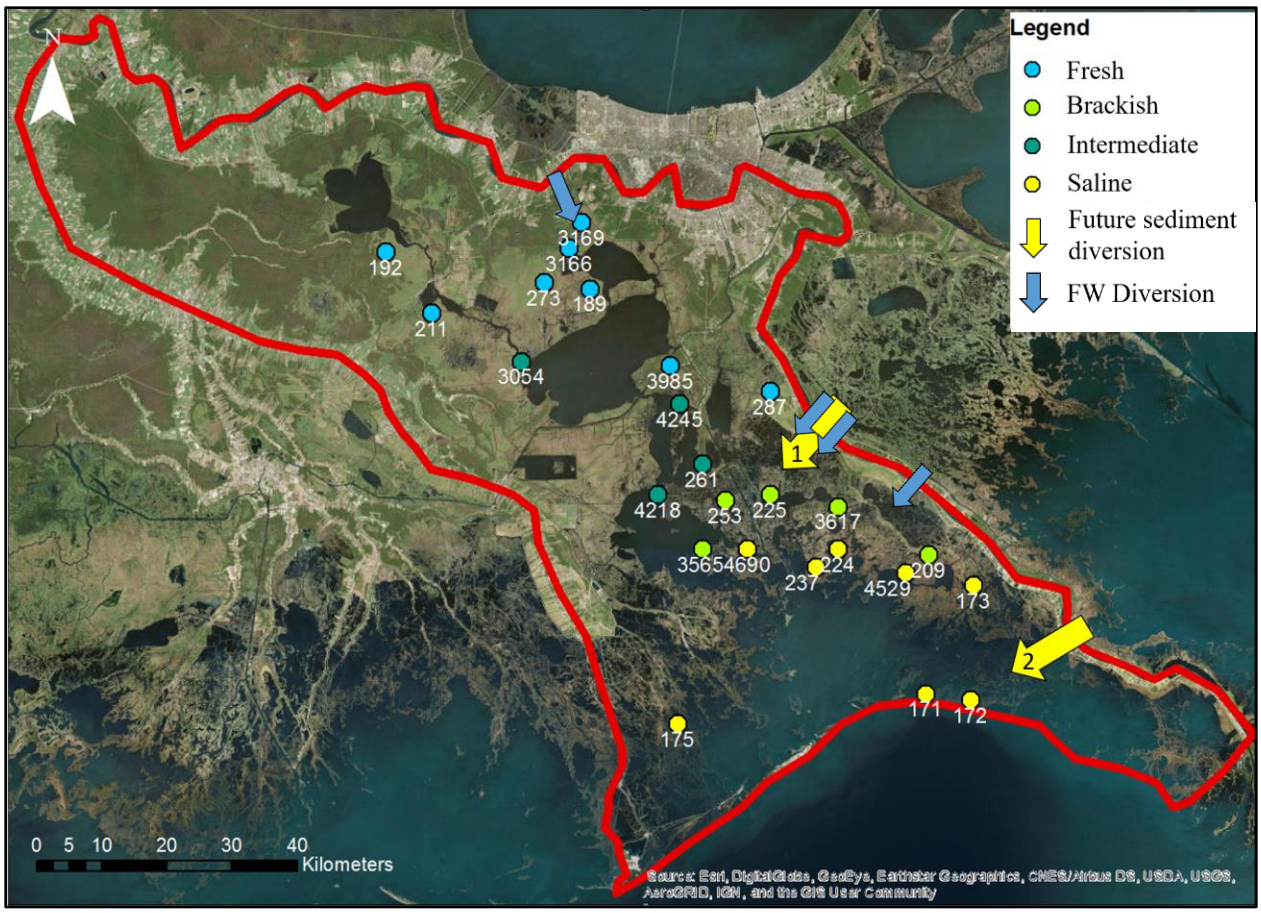

Figure 2. Map of the study area, boundaries of Barataria Basin outlined in red, and CRMS sites listed with their CRMS number and marsh classification. Planned diversions: 1= Mid-Barataria Sediment Diversion, 2= Lower Barataria Sediment Diversion. FW Diversions (upstream to downstream): Davis Pond, Naomi, Myrtle Grove, West Pointe a la Hache)

1.3. Objectives and Hypotheses

The intent of this investigation is to quantify the long-term marsh vertical accretion rates in Barataria Basin to assess background basin-wide trends and spatial variability or trends. This information will aide future restoration efforts in the basin and throughout the delta. Observation and understanding of the controlling factors for marsh accretion rates in this basin is also a major objective. To accomplish this, long-term accretion rates were analyzed using ^{137}Cs and ^{210}Pb radiochemistry, and bulk material compositions to determine mineral versus organic sediment accumulation rates were determined at 25 Coastwide Reference Monitoring System (CRMS)

sites. In an effort to understand components of the sedimentological dynamics, the contributions of hurricane event sedimentation was examined. Comparison of long-term rates produced by this study and available CRMS short-term data will examine how time dependent factors (i.e. period of observation) can change observed trends.

Methods

2.1. Core Acquisition and Sampling

Data for this investigation comes from 25 cores of approximately 40-50 cm depth that were collected in the spring and fall of 2016 at CRMS sites across Barataria Basin (Figure 1). Core samples were analyzed for long-term accretion rates (^{210}Pb and ^{137}Cs), organic matter content, bulk density, and grain size. The diverse sites selected for this study represent a swath across the entire basin from fresh water environments north of Lake Salvador to saline conditions near the Gulf of Mexico. According to CRMS classification, the sites were spread amongst different marsh types (8 being freshwater, 4 intermediate, 5 brackish, and 8 saline according to the mean 2016 growing season salinity, see Figure 2). The CRMS salinity classifications are calculated based on a score generated from vegetative abundance of given species and is derived from Visser et al. (2002). Most of the methods for sampling and analysis were modified from the steps outlined by DeLaune et al. (1978) and Hatton et al. (1983) and are detailed below.

Cores were extracted using an aluminum push core device that is 60.8 cm long. CRMS 287, a freshwater site near the channel of the Mississippi River, experienced 73% compaction during its collection, which resulted in 16.25 cm (8 intervals) of useable core. Therefore, that core and its intervals were excluded in all data analysis. The remaining 24 cores had percentages ranging from 4.5 to 36.1 % compaction. After collection, the cores were frozen in cold storage to prevent internal mixing, mold growth, and to ensure the stratigraphy remained intact. Freezing also facilitates cutting of the cores on a more rigid sample. A band saw was used to cut the cores into discs at the approximately 2 cm spaced intervals. One quarter of the disc was used for bulk density and organic matter testing. Thomas Blanchard at LSU'S Department of Oceanography

conducted organic matter and bulk density measurements, as outlined below. The remaining ¾ was used for ^{137}Cs and ^{210}Pb detection and grain size analyses, outlined below. A 5-10 g aliquot of the ¾ interval was taken out for later use in grain size analysis.

2.2. Organic Matter Testing and Bulk Density Determination

Bulk density measurements take the total mass of the dried sample and divide it by its volume. Organic matter and mineral mass weight percentages were determined using the Loss on Ignition (LoI) method. The LoI method takes dried samples and incinerates them at 550 °C to burn off any organic matter present (Heiri et al. 2001). Dried samples are weighed prior to and after incineration with the observed difference between those two weights being the total organic matter weight. With total organic matter mass known, the percent mineral mass is calculated by subtracting the percent organic matter from 100.

2.3. Cs^{137} and Pb^{210} Detection and Analysis

2.3.1. ^{137}Cs and ^{210}Pb Detection

Studies of the Louisiana coast going back to the 1970s have used radionuclides, often in conjunction with marker beds or ash beds to quantify long-term marsh accretion rates. Widespread use of ^{137}Cs as a dating agent since the 1970s and has successfully been used across the Northern Hemisphere (Richie et al. 1975, DeLaune et al. 1978, Chmura & Kosters 1994, Milan et al. 1995, Walling & He 1997). Most published literature on the accretion rates seen across the Mississippi River Delta plain agrees on a range of roughly 0.5 cm – 1.50 cm of accretion per year over the last ~50 years (Delaune et al. 1978, Chmura & Kosters 1994, Hatton et al. 1983, Lane et al. 2006, Nyman et al. 2006, Wilson & Allison, 2008, Smith et al. 2015). For this study, ^{137}Cs and ^{210}Pb chronologies were used to gain long-term accretion rates. ^{137}Cs is an

anthropogenic by-product produced by nuclear fission with a half-life of 30.17 years (Ritchie & McHenry 1990). Appearance of the isotope came with the first hydrogen bomb testing in 1954 and the peak of observed ^{137}Cs levels that occurred in 1963 is observable in sediments across the globe, especially in the Northern Hemisphere (Cambray et al. 1976).

A number of assumptions have to be made in order to use ^{137}Cs dating. They include: rapid adsorption of ^{137}Cs to particles, immobility of ^{137}Cs once adsorbed, little to no reworking of sediments once deposited, and adjustment for the depth of the biological and physical mixed surface layer (DeLaune et al. 1978, Milan et al. 1994, MacKenzie et al. 2011, Corbett & Walsh 2015). The majority of the study area in Barataria Basin is rapidly accreting, lacks major reworking, and is densely vegetated marsh so the use of ^{137}Cs is reasonable (Appleby & Oldfield 1978, Delaune et al 1978, Chmura & Kosters 1994, Corbett et al. 2015). The isotope adsorbs onto fine grain suspended sediment particles throughout transport and during deposition (Smith & Walton 1980, Wise 1980).

^{210}Pb is naturally occurring isotope that is a part of the ^{222}Rn and ^{238}U decay series with a half-life of 22.3 years. ^{210}Pb has the capability of providing a deeper chronology because of its natural occurrence (Cutshall et al. 1983, Binford 1990, MacKenzie et al. 2011), and ^{210}Pb is used as a corroborative agent against ^{137}Cs in dating marsh soils. Similar to ^{137}Cs, ^{210}Pb preferentially adsorbs to fine grained particles. The same assumptions made for the use of ^{137}Cs dating apply to ^{210}Pb and are limitations to accuracy for both methods (Cutshall et al. 1983, Binfield 1990, Corbett & Walsh 2015). With a half-life of 22.3 years, the measurement accuracy for ^{210}Pb is considered to be 5 half-lives (~100-110 years; Appleby & Oldfield 1977, Appleby 2008, Swarzenski 2014, Corbett & Walsh 2015). Excess ^{210}Pb is gained from atmospheric fallout of ^{222}Rn whereas supported is produced from *in-situ* production from decay of ^{238}U daughter

products from the protolith (Appleby 2008, Swarzenski 2014). Determination of excess versus supported ^{210}Pb is needed to calculate the rate of decay for use of the ^{210}Pb chronometer. Ideal down core profiles show a logarithmic decay of the excess ^{210}Pb with depth until a return to supported ^{210}Pb levels (Appleby 2008, Swarzenski 2014).

Samples for ^{137}Cs and ^{210}Pb detection were dried in an oven at 55° C until completely dry. Dry weight was measured and weight percent water content was calculated. Once the samples were dried and weighed, they were pulverized using a mortar and pestle to homogenize the samples. Samples were then packed in plastic petri dishes, weighed, and sealed with electrical tape around the edge of the lid and dish and allowed to reach secular equilibrium (3 weeks). Low Energy Germanium (LEGe) and Broad Energy Germanium (BEGe) detectors were used to analyze the samples and both are planar geometry and Δ germanium based. LEGe and BEGe detectors from Canberra were used because both styles can accurately assess the keV values needed for ^{137}Cs, ^{210}Pb, and the daughter isotopes of ^{222}Rn and ^{238}U necessary (^{137}Cs photopeak at 661.7 keV, ^{210}Pb photopeak at 46.5 keV, $^{234\text{Th}}$ at 63 keV, ^{212}Pb at 238.6 keV, ^{214} Pb at 295 keV, ^{214}Pb at 352 keV, and ^{214}Bi at 609 keV). Samples were processed in the detectors for 20-24 hours. In addition to the 20-24 hour standard counting time, transmissions counts with an active Pb source were run for 100 seconds in order to improve the accuracy of the ^{210}Pb data following the methods of Cutshall et al. (1983) and Murray et al. (1987). The units of measurement for the radioactivity used in this study are disintegrations per minute (dpm) or 1/60th of a Becquerel (Bq).

2.3.2. Calculating Vertical Accretion Rate and Mass Accumulation Rate using ^{137}Cs and ^{210}Pb radiochemistry

Calculating sediment vertical accretion using ^{137}Cs rates is relatively straightforward and done directly with the dpm activity measured from gamma detection analysis. The interval that contains the peak level of ^{137}Cs activity is dated as 1963 (Richie et al. 1975, DeLaune et al. 1978, Chmura & Kosters 1994, Milan et al. 1995, Walling & He 1997). In order to calculate the vertical accretion rate (VAR, cm/year), the midpoint depth of the peak interval (D_m) is divided by the time difference between deposition and collection, which for this study is 53 years (2016-1963= 53).

$$^{137}Cs\ VAR = \frac{D_m}{53\ years}$$

To calculate ^{137}Cs mass accumulation rate (MAR), cumulative mass per area (M_i) is used. An interval's mass per area is calculated by dividing the dry mass of the interval by its area (81.07 cm^2 used for all intervals). MAR is calculated by dividing the summed mass per area of the peak interval ($g \cdot cm^{-2}$) and all intervals above it by 53 years to calculate a rate in $g \cdot cm^{-2} year^{-1}$ or $kg \cdot m^{-2} year^{-1}$.

$$^{137}Cs\ MAR = \frac{M_i}{53\ years}$$

Several established models utilize ^{210}Pb excess activity to determine sediment vertical accretion rates. The Constant Rate of Supply (CRS) and Constant Flux Constant Sedimentation (CFCS) models are the two models used in this study. The CFCS model equation is shown below:

$$A_z = A_0 e^{-\lambda(z/S)}$$

where A_z is ^{210}Pb excess activity at depth z, A_0 is initial ^{210}Pb excess activity, λ is the decay constant, z is depth, and S is sedimentation rate. CFCS model assumes a constant flux of atmospheric ^{210}Pb fallout and constant sedimentation rate throughout the history of the core. Slopes for CFCS VAR calculation are taken from excess ^{210}Pb vs. depth plots and slopes for CFCS MAR are taken from excess ^{210}Pb vs. cumulative mass per area plots and used to calculate sedimentation rate, S, as seen below:

$$S = \lambda / b$$

where b is the slope of the best-fit line of the ln of ^{210}Pb activity plotted against depth or cumulative mass per area. In contrast, the CRS model calculates varying accumulation rates through time (Appleby & Oldfield 1978). The CRS model assumes a constant atmospheric supply of ^{210}Pb fallout (excess ^{210}Pb) but allows for varying sedimentation rates. Many authors contend that the CRS model is often a better fit for wetland or estuarine environments given that they often experience variable accretion rates through time and atmospheric fluxes of ^{210}Pb are believed to be relatively constant in an area over decadal to century time scales (Appleby & Oldfield 1978, Binfield 1990, Appleby 2008, Corbett & Walsh 2015). However, greater depths are required when coring and calculations are more intensive. ^{210}Pb activity for the CRS model is calculated by normalizing the excess ^{210}Pb concentration values (dpm/g) by multiplying them by their bulk density (g/cm^3) and interval thickness (cm) to obtain inventory of ^{210}Pb excess at a given depth, Ax (dpm/cm^2). All inventories are then summed to obtain ΣAx. The sum of an interval's activity and all activities above it for each depth interval is subtracted from ΣAx, to produce an Az value for that interval. The time (t), in years prior to collection date, is calculated for each interval by equation below where:

$$t = \left(\frac{1}{\lambda}\right) * \ln\left(\frac{\Sigma Ax}{Az}\right)$$

where ΣAx is total sum of Ax and Az for a given depth z. CRS VAR is calculated for each individual interval by dividing its cumulative midpoint depth (cm) by t (years). CRS MAR is calculated by dividing the cumulative mass per area (g/cm^2) of an interval by t (years). Average CRS VAR and MAR was calculated for each core by averaging all individual rates a given core.

2.3.3. Modeled ^{210}Pb Activity Calculations

All but four cores (192, 237, 3054, & 3617) had insufficient coring depths to reach the base of ^{210}Pb excess activity. Without a complete inventory, proper calculation of the CRS could be inaccurate (Appleby 2002, Sanchez-Cabeza & Ruiz-Fernández 2012). CRS calculations were completed for all sites using modeled activity that takes into account a missing inventory component. Using methodology from Sanchez-Cabeza and Ruiz-Fernández (2012), modified from Appleby and Oldfield (1978), cores that did not reach a sufficient depth had a missing inventory component (Aj) estimated for them. Missing inventory (dpm/cm^2) is calculated from the equation below:

$$A(j) = \frac{r \cdot C(j)}{\lambda}$$

A(j) is the missing inventory below interval depth j, r is the CFCS MAR (g/cm^{2}year) for the given core, C(j) is the concentration in the last known interval (dpm/g), and λ is the ^{210}Pb decay constant (0.03114 year^{-1}). Once the missing segment is calculated, it can then be added to the known inventory (δA) as a missing bottom interval to calculate the total estimated inventory A(0), shown below.

$$A(0) = \delta A + A(j)$$

Adding modeled points assumes accuracy from the CFCS rate and cannot account for changes that may occur in ^{210}Pb accumulation or accretion rates over that missing interval (Binford 1990, McKenzie et al. 2011, Sanchez-Cabeza & Ruiz-Fernandez 2012).

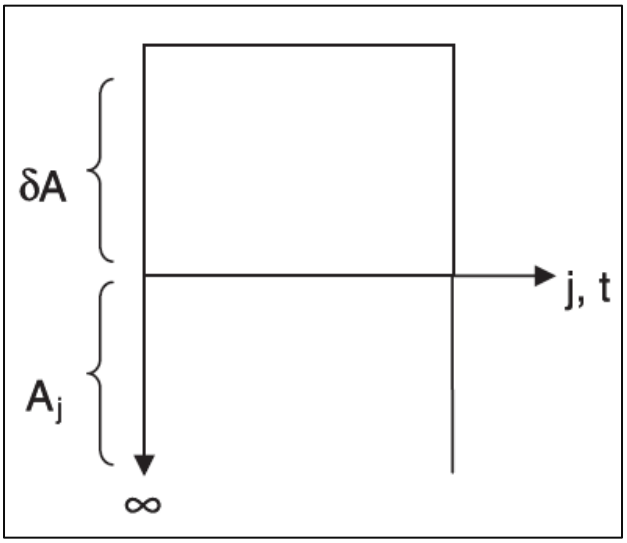

Figure 3. Graphical representation of the missing inventory calculation, from Sanchez-Cabeza & Ruiz-Fernández (2012)

Additionally, this data represents an approximation and does not represent dated intervals (Binford 1990, McKenzie et al. 2011). Given that the CFCS rate is used to calculate A_j, the accuracy of modeled inventory is dependent on the CFCS rate. CRS rates calculated using the modeled activity, as outlined above, will be referred to as *modeled* CRS and CRS rates without the modeled activity will be referred to as *non-modeled*.

2.4. Grain Size Analysis

Due to the highly organic-rich nature of the samples, an organic matter digestion had to be run to remove organic material prior to grain size analysis. Samples were placed in 50 mL plastic sample tubes and 5-7 mL of Sodium Hexametaphosphate $(NaPO_3)_6$ was then added as a

deflocculating agent. The sample was then run on an agitator to thoroughly mix the sample and get the grains into solution. Samples were then washed through an 850 µm mesh sieve because most all sediments in the study area are << 850 µm (Xu et al. 2016). The test tubes were filled to about 90% and then centrifuged for 30 minutes to 1 hour. The supernatant was then removed and 3 ml of $(NaPO_3)_6$ and 5-7ml of Hydrogen Peroxide (H_2O_2) were added and samples were agitated to begin the organic matter digestion process. The samples then were left to react at room temperature for an hour. To expedite the digestion process, samples were heated in an oven at 55° C for 1-2 hours and subsequently to a hot water bath at 70°C for 48 hours. Completion of the digestion process was determined by a cessation of bubbles forming. Acetone was added in cases when necessary to slow the reaction so it did not lose sample or contaminate other samples by overflowing out of the test tube. If any samples had sediment present in the supernatant after the digestion, they were re-run through the centrifuge and digestion process. If the supernatant was clear, it was then removed with a syringe and 3-5 mL of $(NaPO_3)_6$ was added to the test tube. Samples were agitated again and transferred to a plastic 50 mL sample tube, filled up to the 40 mL with $(NaPO_3)_6$, and capped. A Beckman-Coulter Laser Diffraction Particle Size Analyzer (LDPSA) was used to determine grain size distributions on each individual interval. LSU undergraduate Jonathan Camelo ran the majority of the samples and adjusted the operating procedures for the organic matter digestion process specifically for this study.

2.5. Event Sedimentation Analysis

As explained previously, dry mineral mass for each interval was determined by the LoI method. Mineral mass accumulation (MMA) in $kg \cdot m^{-2} year^{-1}$ was calculated for each interval by dividing the cumulative mass per area of the interval by its time since 2016 (t, in years), seen below:

$$MMA = \frac{M_{mi}}{t}$$

where M_{mi} is the cumulative mass per area of the mineral mass at depth i. An average thickness of 1.85 cm is assumed for all intervals, so volume calculations are disregarded. Interval values of mineral mass per area with depth were plotted against the mean and one standard deviation in order to identify intervals of anomalously high amounts of mineral sediment deposition at each site, following methodology from Smith et al. (2015). Given that riverine input has been largely trivial since major levee construction (post-1927), hurricanes and winter storms are the primary sources of such an anomalous event, especially in more inland areas. This method allows for an objective, broad look at quantifying what event sedimentation may look like in the sediment record. A punctuated high-energy event (i.e. hurricane or winter storm) will likely show a discrete signal and should appear as an anomalously high mineral mass relative to the background rates (Smith et al. 2015). Intervals that have a mineral mass per area above the mean plus one standard deviation are labeled as potential event sedimentation. With the age-depth relationships calculated from the ^{137}Cs and ^{210}Pb dating, these events were assigned an age and compared to dates of known storm passages. Error brackets for each core were calculated by dividing the average thickness (1.85 cm) by the respective average accretion rate for the given site, following methods outlined in Smith et al. (2015). NOAA's Historical Hurricane Tracks tool allowed for the identification of all major storms that have passed through Barataria Basin in the concerned time window (1910-2016). The search radius used was 100 km from the averaged latitude and longitude of all of the sites (29.5981 N, -90.0841 W). For the purposes of this study, storms classified as Category 1 hurricanes or greater were included. Hurricanes were identified

as the potential source of mineral deposition if the dates of the storm fell within in the age error bracket associated with each interval.

Results

3.1. ^{137}Cs Results

In total, 25 different cores sites and 539 individual depth intervals were analyzed for ^{137}Cs and ^{210}Pb radiochemistry (see Appendix A for additional site information). A majority of the cores exhibit the typical trend observed with a clear peak defined at depth and return to lower values, exemplified by Figure 4a. Some cores (CRMS 209, 211, 253, 273, 4245, & 4690) had peaks occurring at the bottom interval (see Figure 4b). When the bottom interval contains the ^{137}Cs peak, the rates for those sites represent a minimum accretion rate because the depth of the 1963 horizon cannot be confirmed without a return to lower values (Figure 4b). The third trend observed was a lack of a clear peak (see Figure 4c). This was observed in the samples from the most coastal sites (171, 172 & 175), which showed ^{137}Cs activities below 1 dpm/g with average peak activity being 0.51 ± 0.07 dpm/g compared to an average peak activity of 4.32 ± 1.97 across the remaining sites (Figure 4c). The ^{137}Cs results trend is listed for each site in Tables 1A and 1B along with marsh classification and calculated vertical accretion rates (VAR) and mass accumulation rates (MAR) and all results can be found in Appendix B. Basin wide results averaged a ^{137}Cs VAR of 0.63 ± 0.16 cm/year, with a maximum of ≥ 0.93 ± 0.02 cm/year at intermediate site 4245, and minimum of 0.27 ± 0.02 cm/year at freshwater site 192 (Table 1a). The average ^{137}Cs MAR is 1.47 ± 0.77 kg·m^{-2}year^{-1}, with a maximum of 3.49 kg·m^{-2}year^{-1} at saline site 171, and a minimum of 0.51 kg·m^{-2}year^{-1} at freshwater site 189 (Table 1b).

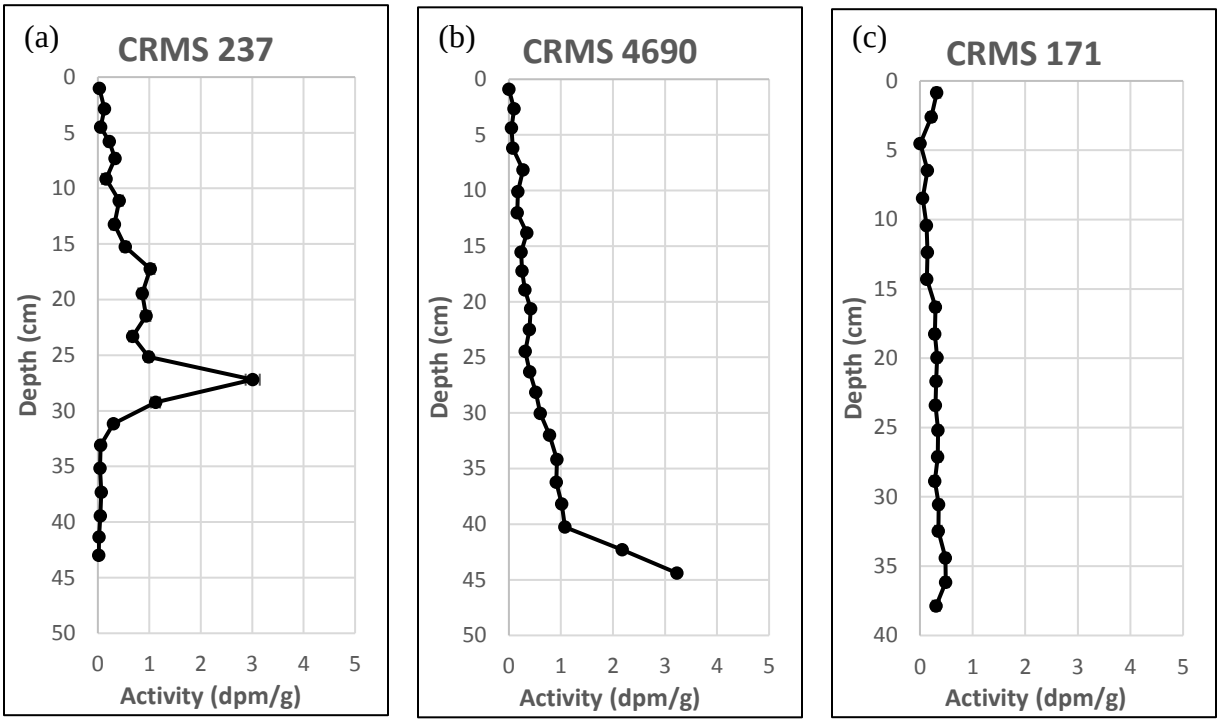

Figure 4. (a) ^{137}Cs profile of CRMS site 237 with clear peak activity, shown with a primary peak of 3.01 +/- 0.14 dpm/g at 27.2 ± 0.95 cm depth resulting in a VAR of 0.51 ± 0.02 cm/year. For all ^{137}Cs profiles, x-error bars are the dpm/g error measurements from the detector and y-error bars are ½ the average interval thickness for the core. (b) ^{137}Cs profile of CRMS site 4690, example of what a profile with a peak ^{137}Cs activity at the base interval with 3.23 ± 0.11 dpm/g at 44.4 ± 0.98 cm depth, resulting in an accretion rate of ≥ 0.84 ± 0.02 cm/year. (c) ^{137}Cs profile of CRMS site 171, an example of a profile with low ^{137}Cs activity. The peak activity is 0.49 ± 0.6 dpm/g at 36.15 ± 0.92 cm depth, resulting in an accretion rate of 36.15 cm/53 years= 0.68 ± 0.02 cm/year

3.2. ^{210}Pb Results

Four of the cores (192, 237, 3054, & 3617) had sufficient depths cored to contain the entire ^{210}Pb inventory (example in Figure 5a). The remainder either showed little to no decay with depth (see Figure 5b) or insufficient decay that did not return to the supported levels (see Figure 5c). The Constant Rate of Supply (CRS) and Constant Flux Constant Sedimentation (CFCS) models were used to calculate VAR for all sites except CRMS 287, which, as mentioned previously, was excluded due to high compaction. CRS results presented are site average values

derived from all intervals at that site to produce one value which could be more easily compared to the ^{137}Cs rates. The results presented in Table 1a indicate that the non-modeled CRS average rates better correlate with the ^{137}Cs data than the CFCS or modeled activity CRS average rates. For example, some CFCS calculations in this study (e.g. sites 175, 225, 253, 4690; Table 1a) gave accretion rates that were an order of magnitude higher than reported rates, or negative due to high activity observed in the base of cores (Figure 5b). Specifically for site 3169, which is in the direct outflow of the Davis Pond diversion, it is likely that opening of the diversion may have invalidated some of the assumptions necessary for the CFCS method. With the opening of the diversion that likely greatly altered the sedimentation rate in that area and may have allowed recent surface to percolate through the soil, both of which would invalidate the method. The CFCS method is the least adaptive and assumes constant flux of atmospheric ^{210}Pb, constant sediment accumulation, and constant specific activity of those sediments. It is the simplest and easiest method to calculate but also the most susceptible to invalidation of assumptions.

CFCS VAR values ranged from -12.46 cm/year to 51.9 cm/year with an average of 3.40 ± 11.40 cm/year (Table 1a). Since the modeled activity CRS rates required using the CFCS rate in the estimations, modeled CRS had similar issues as the CFCS values (relatively unrealistic values obtained). Modeled CRS VAR values were not calculated for sites having a negative CFCS rate but the remaining values ranged from 0.58 cm/year to 18.17 cm/year with an average of 3.47 ± 4.43 cm/year (Table 1a). The MAR values for both are similarly erratic and unreasonable, with CFCS values ranging from -17.40 $kg \cdot cm^{-2} year^{-1}$ to 207.6 $kg \cdot cm^{-2} year^{-1}$ and modeled CRS ranging from 0.91 $kg \cdot cm^{-2} year^{-1}$ to 60.09 $kg \cdot cm^{-2} year^{-1}$ with an average of 9.56 ± 14.66 $kg \cdot cm^{-2} year^{-1}$. Given such variable and unlikely results, CFCS results were not used further other than their initial calculations. While some results from the CFCS produced reasonable

results, the majority did not as indicated by the lack of full inventoried cores (Figure 5, Appendix B). On the positive side, our findings show non-modeled CRS average VAR 0.70 ± 0.20 cm/year, with a maximum of 1.15 ± 0.38 cm/year at freshwater site 3985, and a minimum of 0.42 ± 0.06 cm/year at saline site 4690. These results most closely agreed with the rates produced by the ^{137}Cs data, despite a majoiy missing activity (Table 1a, Appendix B). The assumptions necessary for the CRS method to be valid are less rigid with only atmospheric flux needing to be constant and allowing for variability in accumulation rates and specific activity. As such, variability due to differences in sedimentation or percent organic matter are accounted for and the *non-moldeled* CRS proves to be the best-fit method for use of the ^{210}Pb data.

3.3. Average Vertical Accretion and Mass Accumulation Rates

An overall average VAR and MAR for each site was calculated by averaging ^{137}Cs and non-modeled CRS data (Tables 1a & 1b). CFCS and modeled CRS data were excluded because of their irregularities and wide disagreement with reported values, as discussed above. The average VAR for all 24 sites is 0.67 ± 0.16 cm/year. Average VAR by marsh type was 0.65 ± 0.12 cm/year for fresh, 0.82 ± 0.20 cm/year for intermediate, 0.62 ± 0.12 cm/year for brackish and 0.64 ± 0.10 cm/year for saline (see Figure 6). Two sample equal variance T-tests were run amongst the average VARs for the different marsh types. Results of the t-tests indicate that only the intermediate to saline relationship is proven to be statistically significant (α=0.056) while the remaining comparisons had α-values > 0.1.

Table 1. (a) Total (organic + inorganic) Vertical Accretion Rate (VAR) calculated from ^{137}Cs and ^{210}Pb detection analysis, shown by CRMS site number along with marsh classification (F=freshwater, I=intermediate, B=brackish, and S=saline). ^{137}Cs rates with ≥ have the peak activity in the bottom interval and represent a minimum calculated accretion rate, n/d= not determined, * signifies CRS rates that were calculated using modeled activities to complete the ^{210}Pb inventory. ^{137}Cs results trend identifies the results type from the classification used in Figure 4.

CRMS Site	^{137}Cs results trend	Marsh Type	^{137}Cs VAR (cm/year)	^{210}Pb CFCS VAR (cm/year)	^{210}Pb CRS averaged VAR (cm/year)	^{210}Pb CRS averaged modeled VAR (cm/year)*	**Average VAR (cm/year)**
171	b	S	0.68	4.15	0.63	4.95	**0.66**
172	b	S	0.58	2.36	0.89	2.08	**0.75**
173	a	S	0.50	1.16	0.49	1.44	**0.50**
175	b	S	0.66	51.90	0.79	n/d	**0.73**
189	a	F	0.57	1.02	0.61	1.02	**0.60**
192	a	F	0.27	0.48	0.75	1.03	**0.52**
209	b	B	≥0.83	2.12	0.62	1.47	**0.74**
211	b	F	≥0.56	0.97	0.48	1.20	**0.53**
224	a	S	0.73	1.06	0.50	0.87	**0.62**
225	a	B	0.62	7.60	0.56	8.62	**0.60**
237	a	S	0.51	1.10	0.51	0.89	**0.52**
253	b	B	≥0.75	-7.98	0.78	n/d	**0.77**
261	b	I	0.86	1.06	0.78	1.30	**0.83**
273	b	F	≥0.69	-12.46	0.83	n/d	**0.77**
287	-	F	n/d	n/d	n/d	n/d	**n/d**
3054	a	I	0.49	0.42	0.59	0.79	**0.55**
3166	b	F	0.64	-2.19	0.62	n/d	**0.64**
3169	b	F	0.74	-1.34	0.66	n/d	**0.71**
3565	a	B	0.55	0.29	0.56	1.22	**0.56**
3617	a	B	0.30	0.29	0.63	0.58	**0.46**
3985	a	F	0.48	0.80	1.15	1.27	**0.82**
4218	b	I	≥0.71	4.04	1.09	3.62	**0.90**
4245	b	I	≥0.93	5.56	1.07	6.82	**1.00**
4529	a	S	0.58	6.23	0.88	8.56	**0.73**
4690	b	S	≥0.84	12.98	0.42	18.17	**0.63**

Table 1. (b) Total (organic + inorganic) Mass Accretion Rate (MAR) calculated from ^{137}Cs and ^{210}Pb analysis, at each CRMS site. Marsh type (F=freshwater, I=intermediate, B=brackish, S=saline). ^{210}Pb results trend identifies the result type from the classification used in Figure 5.

CRMS Site	^{210}Pb results trend	Marsh Type	^{137}Cs MAR ($kg \cdot m^{-2}$ $year^{-1}$)	^{210}Pb CFCS MAR ($kg \cdot m^{-2}$ $year^{-1}$)	^{210}Pb CRS averaged MAR ($kg \cdot m^{-2}$ $year^{-1}$)	^{210}Pb CRS average model MAR* ($kg \cdot m^{-2}$ $year^{-1}$)	Average MAR ($kg \cdot m^{-2}$ $year^{-1}$)
171	c	S	3.49	21.33	3.50	27.56	**3.50**
172	c	S	2.01	7.08	2.13	5.67	**2.07**
173	c	S	0.78	1.78	0.71	1.60	**0.74**
175	c	S	2.51	207.6	2.94	n/a	**2.73**
189	c	F	0.51	0.92	0.55	0.91	**0.53**
192	a	F	0.63	2.10	1.52	2.24	**1.07**
209	c	B	≥1.76	4.30	1.52	3.53	**1.64**
211	c	F	≥0.81	1.39	0.69	1.72	**0.75**
224	c	S	2.37	3.17	1.78	3.01	**2.07**
225	c	B	1.30	23.07	1.49	21.42	**1.39**
237	c	S	1.38	2.54	1.51	2.57	**1.44**
253	b	B	≥1.71	-17.40	2.10	n/a	**1.90**
261	a	I	2.04	2.52	1.69	2.85	**1.86**
273	b	F	≥0.69	-12.36	0.87	n/a	**0.78**
287	-	F	n/d	n/d	0.40	n/a	**n/d**
3054	a	I	0.96	1.22	1.23	1.69	**1.09**
3166	b	F	0.74	-2.48	0.85	n/a	**0.80**
3169	b	F	2.07	-5.06	2.64	n/a	**2.35**
3565	b	B	1.06	2.97	1.33	3.16	**1.19**
3617	a	B	0.65	1.70	1.24	1.86	**0.94**
3985	c	F	0.75	1.25	0.83	1.71	**0.79**
4218	c	I	1.07	5.46	1.51	4.84	**1.29**
4245	c	I	≥1.84	11.08	2.19	13.69	**2.02**
4529	b	S	1.81	17.90	2.57	21.53	**2.19**
4690	c	S	2.33	42.08	3.04	60.09	**2.69**

\

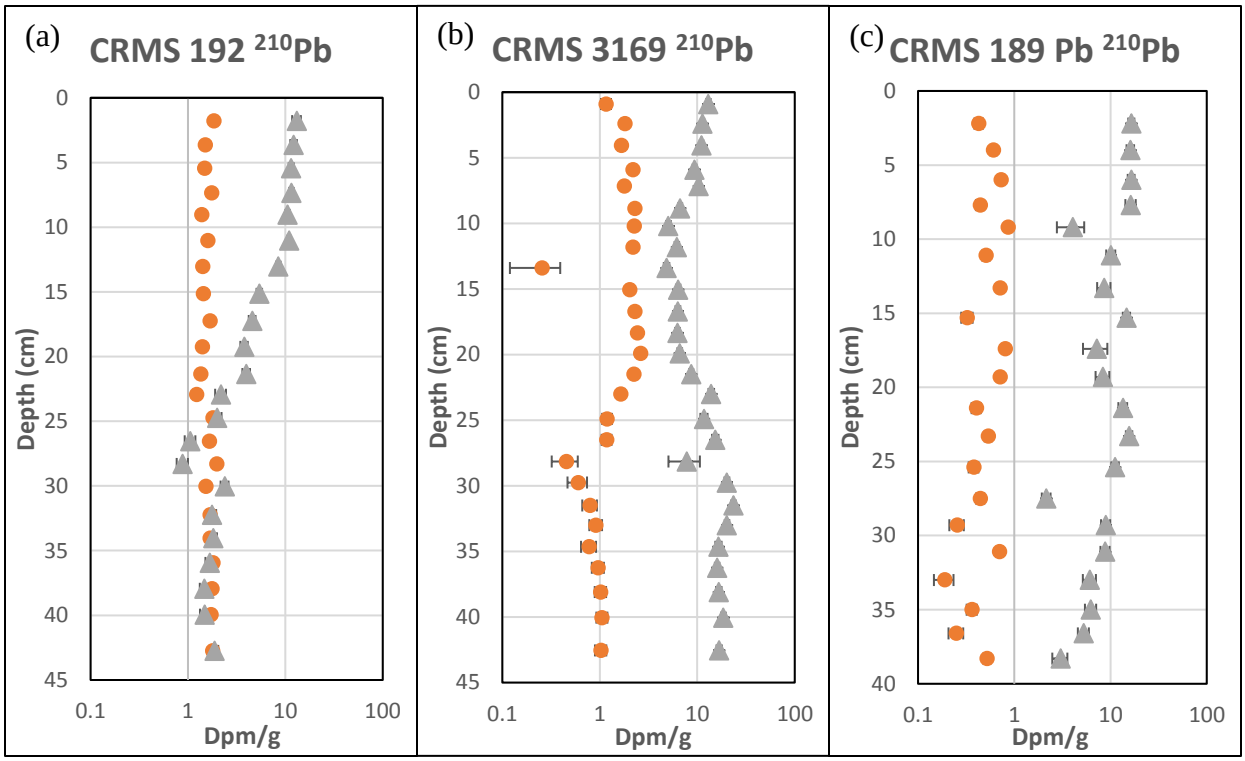

Figure 5. The orange circles represent supported ^{210}Pb and the grey triangles represent excess ^{210}Pb (a) ^{210}Pb profile from CRMS 192 showing an ideal example with a full inventory. (b) ^{210}Pb profile from CRMS 3169 showing an example of shows irregular decay. (c) ^{210}Pb profile from CRMS 189 showing an example that shows down core decay but an insufficient amount to return to supported levels.

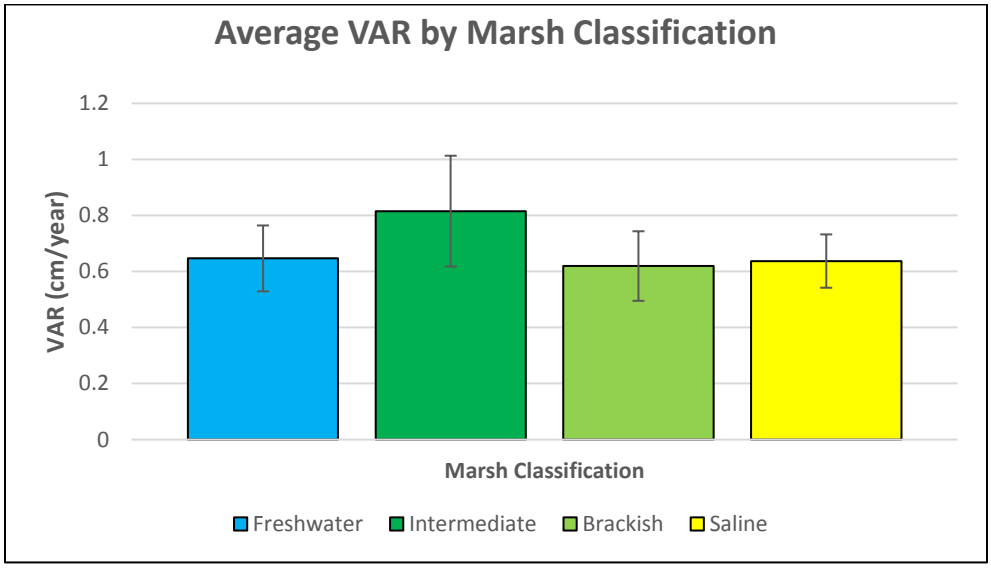

Figure 6. A comparison of the average VAR amongst the different marsh salinity classifications observed within Barataria Basin. Fresh sites n=7, intermediate sites n=4, brackish site n=5, and saline sites n=8.

3.4. Bulk Density and Organic Matter

Table 2 displays the results of bulk density and organic matter percentage for each site classified by their respective marsh type. The average measured bulk density for the entire data set is 0.23 ± 0.15 g/cm^3 and the average percent organic matter is 36.94 ± 21.85 % (all data in Appendix D). On average, fresh marsh sites show a lower bulk density and higher organic matter percentage. A strong trend between greater bulk density and lower organic matter percentage is observed in these data (Figure 7).

Table 2. Average bulk density (BD) and organic matter (OM) percentages listed by CRMS site and salinity classification. ± error shown is 1 standard deviation. Averages for each type shown in bold.

Salinity Classification	CRMS Site	Average BD (g/cm^3)	Average OM
Fresh	192	0.32 ± 0.12	26 ± 9%
	211	0.11 ± 0.02	43 ± 9%
	273	0.07 ± 0.01	79 ± 7%
	189	0.06 ± 0.02	85 ± 19%
	3166	0.09 ± 0.03	67 ± 18%
	3169	0.27 ± 0.19	44 ± 29%
	3985	0.12 ± 0.05	63 ± 16%
	287	0.06 ± 0.02	69 ± 7%
		0.14 ± 0.10	**60 ± 20 %**
Intermediate	3054	0.27 ± 0.16	36 ± 15%
	4245	0.17 ± 0.04	37 ± 5%
	261	0.24 ± 0.06	33 ± 6%
	4218	0.14 ± 0.04	37 ± 6%
		0.20 ± 0.06	**35 ± 2%**
Brackish	209	0.21 ± 0.07	33 ± 9%
	3617	0.47 ± 0.30	23 ± 20%
	225	0.18 ± 0.06	40 ± 10%
	253	0.22 ± 0.05	26 ± 4%
	3565	0.16 ± 0.06	41 ± 11%
		0.25 ± 0.12	**33 ± 8 %**
Saline	4690	0.23 ± 0.07	22 ± 7%
	237	0.25 ± 0.13	29 ± 11%
	224	0.30 ± 0.17	28 ± 12%
	4529	0.25 ± 0.15	27 ± 16%
	173	0.18 ± 0.05	32 ± 7%
	171	0.42 ± 0.10	13 ± 4%
	172	0.34 ± 0.09	16 ± 4%
	175	0.41 ± 0.09	15 ± 4%
		0.30 ± 0.09	**23 ± 7%**

.

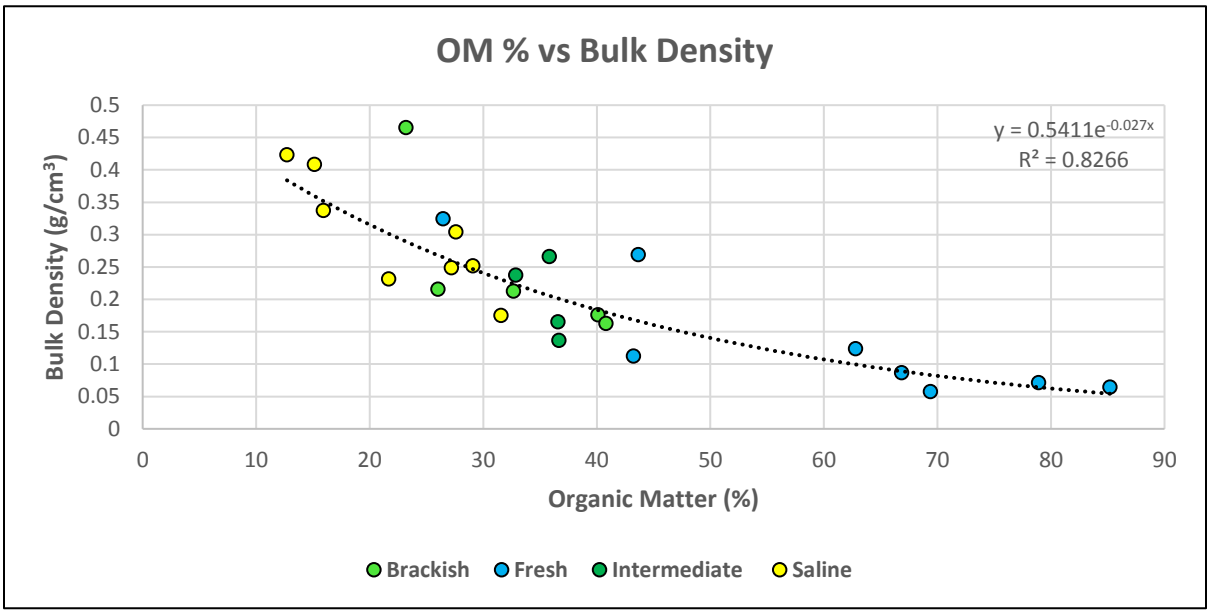

Figure 7. Organic Matter fraction plotted against Bulk Density (g/cm^3). The trend line shows an r^2=0.8266 which is indicative of a relatively strong correlation between the two.

3.5. Grain Size Analysis

Seven cores spread throughout the basin were run for grain size analysis at 2 cm intervals (sites 172, 175, 192, 209, 3054, 3565, and 4218). Below, Table 3 presents marsh classification, averaged mean, averaged median, sorting, skewness, and kurtosis values, compiled by Jonathan Camelo. The average grain size falls within fine silt (6-7 ϕ, 7.8 - 15.6 µm) to medium silt (5-6 ϕ, 15.6 - 31 µm) range. Two of the brackish and saline sites show a coarser mean and median grain size when compared to the intermediate and fresh sites. Positive skew values from all sites show sorting is generally poor, and lean towards more fine grains. Agreement between the mean and median values explains the low degree of skewness observed.

Table 3. Grain size results from Jonathan Camelo by marsh type (F=freshwater, I=intermediate, B=brackish, and S=saline). Errors listed in mean and median are one standard deviation.

CRMS site	Marsh Type	Mean (μm)	Median (μm)	Sorting	Skewness	Kurtosis
192	F	10.05 ± 1.71	10.76 ± 2.16	2.04	0.07	0.81
3054	I	10.61 ± 0.74	12.12 ± 1.22	2.00	0.14	0.81
4218	I	12.76 ± 1.28	10.66 ± 0.74	1.86	0.21	0.89
209	B	17.02 ± 2.29	20.45 ± 3.40	1.81	0.24	0.96
3565	B	7.57 ± 0.62	7.97 ± 0.88	1.80	0.06	0.86
172	S	11.75 ± 1.69	13.44 ± 2.21	2.31	0.31	0.90
175	S	17.18 ± 1.17	22.07 ± 2.03	1.84	0.32	0.97

3.6. Mineral Mass per Area and Mineral Mass Accumulation Rates

The mineral mass per area trends almost exactly mimic the organic matter and bulk density trends. Examples of individual plots are shown in Figure 8. Average mineral mass accumulation (MMA) ranged from 0.09 ± 0.10 $kg \cdot m^{-2}$ $year^{-1}$ at site 189 to 3.26 ± 1.60 $kg \cdot m^{-2}$ $year^{-1}$ at site 273, with an average of 1.25 ± 0.82 $kg \cdot m^{-2}$ $year^{-1}$. Saline sites show the highest MMA rates at 1.72 ± 0.71 $kg \cdot m^{-2} year^{-1}$ while intermediate sites the lowest at 0.86 ± 0.27 $kg \cdot m^{-2} year^{-1}$ (Table 4).

Table 4. Results of the Mineral Mass Accumulation trends for each site in the study area. Shown below are the site number, the average mineral mass per area (MMPA) ± 1 standard deviation, and the average MMA value ± one standard deviation. MMPA values with depth for specific sites found in Figure 8 and Appendix D.

CRMS Site	Marsh Type	Average Mineral Mass per Area	Average MMA ($kg \cdot m^{-2}$ $year^{-1}$)
171	S	6.93 ± 2.32	2.82 ± 0.26
172	S	4.94 ± 1.71	1.95 ± 0.24
173	S	2.10 ± 0.73	0.65 ± 0.10
175	S	6.04 ± 1.66	2.53 ± 0.22
189	F	0.19 ± 0.25	0.09 ± 0.10
192	F	4.87 ± 2.65	0.88 ± 0.29
209	B	2.83 ± 1.35	1.37 ± 0.23
211	F	1.09 ± 0.25	0.10 ± 0.18
224	S	4.71 ± 3.59	1.73 ± 0.28
225	B	2.09 ± 0.92	0.94 ± 0.21
237	S	3.40 ± 1.87	1.20 ± 0.26
253	B	1.65 ± 0.97	1.47 ± 0.16
261	I	2.83 ± 0.82	1.16 ± 0.11
273	F	0.29 ± 0.13	3.26 ± 1.60
287	F	n/a	n/a
3054	I	3.20 ± 2.61	0.59 ± 0.20
3166	F	0.60 ± 0.51	0.38 ± 0.15
3169	F	3.17 ± 3.06	2.06 ± 0.55
3565	B	1.82 ± 1.20	0.84 ± 0.27
3617	B	8.11 ± 5.85	1.10 ± 0.72
3985	F	0.94 ± 0.68	0.35 ± 0.11
4218	I	1.45 ± 0.52	0.67 ± 0.10
4245	I	2.30 ± 0.66	1.01 ± 0.11
4529	S	4.00 ± 3.21	1.55 ± 0.46
4690	S	3.43 ± 1.09	1.29 ± 0.23
Averages			
Fresh	-	**1.59 ± 1.76**	**1.02 ± 1.20**
Intermediate	-	**2.45 ± 0.76**	**0.86 ± 0.27**
Brackish	-	**3.30 ± 2.73**	**1.14 ± 0.27**
Saline	-	**4.44 ± 1.55**	**1.72 ± 0.71**

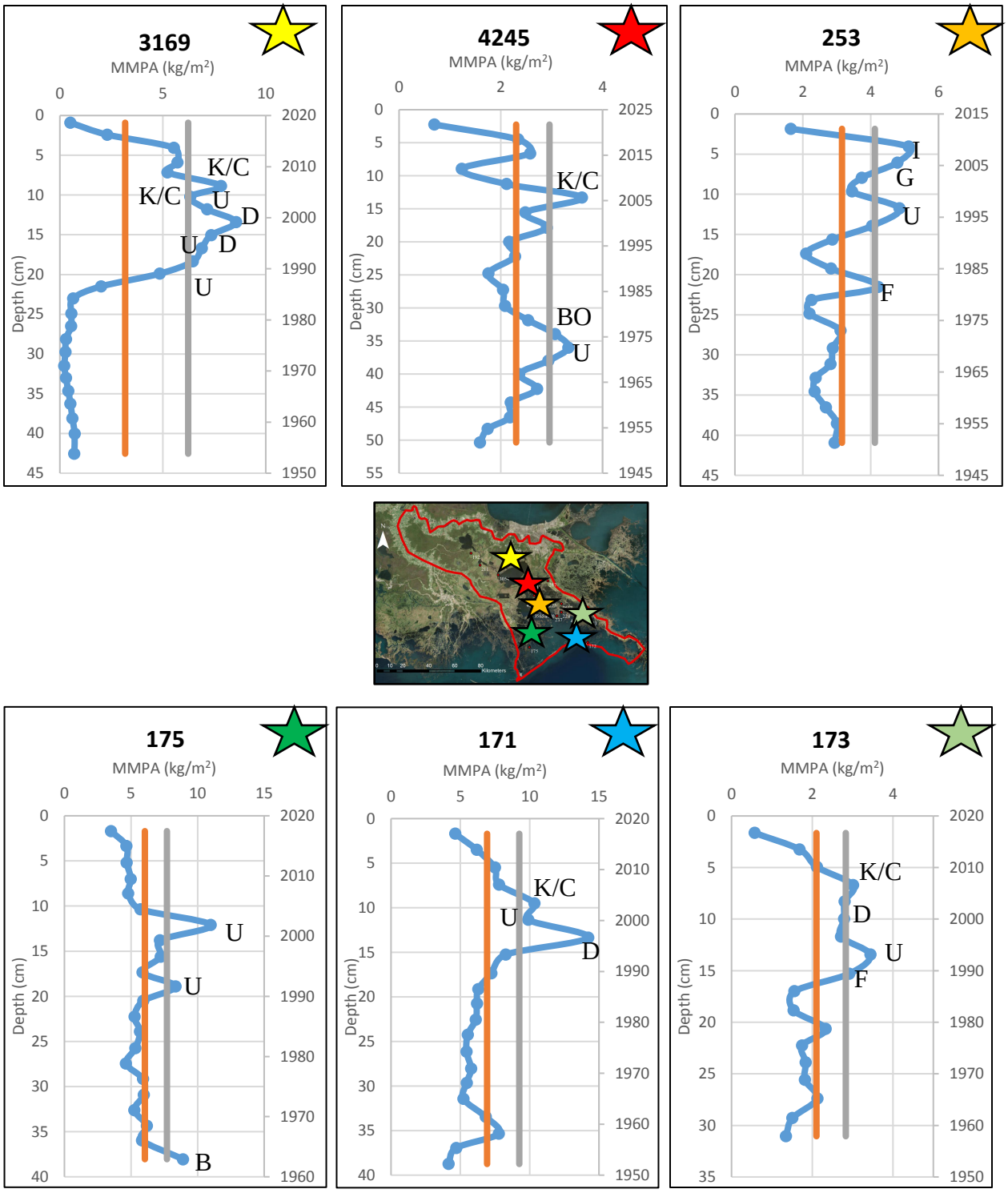

Figure 8. Mineral mass per area (kg/m^2) profiles for CRMS sites labeled with events (I= Isaac (2012) G= Gustav (2008) K/C=Katrina/Cindy (2005) D=Danny (1997) F=Florence (1988) BO= Bob (1979) B= Betsy (1965) U=undesignated event). Secondary axis shows years from the average VAR rates. Inset map with stars shows locations of profiles with stars representing the locations in the upper right corner of the graphs. Of note, K/C in seen in 4 of 6 across the basin.

3.7. Event Sedimentation Analysis

The following hurricanes passed within the study and matched timing with an interval: Isaac 2012, Gustav 2008, Katrina & Cindy 2005, Danny 1997, Florence 1988, Bob 1979, Betsy 1965, Flossy 1956, Hurricane #5 of 1948 (later named Charlie), and Hurricane #4 of 1947 (later named George; map of paths found in Appendix E). Age dates from the average VAR were used when investigating for the presence of storm sedimentation, as shown in Figure 8 (remaining MMPA data in Appendix D). There are instances when hurricanes Isaac and Gustav or Gustav and Katrina overlapped on an interval due to the timing between the storms with the error range of interval dating (±2-4 years). Three such intervals were observed CRMS site 173 at 6.7 cm, 9.15 cm, and 15.3 cm depth (Figure 8). The peak at 6.7 cm corresponds to 2004.85 ± 3.73 years (Katrina/Cindy 2005), 9.15 cm corresponds with 1998.15 ± 3.73 years (Danny 1997), and 15.3 corresponds with 1991.25 ± 3.73 years (Florence 1988). Due to close timing and error range calculations, 5 of the 48 had two potential storms associated with that deposits (2 with Isaac-Gustav overlap and 3 with Gustav-Katrina/Cindy overlap). A total of 48 unique intervals of the 531 (9.0%) intervals analyzed matched with a known hurricane event. Of the 48 mineral sediment events identified, 30 are identified from hurricane events since 1997 (Isaac 2012: 5, Gustav 2008: 6, Katrina 2005:13, Danny 1997:6). The remaining hurricanes that predate 1997 did not have more than five matches each (Table 5). An additional 27 intervals of high mineral mass accumulation were identified as being undesignated events with no time match to hurricane activity (see Figure 8 for examples).

Table 5. Summary of the hurricane sedimentation events using the MMA method (shown in Figure 8). "# of intervals" column represents the number of intervals across all sites that matches with a hurricane passage.

Year	Hurricane Name	# of intervals in Barataria cores
2012	Isaac	5
2008	Gustav	6
2005	Katrina/Cindy	13
1997	Danny	6
1988	Florence	3
1979	Bob	5
1965	Betsy	4
1956	Flossy	3
1948	Hurricane #5 (Charlie)	2
1947	Hurricane #4 (George)	1
-	Undesignated events	27

Discussion

4.1. Long-Term Vertical Accretion Rates in Barataria Basin

Comparison of this study's results to previous work using radiochemistry have found that this study's results fall within the range of vertical accretion rates (0.5-1.5 cm/year) previously published (DeLaune et al. 1978, Hatton et al. 1983, Baumann et al. 1984, Chmura & Kosters 1994, Lane et al. 2006, Feijtel et al. 1988, Nyman et al. 2006, Wilson & Allison, 2008). Given that a majority of prior results have also used radiochemistry, it is expected that the results from this study should compare well. Distinctions have been made by classifying sites according to marsh salinity (fresh, intermediate, brackish, saline) and location (back marsh vs. channel-side vs. coastal). In general, the compiled published data shows that channelside or coastal sites have been found to have higher accretion rates than back marsh sites (DeLaune et al. 1978, Hatton et al. 1983, Baumann et al. 1984, Feijtel et al. 1988, Chmura & Kosters 1994, Lane et al. 2006, Nyman et al. 2006). Individual site geomorphological, hydrological, salinity, and flora patterns all play a role in determining accretion rates for an area (Baumann et al. 1984, Reed 1995, Callaway & DeLaune 1997, Nyman et al. 2006, Wilson & Allison 2008) but just how they all relate together can be difficult to understand beyond a local scale (Nuebauer 2008).

The basin average VAR is 0.67 ± 0.14 cm/year and falls within the range of VARs that have been documented in this region (DeLaune et al. 1978, Hatton et al. 1983, Baumann et al. 1984, Chmura & Kosters 1994, Lane et al. 2006, Feijtel et al. 1988, Nyman et al. 2006, Wilson & Allison, 2008). Spatial analysis of VAR within the basin shows there is not an immediately obvious spatial trend west to east or across the salinity zones north to south (see Figure 9). As mentioned previously, only the intermediate to saline comparison showed a statistically significant difference. However, satellite imagery and GIS software were used to measure

approximate distances to the nearest channel or water body to assess small-scale variability. Sites 3166 and 3169 were excluded from this analysis due to their proximity to the Davis Pond Freshwater Diversion but the remainder were classified as interior, channel-side, or open bay (Table 6). Average values for the classifications are as follows: interior 0.67 ± 0.21 cm/year, channel-side 0.64 ± 0.15 cm/year, and open bay 0.65 ± 0.13 cm/year. Unlike previous studies, not much of a difference was found in the observed VAR between interior (backmarsh) and channel-side or open bay marshes (Figures 10a & 10 b). Studies that have examined the difference between these areas but have generally found that channelside sites have larger long-term and short-term accretion rates due to their proximity to a sediment source (e,g, DeLaune et al. 1978, Hatton et al. 1983, DeLaune et al. 1983, Reed 1992), which is not observed here. Perhaps comparison of these marsh area in closer proximity of one another or along a carefully chosen transect may reveal a more clear trend than observed here.

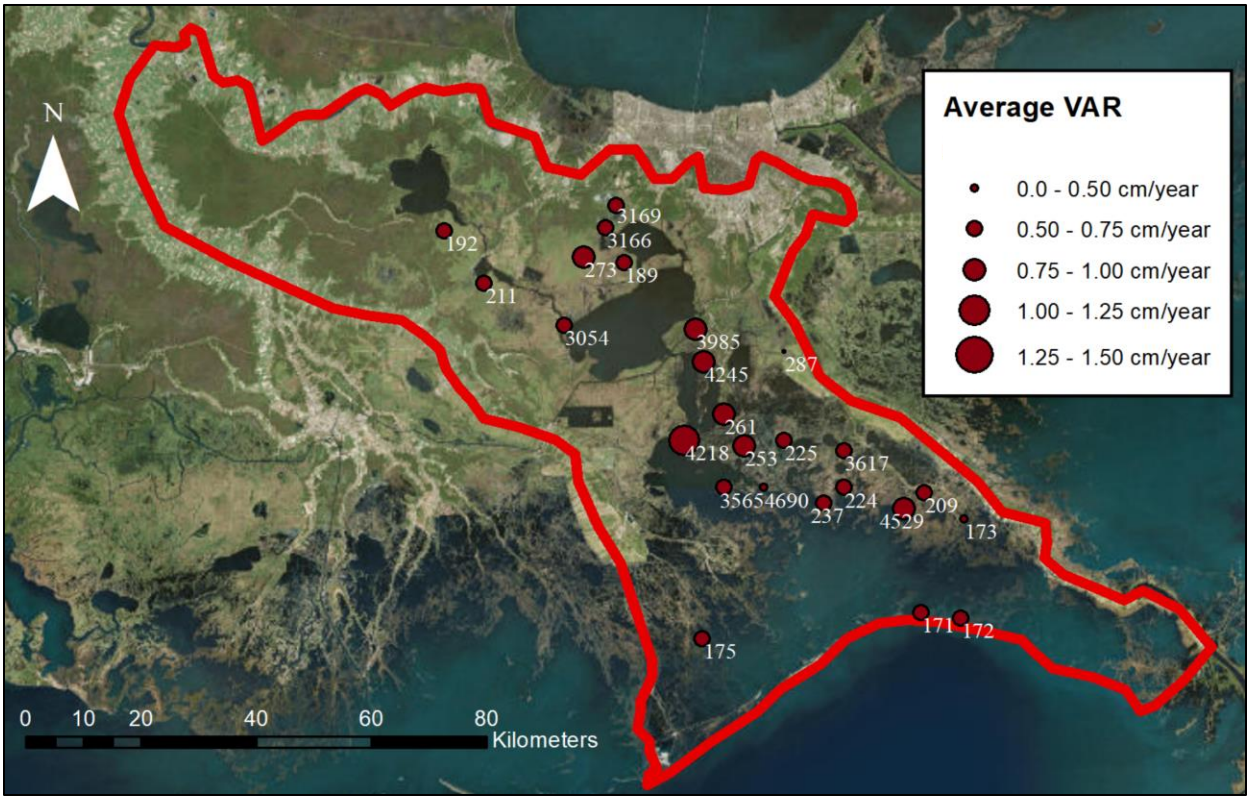

Figure 9. Map of study area and site with the associated average total vertical accretion rate plotted at its location. No first-order spatial trends are discernible from this data.

Table 6. List of all sites classified by their nearest water body and the distance to that water body. Sites are classified as interior if the distance to a water body is > 100 m, channel-side or open bay if distance is < 100 m, ( ) signifies the closest body to the interior sites.

CRMS Site	Closest Waterbody Type	Approximate distance (m)
171	open bay	0
172	channel-side	25
173	open bay	0
175	open bay	0
189	interior (open bay)	1600
192	interior (open bay)	2000
209	channel-side	50
211	interior (open bay)	1000
224	interior (open bay)	200
225	interior (channel)	125
237	channel-side	0
253	channel-side	0
261	interior (open bay)	750
273	interior (open bay)	2500
287	channel-side	480
3054	channel-side	300
3166	Davis Pond FW Diversion	0
3169	Davis Pond FW Diversion	40
3565	interior (open bay)	400
3617	interior (open bay)	220
3985	open bay	0
4218	interior (channel)	560
4245	interior (open bay)	240
4529	open bay	0
4690	channel-side	40

Salinity decreases inland but the long-term VAR trends observed here do not seem to be determined by that change in salinity and associated vegetation. Intermediate marshes have the highest average VAR at 0.82 ± 0.20 cm/year, but the remaining three areas (fresh, brackish, saline) are within several mm of each other (Figure 6). Despite saline sites on average having roughly double the bulk density and one-half of the organic matter (Table 2), it is interesting to

note almost no difference in the long-term VAR between saline and fresh marshes (Table 1a & 1b; Figure 6). No apparent trend in VAR appears either on a north-south or east-west trend (Figure 9), which suggests there is no apparent connection between VAR and proximity to the Mississippi River. Given that major levees have been in place since 1928, this seems reasonable that no connection would be evident. Site 3169, in the direct outflow of the Davis Pond diversion, is the only site that has the potential to have benefitted from a diversion which suggests that the existing diversions only affect a localized area around the structure. Even then, site 3169 has an elevated MAR and bulk density in the top of the core but no evidence yet to suggest that it has a greater than expected VAR (Table 1a & 1b).

Elevation was determined not to be an important factor in constraining average VAR. Figure 10c and 10d, below, show the 17 sites with elevation data plotted against their average MAR and VAR, respectively. The range of observed elevations in this study was very small: from 0.04 m to 0.24 m above NAVD 88. This limited amount of elevation change likely does not provide a large enough range of to produce statically significant differences based on that factor alone, as have been found in other marsh studies done elsewhere (e.g. Boesch et al. 1994, Cahoon & Reed 1995). Cores come from a broad swath across the entire basin and were not collected with the intent of collection along a specific location's elevation profile. The intrabasinal dynamics (i.e. proximity to a water body, fresh vs. saline) vary greatly so without comparison of elevation within similar environmental conditions in a given area (i.e. backmarsh vs. channelside vs. coastal), any assessment of elevation is not likely to produce a significant trend. Furthermore, given that the range is only 20 cm, it is also likely that such a small amount of elevation change would not act as barrier to hydrologic or sedimentological process to produce different VAR.

Figure 10. (a) Site distance from the nearest waterbody plotted against average MAR values at each site. (b) Site distance from the nearest waterbody plotted against average VAR values at each site. (c) Site elevation against the average MAR (cm/year) for the sites with elevation data in m above sea level (NAVD88). (d) Site elevation against the average VAR for the 17 sites with CRMS data.

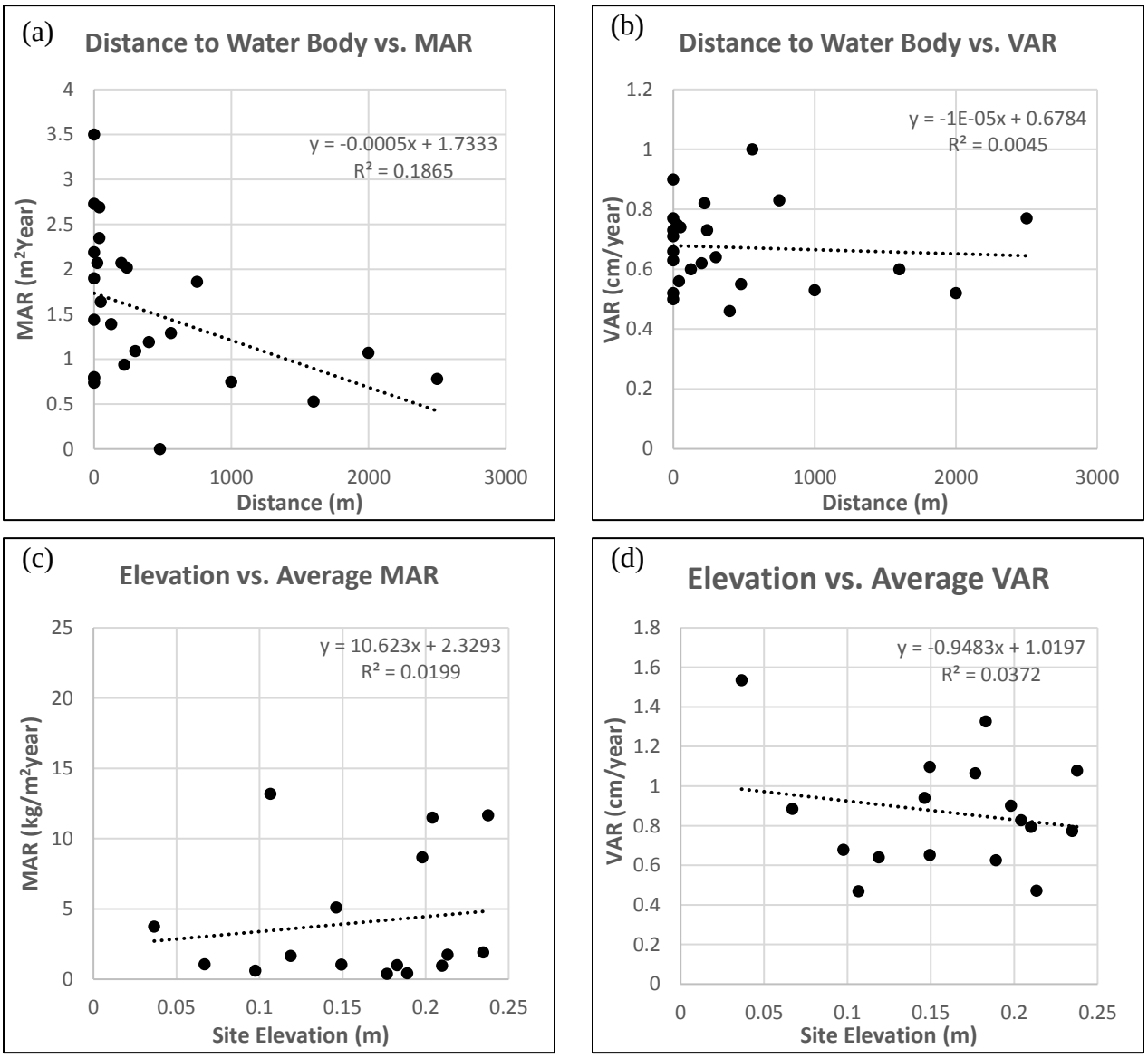

This study confirms the complexity of mineral versus organic matter contribution to VAR. Relative amounts of organic matter versus mineral sediments does not fully determine the VAR observed in Barataria Basin. While freshwater marshes are more organic rich compared to

salt marshes, the VAR were similar (Table 1a, Figures 6 & 9). Individual site dynamics such as proximity to the nearest waterbody, elevation, storm history in addition to salinity and vegetation likely determine rates. The observed VAR patterns in this study do not follow any clear trend related to waterbody distance, elevation, storm history, or salinity individually (Tables 1a & 6, Figures 6 & 9). Due to the highly variable landscapes and site-specific conditions found throughout coastal Louisiana, most previous work suggests that salinity or any other single environmental factor cannot determine accretion rates reliably (Jarvis 2010). A large volume of the marsh vertical accretion rates measured in Louisiana since 1978 is presented in Jarvis (2010) and compares results by wetland type, method used, period of observation, and location such as backmarsh or channelside. On a basin-wide scale, the range and average rate from this study (0.46 – 1.00 cm/year, 0.67 ± 0.14 cm/year) compares well with the range of values compared in Jarvis (2010) (~0.50 to 1.5 cm/year; Table 1a, Figures 6 & 9).

Variation is inherent due to different measurement types, environmental factors (i.e. local shallow subsidence, water body proximity, human activity), and landscape changes all greatly affecting marsh vertical accretion (Jarvis 2010). As such, local sampling and analysis are needed to effectively approximate trends for a site specific area because basin-wide averages do not account for the local complexity. This data provides a good baseline on accretion trends in the basin for the purposes of coastal management and diversion planning, however, local effects are difficult to constrain given the variability inherent to the system.

4.2. Long-Term Mass Accumulation Rates in Barataria Basin

Figure 11a shows MAR plotted spatially in Barataria Basin. The spatial analysis reveals that, in general, sites south of Lake Salvador have larger mass accumulation rates than the sites to the north. Average MAR of the southern sites is 1.88 ± 0.73 $kg \cdot m^{-2} year^{-1}$ whereas the northern

sites averaged 0.95 ± 0.46 $kg \cdot m^{-2} year^{-1}$. Table 7 shows elevated MAR appear to be coincident with lower percentages of organic matter and closer proximity to water bodies allowing more mineral deposition. Organic matter makes up, on average, 28 ± 9% of the mass of the sites south of Lake Salvador compared to 55 ± 21% in the northern sites. Given that organic matter has a lower bulk density than mineral sediments, MAR at sites with low organic content is greater (Hatton et al. 1983, DeLaune et al. 2003, Nyman et al. 2006; Tables 1b, 2, 4). Decoupling between the MAR and VAR trends also suggests that in the fresh water and more inland areas, the accumulation of organic matter and below ground biomass plays a larger role in maintaining elevation capital (Figures 9, 11a, 11b, & Table 7; Cahoon et al. 2011). While not completed in this study, measurements of belowground biomass and compaction of organic matter could be the focus of future work.

MAR findings in this study compare well to previous observation. Hatton et al. (1983) calculated accumulation rates in Barataria Basin and found similar trends as presented in this study. They also found that saline marshes have a higher mass accumulation rates (~2.17 to 3.37 $kg \cdot m^{-2} year^{-1}$) than fresh sites (~0.58 to 1.17 $kg \cdot m^{-2} year^{-1}$) compared to 0.74 to 3.5 $kg \cdot m^{-2} year^{-1}$ for saline and 0.39 to 1.73 $kg \cdot m^{-2} year^{-1}$ for fresh in this study. DeLaune et al. (2003) examined mass accumulation rates at sites near the Caernarvon diversion in Breton Sound and found rates averaging 1.53 ± 1.21 $kg \cdot m^{-2} year^{-1}$ in the upper portion near the diversion and 0.54 ± 0.13 $kg \cdot m^{-2} year^{-1}$ in the lower basin, which has a similar range as the values in this study. Such a trend may serve as confirmation for the anomalous MAR value seen at CRMS site 3169 near the Davis Pond diversion. Planned diversions for Barataria Basin are one to two orders of magnitude larger then existing diversions in the basin so an increase in MAR will likely occur once the Mid and Lower Barataria diversions are constructed. Comparison of the location of the planned diversions

(Figure 2), the MMA and MAR trends from this and other studies suggests they could provide much needed sedimentation to those vulnerable areas. MAR similar to those of this study were found in Nyman et al. (2006), with fresh sites (0.88 $kg \cdot m^{-2} year^{-1}$) having lower values than saline sites (2.38 to 2.59 $kg \cdot m^{-2} year^{-1}$). Previous results and this study's results find that unlike VAR, increased MAR and MMA coincided with a trend of increasing salinity (Table 4 & 7; Figures 11a & 11b).

MMA spatial patterns are shown in Figure 11b. This map shows a similar trend as MAR, although less clear, with the majority of the higher values found south of Lake Salvador. This may be in part due to elevated levels of mineral material accumulating at site 3169 due to the Davis Pond diversion. As seen in the organic matter and bulk density trends, the general trend of increasing MMA is observed when comparing fresh water marshes to saline, intermediate to brackish, intermediate to saline, and brackish to saline (all α values < 0.025). Lake Salvador lies almost exactly on the intermediate to fresh marsh transition (Figure 2). In addition to the salinity transition, Lake Salvador is located in the middle of the basin, which could be creating a hydrologic barrier that keeps mineral material from being distributed as easily in the more northern areas.

Comparison between the MAR and MMA spatial trends with the Couvillion et al. (2017) land loss map highlights that the areas having undergone significant land loss overlap with areas with the greatest MMA (Figure 12a). The more northern, inland areas showing little to no land change in the last ~80 years have much lower MMA values, with exception of site 3169 near the Davis Pond diversion. Additionally, as seen in Figure 12b, the highest MMA values coincided with the sites closest to waterbodies show a large range of MMA values but do have the highest of the sites studied. Shoreline and marsh edge erosion could be a contributing factor to the

elevated levels of mass accumulation in those sites. As outlined in Wilson and Allison (2008), marsh edge erosion can increase the sediment delivered to local the bays and waterbodies. This sediment can be re-suspended and deposited during storm events on the marsh platform during periods of inundation; thus, former marsh edge sediment could be the sustaining material for the elevation of remaining marsh platforms "cannibalization of the marsh edge" sensu (Wilson & Allison 2008, Mariotti & Fagherazzi 2010). Given that there are currently few, if any, outside sources for mineral material to be added to the basin, this may explain the observed differences in MAR and MMA between the areas to the north and south of Lake Salvador.

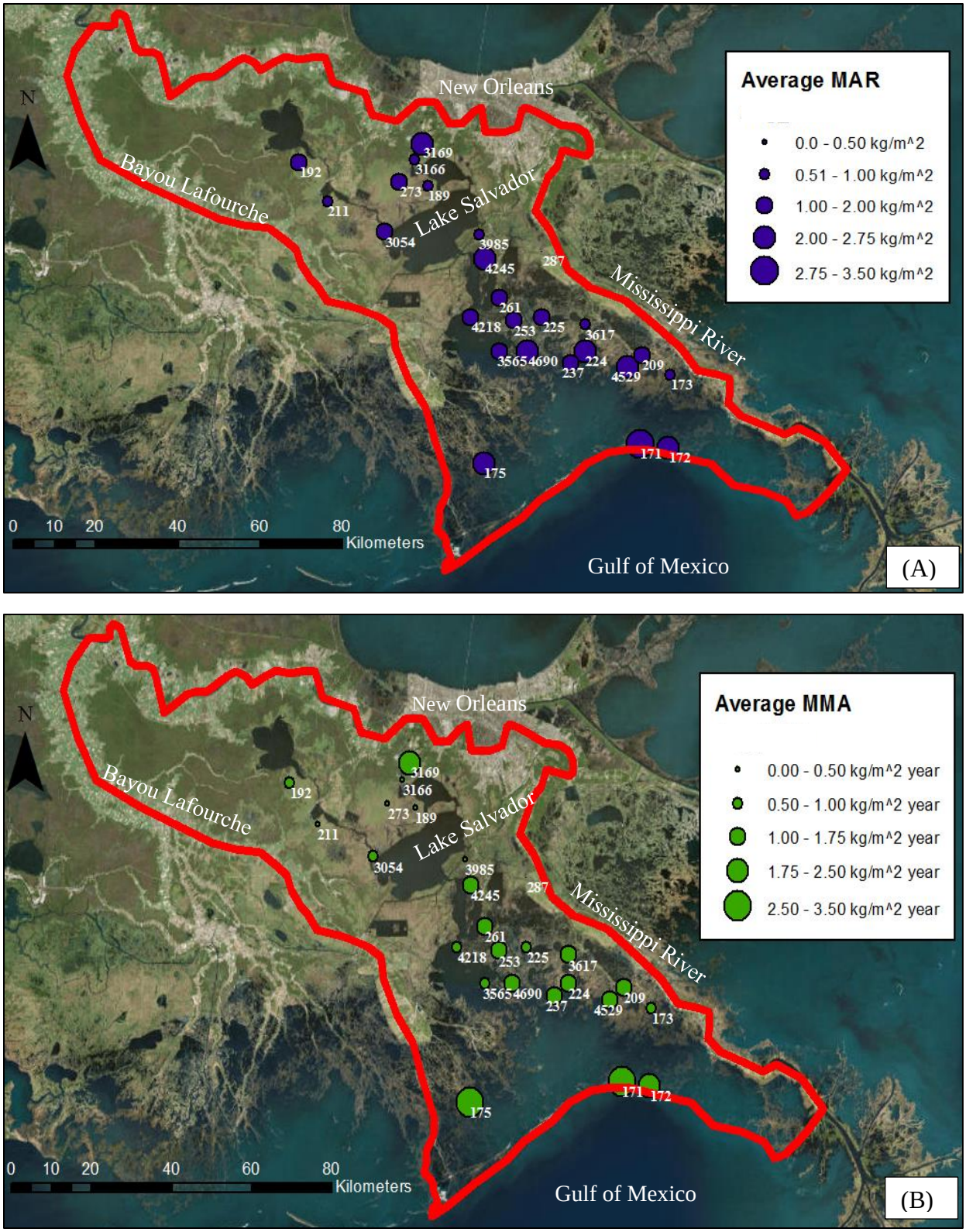

Figure 11. (a) Map of mass accumulation rate (MAR) plotted by site location. (b) Map of mineral mass accumulation (MMA) rates plotted by site location.

Table 7. Comparison of mass accumulation rates (MAR=total inorganic and organic), organic matter %, and distance to nearest waterbody of sites north and south of Lake Salvador, which is near the fresh-intermediate marsh transition.

Sites North of LS	MAR ($kg \cdot m^{-2} year^{-1}$)	MMA ($kg \cdot m^{-2} year^{-1}$)	OM %	Nearest water body (m)	Sites South of LS	MAR ($kg \cdot m^{-2} year^{-1}$)	MMA ($kg \cdot m^{-2} year^{-1}$)	OM %	Nearest water body (m)
189	0.60	0.09	85	1600	171	3.50	2.82	13	0
192	1.28	0.88	26	2000	172	2.07	1.95	16	25
211	1.00	0.1	43	1000	173	0.74	0.65	32	0
273	0.39	0.15	79	2500	175	2.73	2.53	15	0
3054	1.00	0.59	36	300	209	1.64	1.37	33	50
3166	0.41	0.38	67	0	224	2.07	1.73	28	200
3169	1.17	2.06	44	40	225	1.39	0.94	40	125
4245	0.60	0.09	37	240	237	1.44	1.2	29	0
					253	1.90	1.2	26	0
					261	1.86	1.47	33	0
					3565	1.19	1.16	41	750
					3617	0.94	0.84	23	400
					3985	1.73	1.1	63	0
					4218	1.29	0.35	37	220
					4245	2.02	0.67	37	560
					4529	2.19	1.01	27	0
					4690	2.69	1.55	22	40
	0.81 ± 0.35	**0.54 ± 0.68**	**52 ± 22**	**960 ± 970**		**1.85 ± 0.69**	**1.33 ± 0.65**	**30 ± 12**	**139 ± 226**

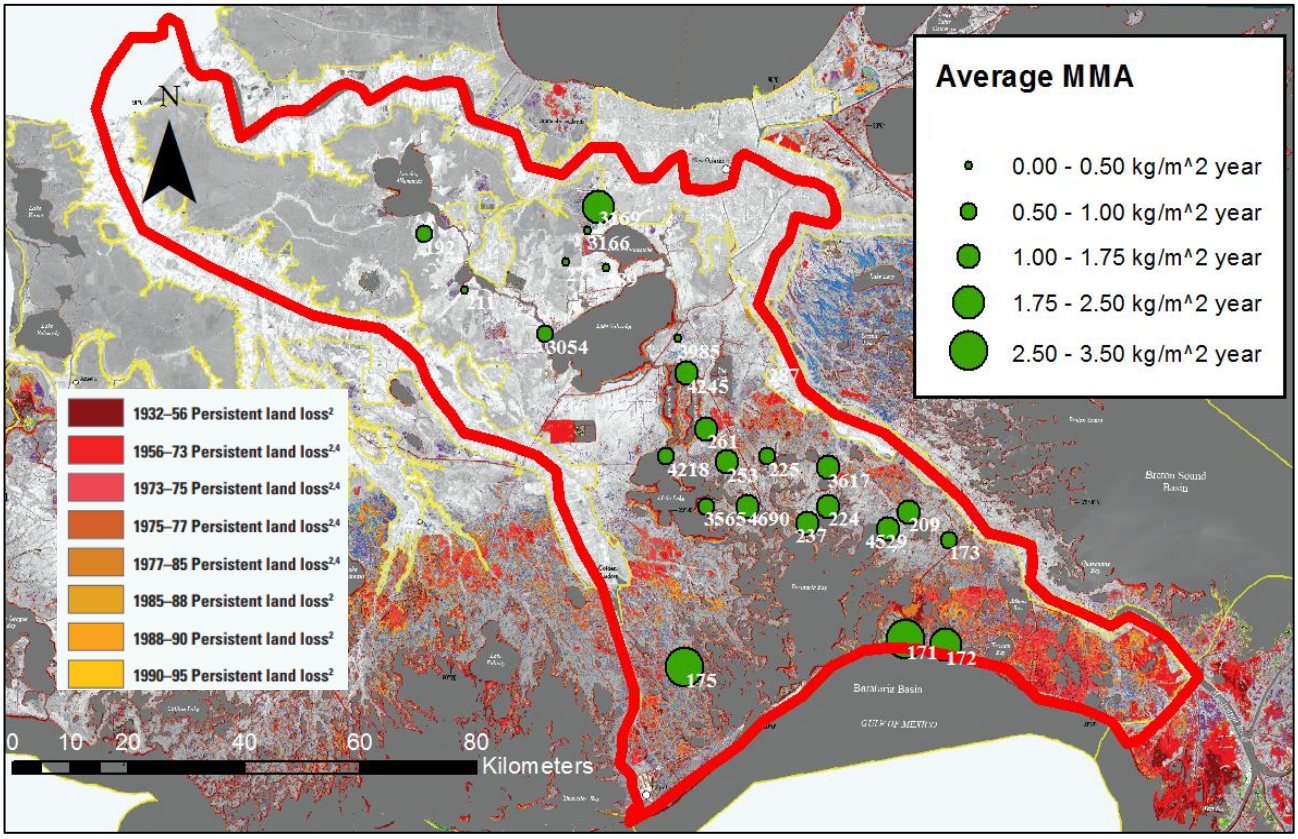

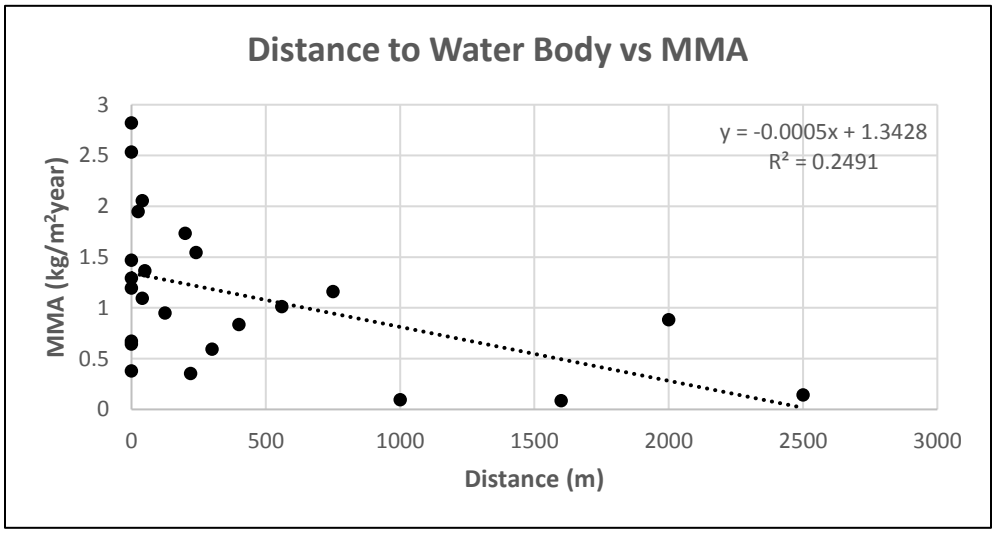

Figure 12. (a) MMA from this study georeferenced over the Couvillion et al. (2017) land loss map. The areas of the map in color are areas that have had persistent land loss between 1932-2014, with cooler colors representing more recent land loss. The majority of loss shown in Barataria Basin in the map above is older, with the red colors indicating losses from 1956-1973 and more focused in the southern and coastal areas of the basin. (b) Distance to water body plotted against MMA.

4.3. Comparison of Study VAR and MAR to CRMS Elevation and Accretion Data

Of the CRMS sites used in this study, 17 have a variety of publically available data including short-term elevation change, short-term VAR, subsidence rates, relative sea level rise, and vertical accretion data associated with the monitoring systems collected by the CPRA and USGS. The remaining 8 (189, 192, 211, 273, 287, 3166, 3169, & 4245) are floating marshes and lack a permanent substrate in which to anchor elevation and accretion measuring equipment. Elevation measurements are made using RSET methodology (Cahoon et al. 2002), short-term vertical accretion data measured using cyro-coring of marker horizons (Cahoon et al. 1996) with all data collection and verification conducted in accordance with the CRMS standards (Folse et al. 2014, Jankowski et al. 2017). The data collected from the CRMS instruments only spans ~ 10 year period as the first CRMS sites measurements came online in 2006. The CRMS short-term data elevation and accretion data observation time averages 8.4 ± 1.01 years, which is roughly an order of magnitude below what the ^{137}Cs and ^{210}Pb radiochemistry reaches (Cs=53 years and Pb= ~ 100 years). The average absolute value differences between short-term (CRMS provided) and the long-term VARs (from this study) is presented in Table 8, also compiled in Figure 13.

Of the 17 sites with short-term data available, 15 had VAR that were higher than the long-term results from this study. Only 5 of 17 had differences that were under 30% different in comparison to the long-term VAR reported here (Table 8, Figure 13 & 14). Differences in observation period can explain why such disagreement in VAR between the data sets exists (Sadler 1981). Storm erosion, variations in sedimentation through time, recent storm flux, varying sediment residence times, sediment diagenesis (i.e compaction), and sediment metabolism of organic material are likely some of mechanisms that are causing this difference (Sadler 1981, Neubauer et al. 2002). Even in unperturbed environments, sediment contributions

are not likely to be completely retained in an area over decadal time scales due to these mechanisms (Sadler 1981, Neubauer et al. 2002). This marsh accretion variability is why the CRS model was chosen for this project. The CRS model allows for variability through time, and a variability in VAR is observed in all sites in this study: generally, there appears to be increase in VAR over time followed by a decrease in more recent years (Figure 15). However, there are limitations to the accuracy of this perceived variability. Variability in rates through time is likely due to the much higher ratio of total activity over remaining activity (ΣAx/Ai) in the bottom intervals (Binford 1990). A larger ratio can skew calculated accretion rates to be lower because it represents more time as the ratio increases (Binford 1990). Additionally, observed rates of shallow subsidence in the region are high (Nienhuis et al. 2016, Jankowski et al. 2017). Compaction is likely the main driver of this subsidence (Dokka & Shinkle 2004) and may be causing the same interval thickness to represent a larger period of time (Figure 15). The similarity of trends of rates through time observed in the CRS method across the basin (Figure 15, Appendix G) suggests this may be the case. This interpretation suggests the trends in the CRS rates show the Sadler effect with higher rates in the short-term returning to lower rates in the long-term (Sadler 1981; Figure 15). Howeve this does not explain a return to lower values in most recent times. One possible interpretation is the fluctuation in accretion rates correlates with land loss rates quantified by Couvillion et al. (2017). Their study shows a large portion of the land loss in Barataria Basin occurred between the 1932-1975, with rates of loss largely slowing in more recent years (Couvillion et al. 2017, Figure 12a). Unfortunately, CRS data shows a return to lower rates after reaching a maximum from ~ 2000-2010 (Figure 15), which does not agree with their findings so this interpretation is rejected.

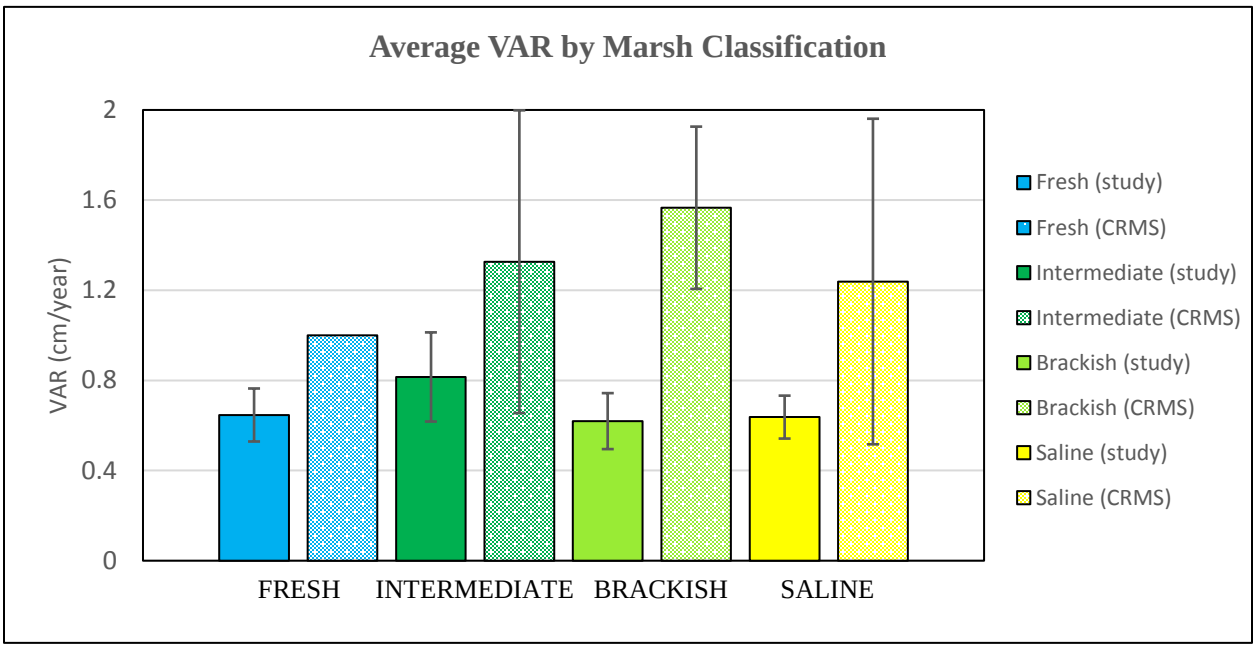

Figure 13. Comparison of the VAR produced by this study to the VAR from the CRMS measurement sites. Study VAR are shown by the solid colors and the CRMS VAR are shown by the light hatching.

Table 8. A comparison of short-term VAR and long-term VAR, from CRMS metadata and this study, respectively. Marsh salinities are represented by the following: F= fresh, I= intermediate, B= brackish and S= saline.

CRMS Site	Marsh Classification	Short-term VAR (cm/yr)	^{137}Cs VAR (cm/year)	Long-term VAR, this study (cm/yr)	Difference (cm/yr)	Percent difference (%)
171	S	1.60	0.68	0.66	0.94	142.33
172	S	1.79	0.58	0.75	1.04	139.02
173	S	0.55	0.50	0.50	0.05	9.32
175	S	0.52	0.66	0.73	-0.21	29.39
209	B	1.19	0.83	0.74	0.45	60.15
224	S	0.48	0.73	0.62	-0.14	22.57
225	B	1.28	0.62	0.60	0.68	113.00
237	S	2.39	0.51	0.52	1.87	359.62
253	B	2.08	0.75	0.77	1.31	169.54
261	I	0.99	0.86	0.83	0.16	19.50
3054	I	0.89	0.49	0.55	0.34	61.94
3565	B	1.54	0.55	0.56	0.98	175.11
3617	B	1.74	0.30	0.56	1.18	210.05
3985	F	1.00	0.48	0.94	0.06	6.12
4218	I	2.10	0.71	1.02	1.08	106.07
4529	S	1.69	0.58	0.87	0.82	94.01
4690	S	0.89	0.84	0.37	0.52	139.75
Average		**1.34 ± 0.59**	**0.63 ± 0.15**	**0.68 ± 0.17**	**0.70 ± 0.52***	**109 ± 91**

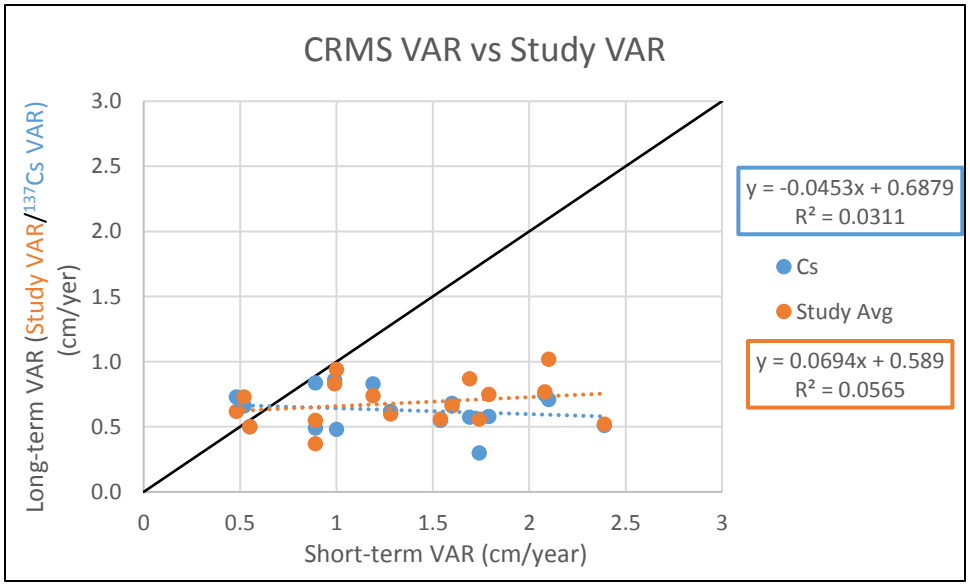

Figure 14. Plot of VAR produced by this study compared to VAR from CRMS data.

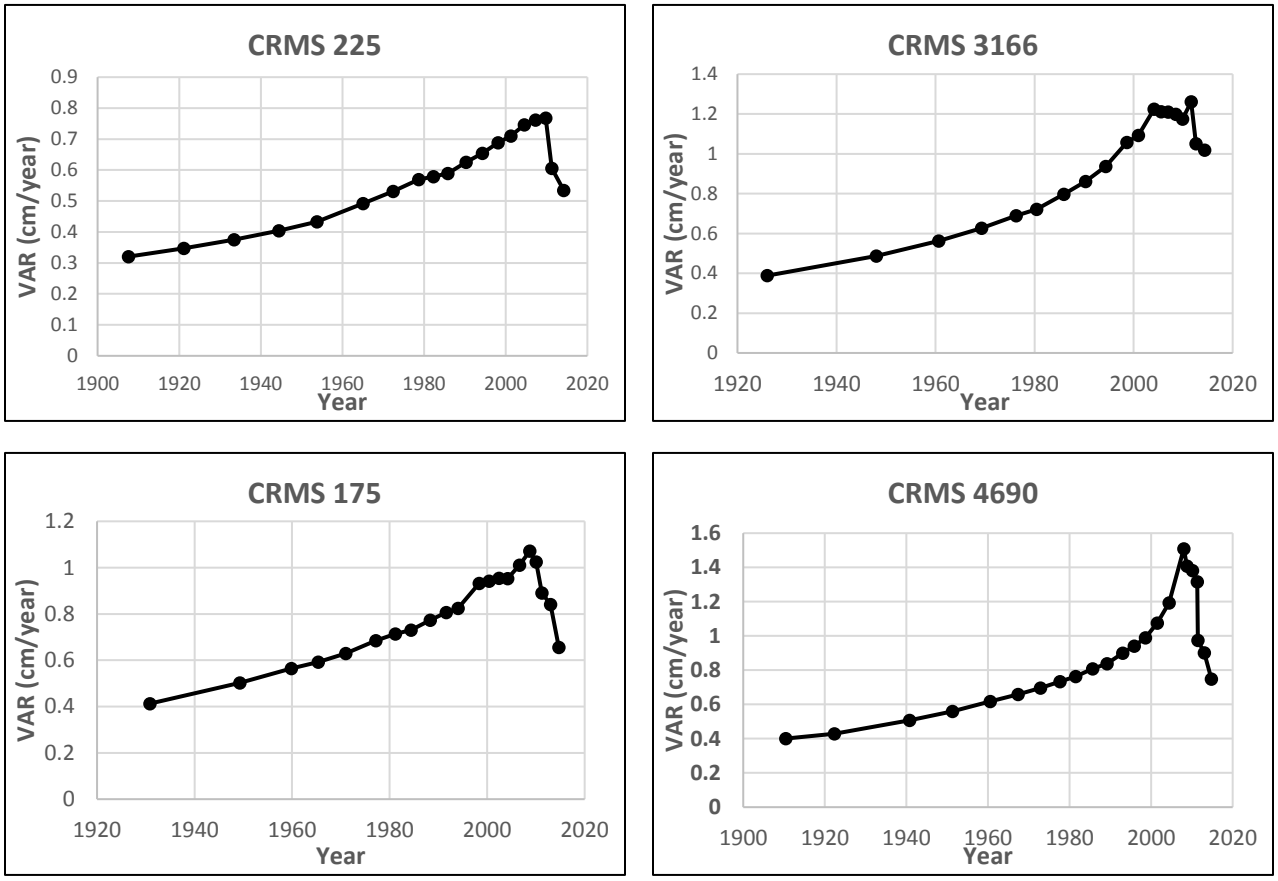

Figure 15. Graphs of select ^{210}Pb CRS model results. The plot shows a peak in VAR in recent times (last 10-15 years) with decrease to lower rates through time. Of note, the spacing between intervals increases with time, as discussed in text. The remainder of the graphs are in Appendix F.

4.4. Event Sedimentation Analysis

While using mineral mass per area trends is a good objective, first-order tool to identify potential storm event layers, we found either that hurricane signals are not created or preserved basin wide after a hurricane event or that other non-hurricane events are present (i.e. winter storms). Not all mineral sedimentation layers identified had an associated hurricane that corresponded to it (Figure 8). Additionally, net contributions associated with hurricanes cannot

easily be constrained due to the irregularity of the landscape it passes through, sediment sourcing, and what measures are used to determine deposition (i.e. residence time of sediments, difficulty extrapolating deposits over path, net effects; Neubauer et al. 2002, Smith et al. 2015). Hurricanes can act as erosive agents in many areas (Barras 2005). Erosive events could remove time in the radiochemical record and could invalidate assumptions required for geochemistry dating (^{137}Cs or ^{210}Pb) by reworking existing surface deposits (Corbett & Walsh 2015). The sourcing of the sediments deposited by hurricanes may also cause a breakdown of assumptions if the sediments deposited are sourced locally (i.e. cannibalization of local fine-grained sediments; Wilson & Allison 2008, Mariotti & Fagherazzi 2010) as opposed to being allochthonous. Preliminary results are too limited to suggest anything but further grain size analysis would allow for a better examination of this possible trend.

Agreement between hurricane path and core location with matched intervals provides a greater degree of confidence in the relationship (Appendix E shows hurricane paths). Some intervals do not seem to have a direct geographic tie to the hurricane path, which speaks to the complexity of matching a hurricane's timing with deposition it may produce, or the more likely possibility that the event identified is not the result of a hurricane but an unrelated event of coincident timing. For example, Danny did not travel directly through Barataria Basin but remained largely offshore except for crossing the Mississippi River in the southern portion of the basin just north of the Bird's Foot Delta. CRMS 171 and 175, located in the southern portion of the basin, have intervals that tie them to Danny's more southern path. CRMS sites 3166 and 3169 also have intervals that matched with the timing of Danny but are the most northern points in the data set. This suggests that some of the matched intervals may just be a coincidence of timing or were produced by a non-hurricane event. Additionally, 3169 is near the Davis Pond

diversion and shows three events after the implementation of that structure (2002) which may be causing those events. Hurricanes Katrina and Cindy both occurred in 2005 and time resolution is not precise enough to be able to determine the difference between storms in the same year, so they are grouped together. Katrina was the largest storm to pass through the search radius in the period of interest. The Katrina/Cindy event produced 15 matched intervals, the most in this basin-wide analysis, further providing confidence in the methodology (Table 5).

Table 9. (a) Mineral mass per area (MMPA) in kg/m^2 contributions by individual hurricanes. Intervals that had dates that potentially tied them to multiple hurricanes are listed out separately from the individual hurricanes.

Sediment Source	MMPA contributed (kg/m^2)	% of total hurricane MMPA	% of Total MMPA Inventory
Isaac (2012)	14.83	5.13	0.88
Isaac/Gustav	9.32	3.23	0.56
Gustav (2008)	11.58	4.01	0.69
Gustav/Katrina	6.30	2.18	0.38
Katrina/Cindy (2005)	58.98	20.42	3.52
Danny (1997)	48.76	16.88	2.91
Florence (1988)	9.78	3.39	0.58
Bob (1979)	32.92	11.39	1.96
Betsy (1965)	59.37	20.55	3.54
Flossy (1956)	18.50	6.40	1.10
Charlie (1948)	9.17	3.17	0.55
George (1947)	7.80	2.70	0.46
Hurricane total	**288.86**	**100**	**17.2**
Undesignated Events	**150.15**	**-**	**9**
Residual	**1237.00**	**-**	**73.8**
Total MMPA Inventory	**1676.01**	**-**	**100**

Table 9. (b) Mineral mass per area in kg/m^2 for the hurricane intervals data placed into context of its salinity and relative contributions to cumulative mineral mass at its location. HI=hurricane interval.

Fresh CRMS Sites	Percent of total MMPA in HI	Intermediate CRMS Sites	Percent of total MMPA in HI	Brackish CRMS Sites	Percent of total MMPA in HI	Saline CRMS Sites	Percent of total MMPA in HI
189	43.0%	**261**	0.0%	**209**	24.7%	**171**	16.9%
192	7.1%	**3054**	28.0%	**225**	18.9%	**172**	16.4%
211	7.5%	**4218**	13.1%	**253**	14.1%	**173**	24.4%
273	20.2%	**4245**	32.3%	**3565**	25.2%	**175**	6.7%
3166	47.3%			**3617**	12.5%	**224**	25.2%
3169	36.4%					**237**	17.6%
3985	19.1%					**4529**	8.8%
Average	25.8 ± 16.5%		18.3 ± 14.7%		19.1 ± 5.9%		15.7 ± 6.9%

Our data shows that hurricanes in the last ~20 years (Danny, Katrina, Gustav, and Isaac) had an observable impact on the mineral sediment accretion trends in Barataria Basin (Table 9). Cumulatively, the hurricane intervals make up 17.2% and undesignated intervals an additional 8.96% of the total sediment budget across all sites (Table 9a). Hurricane intervals make up a larger percentage of the mineral mass observed at fresh marshes (25.8 ± 16.5%) than they do at saline sites (15.7 ± 14.7%) (see Table 9b). Individual contributions by storm are shown in Table 9a. Smith et al. (2015) analyzed hurricane sedimentation from category 3 and above hurricanes (n=7) in the neighboring Breton Sound and found hurricanes contributed 10.9% of the sediment inventory, which is lower than results found in this study. However, this study looked at category 1 and above storms (n=11) which included more storms than Smith et al. (2015), and may explain why the total impact is greater. The contribution from undesignated events in this study (9%) are also greater than Smith et al. (2015) (2.9%). Both studies show there is a measurable impact by hurricanes on the sediment budgets of Louisiana coastal marshes. However, due to a

limited time period and records that post-date the implementation of the levee system, it is possible that the observed impact of storms is amplified in recent years (Sadler 1981). The current delta system has been building over 1000s of years (Roberts 1997, Blum & Roberts 2009) and known hurricane record only represent a small portion of that time (~70 years). Storms also may have a larger impact in the basin post-levee construction since few other means of sediment distribution are present. If that is that case, the majority of sediments deposited over the last ~100 years (at least 73.8% of mineral mass budget, Table 9a) were likely sourced from pre-dam fluvial deposition, regular tidal activity, and/or minor storms. As discussed in 4.2, the elevated mineral material may be a result of reworking eroded marsh edge sediments as opposed to bringing in outside sourced material (Wilson & Allison 2008).

When compared to the basin average grain size ($\bar{x}$=12.8 μm), hurricane intervals only have a slightly larger grain size ($\bar{x}$=13.1 μm). However, this small of a difference is not statistically significant. This may provide further evidence that the hurricane deposits are depositing reworked material, in which case it is expected that storm intervals would have a similar grain size to existing marsh material. Figure 16, below, shows examples of grain size trend profiles overlain with the event sedimentation profile used in identifying storm events. Typified by the selected profiles, some of the cores qualitatively show a positive correlation between MMPA and grain size but others show an opposite trend. Further analyses and a more in-depth quantitative analysis is needed to confirm or deny these connection and could be an area for future work.

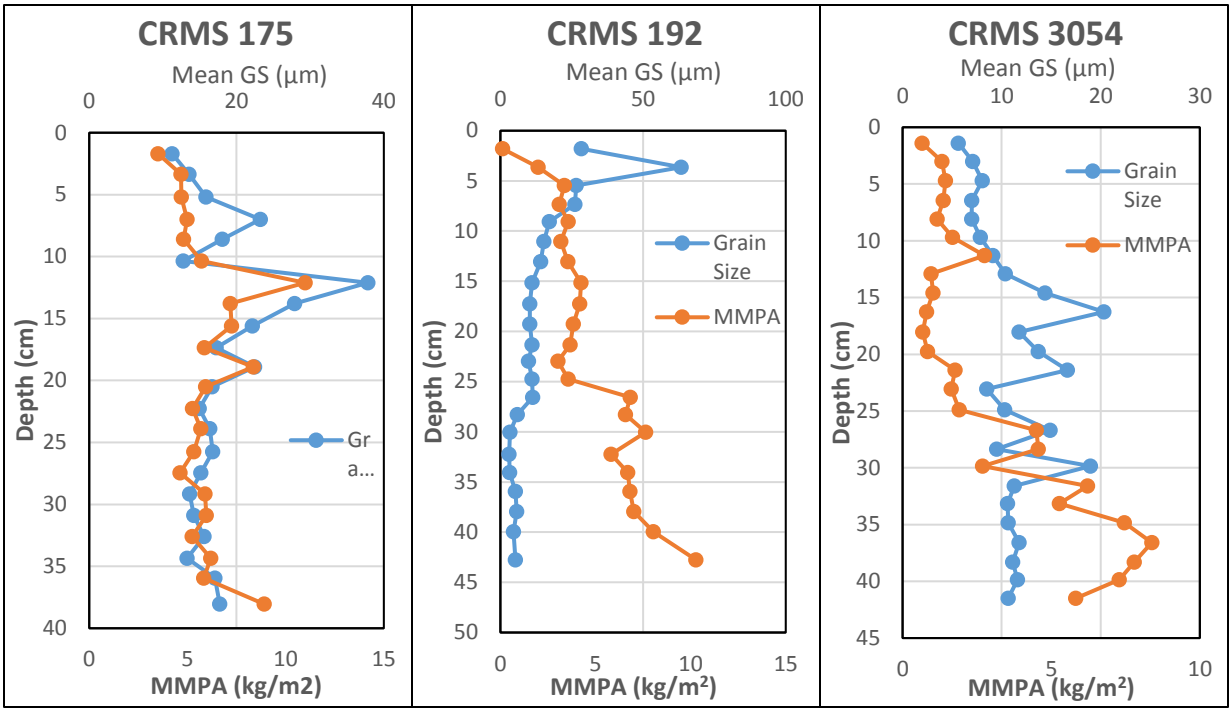

Figure 16. 3 examples of mean grain size profiles compared against down core mineral mass per area trends (MMPA). Of note, CRMS 175 largely shows a positive connection while CRM 192 and 3054 show mixed results with both positive and negative connections.

Conclusions

The average VAR produced by this study (0.67 ± 0.16 cm/year) agrees with the published range of values for coastal Louisiana (0.5-1.5 cm/year). Evidence from this study shows the VAR trends do not follow a basin wide spatial trend. This is likely due to the variability of environments over which the sites originate and the broad span of the basin they encompass. However, MAR values south of Lake Salvador are significantly higher than those to the north of Lake Salvador. This is trend is further confirmed by the higher bulk densities and mineral mass weight percent observed in the more coastal and saline sites. Despite their differences in mineral mass content, similar VAR throughout suggests that both organic and mineral material are contributing factors to elevation capital in Barataria Basin: the southern more saline marshes are accreting with 70% mineral sediment compared to 48% in the more organic-rich freshwater marshes to the north. Long-term investigation of sediment residence times variance and how compaction rates for mineral and organic material differ would help to better quantify the contribution of organic or mineral mass to marsh elevation capital. Furthermore, the area with the largest amounts of historical land loss, in large part, coincides with the areas showing elevated MAR values. Marsh edge erosion and subsequent resuspension of this material is one possible explanation of the elevated MAR values in the southern and central regions of the basin. Mineral mass accumulation data shows that hurricane deposits are present within the basin with Category 1 and above hurricanes since 1947 comprising ~17% of the budget and undesignated events an additional ~9%. Hurricanes and other storm events likely play a role in distributing sediments within the basin but MMA results and preliminary grain size data suggest that the majority of sediments are residual and likely not resultant of large-scale event deposition.

References

Appleby, P. G. (2002). Chronostratigraphic techniques in recent sediments. *Tracking environmental change using lake sediments* (pp. 171-203). Springer, Dordrecht.

Appleby, P. G. (2008). Three decades of dating recent sediments by fallout radionuclides: a review. *The Holocene* 18(1), 83-93.

Appleby, P. G., & Oldfield, F. (1978). The calculation of lead-210 dates assuming a constant rate of supply of unsupported 210Pb to the sediment. Catena, 5(1), 1-8.

Appleby, P. G., & Oldfieldz, F. (1983). The assessment of 210Pb data from sites with varying sediment accumulation rates. Hydrobiologia, 103(1), 29-35.

Barras, J. A. (2005). Land area changes in coastal Louisiana after Hurricanes Katrina and Rita. *Science and the storms: the USGS response to the hurricanes of*, 98-113.

Baumann, R. H., Day, J. W., & Miller, C. A. (1984). Mississippi deltaic wetland survival: sedimentation versus coastal submergence. *Science*, *224*(4653), 1093-1095.

Baustian, J. J., Mendelssohn, I. A., & Hester, M. W. (2012). Vegetation's importance in regulating surface elevation in a coastal salt marsh facing elevated rates of sea level rise. *Global Change Biology*, *18*(11), 3377-3382.

Baustian, J. J., & Mendelssohn, I. A. (2015). Hurricane-induced sedimentation improves marsh resilience and vegetation vigor under high rates of relative sea level rise. *Wetlands*, 35(4), 795-802.

Bentley, S. J., Freeman, A. M., Willson, C. S., Cable, J. E., & Giosan, L. (2014). Using what we have: Optimizing sediment management in Mississippi River delta restoration to improve the economic viability of the nation. In *Perspectives on the Restoration of the Mississippi Delta* (pp. 85-97). Springer Netherlands.

Bentley, S. J., Blum, M. D., Maloney, J., Pond, L., & Paulsell, R. (2016). The Mississippi River source-to-sink system: Perspectives on tectonic, climatic, and anthropogenic influences, Miocene to Anthropocene. Earth-Science Reviews, 153, 139-174.

Bierman, V. J., Hinz, S. C., Zhu, D. W., Wiseman, W. J., Rabalais, N. N., & Turner, R. E. (1994). A preliminary mass balance model of primary productivity and dissolved oxygen in the Mississippi River plume/inner Gulf Shelf region. *Estuaries and Coasts*, *17*(4), 886-899.

Binford, M. W. (1990). Calculation and uncertainty analysis of 210 Pb dates for PIRLA project lake sediment cores. *Journal of Paleolimnology*, 3(3), 253-267.

Blum, M. D., & Roberts, H. H. (2009). Drowning of the Mississippi Delta due to insufficient sediment supply and global sea-level rise. *Nature Geoscience*, 2(7), 488-491.

Board, O. S., & National Research Council. (2006). *Drawing Louisiana's New Map: Addressing Land Loss in Coastal Louisiana*. National Academies Press.

Boesch, D. F., Josselyn, M. N., Mehta, A. J., Morris, J. T., Nuttle, W. K., Simenstad, C. A., & Swift, D. J. (1994). Scientific assessment of coastal wetland loss, restoration and management in Louisiana. *Journal of Coastal Research*, i-103.

Bricker-Urso, S., Nixon, S.W., Cochran, J.K., Hirschberg, D.J., Hunt, C. (1989). Accretion rates and sediment accumulation in Rhode Island salt marshes. *Estuaries* 12, 300-317.

Cahoon, D. R., Lynch, J. C., & Knaus, R. M. (1996). Improved cryogenic coring device for sampling wetland soils. *Journal of Sedimentary Research*, 66(5).

Cahoon, D. R., Lynch, J. C., Perez, B. C., Segura, B., Holland, R. D., Stelly, C., Hensel, P. (2002). High-Precision Measurements of Wetland Sediment Elevation: II. The Rod Surface Elevation Table. *Journal of Sedimentary Research, 72*(5), 734-739. doi:10.1306/020702720734

Cahoon, D. R., & Reed, D. J. (1995). Relationships among marsh surface topography, hydroperiod, and soil accretion in a deteriorating Louisiana salt marsh. *Journal of Coastal Research*, 357-36

Cahoon, D. R., White, D. A., & Lynch, J. C. (2011). Sediment infilling and wetland formation dynamics in an active crevasse splay of the Mississippi River delta. *Geomorphology*, *131*(3-4), 57-68.

Callaway, J. C., DeLaune, R. D., & Patrick Jr, W. H. (1997). Sediment accretion rates from four coastal wetlands along the Gulf of Mexico. *Journal of Coastal Research*, 181-191.

Cambray, R. S., Eakins, J. D., Peirson, D. H., & Fisher, E. M. R. (1976). *Radioactive fallout in air and rain: results to the end of 1975* (No. AERE-R-8267). CM-P00068548.

Chmura, G. L., & Kosters, E. C. (1994). Storm deposition and 137Cs accumulation in fine-grained marsh sediments of the Mississippi Delta Plain. *Estuarine, Coastal and Shelf Science*, *39*(1), 33-44.

Coleman, J.M., Roberts, H.H., and Stone, G.W. Mississippi River delta: an overview. *Journal of Coastal Research* (1998): 699-716.

Condrey, R. E., Hoffman, P. E., & Evers, D. E. (2014). The last naturally active delta complexes of the Mississippi River (LNDM): discovery and implications. In *Perspectives on the Restoration of the Mississippi Delta* (pp. 33-50). Springer, Dordrecht.

Corbett, D., & Walsh, J. (2015). 210 Lead and 137 Cesium: establishing a chronology for the last century. *Handbook of Sea-Level Research* (1st ed., Vol. 1, pp. 361-372). John Wiley & Sons, Ltd.

Couvillion, B.R., Beck, H., Schoolmaster, D., and Fischer, M. (2017). Land area change in coastal Louisiana 1932 to 2016: *U.S. Geological Survey Scientific Investigations Map 3381*, 16 p. pamphlet, https://doi.org/10.3133/sim3381.

CPRA of Louisiana. (2017). Louisiana's Comprehensive Master Plan for a Sustainable Coast. Coastal Protection and Restoration Authority of Louisiana. Baton Rouge, LA.

CPRA (2017a). Mid-Barataria Sediment Diversion." Coastal Protection and Restoration Authority, coastal.la.gov/mid-basin-sediment-diversion-program/collaborative-delivery-market-sounding-mbsd/.

CPRA. (2017b, October 18). $1.2 billion in coastal projects in Southeast Louisiana spotlighted at CPRA's October board meeting [Press release]. Retrieved November 6, 2017, from http://coastal.la.gov/wp-content/uploads/2017/10/2017.10.18-CPRA-Board-Meeting-Press-Release.pdf

Craft, C. B., Seneca, E. D., & Broome, S. W. (1993). Vertical accretion in microtidal regularly and irregularly flooded estuarine marshes. *Estuarine, Coastal and Shelf Science*, *37*(4), 371-386.

Cutshall, N. H., Larsen, I. L., & Olsen, C. R. (1983). Direct analysis of 210Pb in sediment samples: self-absorption corrections. *Nuclear Instruments and Methods in Physics Research*, 206(1-2), 309-312.

CWPPRA (2017). The Barataria Basin. Retrieved November 06, 2017, from https://www.lacoast.gov/new/About/Basin_data/ba/Default.aspx

Day, J. W., Barras, J., Clairain, E., Johnston, J., Justic, D., Kemp, G. P., & Templet, P. (2005). Implications of global climatic change and energy cost and availability for the restoration of the Mississippi delta. *Ecological Engineering*, *24*(4), 253-265.

Day, J. W., Lane, R. R., D'Elia, C. F., Wiegman, A. R., Rutherford, J. S., Shaffer, G. P., & Kemp, G. P. (2018). Large infrequently operated river diversions for Mississippi delta restoration. In *Mississippi Delta Restoration* (pp. 113-133). Springer, Cham.

DeLaune, R. D., Patrick Jr, W. H., & Buresh, R. J. (1978). Sedimentation rates determined by 137Cs dating in a rapidly accreting salt marsh. *Nature*, 275(5680), 532.

DeLaune, R. D., Baumann, R. H., & Gosselink, J. G. (1983). Relationships among vertical accretion, coastal submergence, and erosion in a Louisiana Gulf Coast marsh. *Journal of Sedimentary Research*, 53(1).

DeLaune, R. D., Pezeshki, S. R., Pardue, J. H., Whitcomb, J. H., & Patrick Jr, W. H. (1990). Some influences of sediment addition to a deteriorating salt marsh in the Mississippi River deltaic plain: a pilot study. *Journal of Coastal Research*, 181-188.

DeLaune, R. D., Jugsujinda, A., Peterson, G. W., & Patrick Jr, W. H. (2003). Impact of Mississippi River freshwater reintroduction on enhancing marsh accretionary processes in a Louisiana estuary. *Estuarine, Coastal and Shelf Science*, 58(3), 653-662.

Dokka, R. K. (2006). Modern-day tectonic subsidence in coastal Louisiana. *Geology*, *34*(4), 281-284.

Feijtel, T. C., DeLaune, R. D., & Patrick, W. H. (1988). Seasonal pore water dynamics in marshes of Barataria Basin, Louisiana. *Soil Science Society of America Journal*, 52(1), 59-67.

Folse, T. M., L. A. Sharp, J. L. West, M. K. Hymel, J. P. Troutman, T. McGinnis, D. Weifenbach, W. M. Boshart, L. B. Rodrigue, D. C. Richardi, W. B. Wood, and C. M. Miller. (2014). A Standard Operating Procedures Manual for the Coast-wide Reference Monitoring System-Wetlands: Methods for Site Establishment, Data Collection, and Quality Assurance/Quality Control. Louisiana Coastal Protection and Restoration Authority, Office of Coastal Protection and Restoration. Baton Rouge, LA. 228 pp.

Gagliano, S. M., Meyer-Arendt, K. J., & Wicker, K. M. (1981). Land loss in the Mississippi River deltaic plain. *GCAGS Transactions 31*.

Gagliano, S. M. (1998). Faulting, subsidence and land loss in coastal Louisiana. *Coastal Environments Inc., Baton Rouge, LA.*

González, J.L., and Tornqvist, T.E. Coastal Louisiana in crisis: Subsidence or sea level rise?. *EOS, Transactions American Geophysical Union* 87.45 (2006): 493-498.

Hatton, R. S., DeLaune, R. D., & Patrick, W. H. (1983). Sedimentation, accretion, and subsidence in marshes of Barataria Basin, Louisiana. *Limnology and Oceanography*, 28(3), 494-502.

Heiri, O., Lotter, A. F., & Lemcke, G. (2001). Loss on ignition as a method for estimating organic and carbonate content in sediments: reproducibility and comparability of results. *Journal of paleolimnology*, 25(1), 101-110.

Henry, K. M., & Twilley, R. R. (2013). Soil development in a coastal Louisiana wetland during a climate-induced vegetation shift from salt marsh to mangrove. *Journal of Coastal Research*, 29(6), 1273-1283.

Jankowski, K. L., Törnqvist, T. E., & Fernandes, A. M. (2017). "Vulnerability of Louisiana's coastal wetlands to present-day rates of relative sea-level rise". *Nature Communications*, 8, 14792.

Jarvis, J. C. (2010). Vertical accretion rates in coastal Louisiana: A review of the scientific literature (No. ERDC/EL-TN-10-5). *Engineer Research and Development Center Vicksburg MS Environmental Lab.*

Kesel, R. H. (1989). The role of the Mississippi River in wetland loss in southeastern Louisiana, USA. *Environmental Geology*, 13(3), 183-193.

Kesel, R. H. (2003). Human modifications to the sediment regime of the Lower Mississippi River flood plain. *Geomorphology*, 56(3), 325-334.

Kim, W., Mohrig, D., Twilley, R., Paola, C., & Parker, G. (2009). Is it feasible to build new land in the Mississippi River Delta?.*EOS, Transactions American Geophysical Union*, 90(42), 373-374.

Kolker, A. S., Allison, M. A., & Hameed, S. (2011). An evaluation of subsidence rates and sea-level variability in the northern Gulf of Mexico. *Geophysical Research Letters*, *38*(21).

Leonard, L.A., Hine, A.C., Luther, M.E., (1995). Surficial sediment transport and deposition processes in a Juncus roemerianus marsh, west-central Florida. *Journal of Coastal Research* 11, 322e336.

MacKenzie, A. B., Hardie, S. M. L., Farmer, J. G., Eades, L. J., & Pulford, I. D. (2011). Analytical and sampling constraints in 210 Pb dating. *Science of the Total Environment*, 409(7), 1298-1304.

Mariotti, G., & Fagherazzi, S. (2010). A numerical model for the coupled long-term evolution of salt marshes and tidal flats. *Journal of Geophysical Research: Earth Surface*, 115(F1).

Meade, R. H., & Moody, J. A. (2010). Causes for the decline of suspended-sediment discharge in the Mississippi River system, 1940–2007. *Hydrological Processes*, 24(1), 35-49.

Milan, C. S., Swenson, E. M., Turner, R. E., & Lee, J. M. (1995). Assessment of the method for estimating sediment accumulation rates: Louisiana salt marshes. *Journal of Coastal Research*, 296-307

Mitsch, W. J., Day Jr, J. W., Gilliam, J. W., Groffman, P. M., Hey, D. L., Randall, G. W., & Wang, N. (2001). Reducing Nitrogen Loading to the Gulf of Mexico from the Mississippi River Basin: Strategies to Counter a Persistent Ecological Problem: Ecotechnology—the use of natural ecosystems to solve environmental problems—should be a part of efforts to shrink the zone of hypoxia in the Gulf of Mexico. *BioScience*, *51*(5), 373-388.

Morton, R., & White, W. (1997). Characteristics of and Corrections for Core Shortening in Unconsolidated Sediments. *Journal of Coastal Research*, 13(3), 761-769.

Murray, A., Marten, R., Johnston, A., & Martin, P. (1987). Analysis for naturally occurring radionuclides at environmental concentrations by gamma spectrometry. *Journal of Radioanalytical and Nuclear Chemistry*, 115(2), 263-288.

Neupane, Jeevan, Water Quality Modeling of Freshwater Diversions in the Barataria Basin (2010). *University of New Orleans Theses and Dissertations*. Paper 1255

Neubauer, S. C., Anderson, I. C., Constantine, J. A., & Kuehl, S. A. (2002). Sediment deposition and accretion in a mid-Atlantic (USA) tidal freshwater marsh. *Estuarine, Coastal and Shelf Science*, 54(4), 713-727.

Neubauer, S. C. (2008). Contributions of mineral and organic components to tidal freshwater marsh accretion. *Estuarine, Coastal and Shelf Science*, *78*(1), 78-88.

Nienhuis, J. & Törnqvist, T., Jankowski, K.L. & Fernandes, A. & E. Keogh, M. (2017). A new subsidence map for coastal Louisiana. *GSA Today*. 27. 58-59.

Nyman, J. A., DeLaune, R. D., & Patrick, W. H. (1990). Wetland soil formation in the rapidly subsiding Mississippi River deltaic plain: Mineral and organic matter relationships. *Estuarine, Coastal and Shelf Science*, *31*(1), 57-69.

Nyman, J., DeLaune, R., Roberts, H., & Patrick, W. (1993). Relationship between vegetation and soil formation in a rapidly submerging coastal marsh. *Marine Ecology Progress Series, 96*(3), 269-279

Nyman, J. A., Crozier, C. R., & DeLaune, R. D. (1995). Roles and patterns of hurricane sedimentation in an estuarine marsh landscape. *Estuarine, Coastal and Shelf Science*, *40*(6), 665-679.

Nyman, J. A., Walters, R. J., Delaune, R. D., & Patrick, W. H. (2006). Marsh vertical accretion via vegetative growth. *Estuarine, Coastal and Shelf Science*, *69*(3), 370-380.

Penland, S., Ritchie, W., Boyd, R., Gerdes, R. G., & Suter, J. R. (1986). The Bayou Lafourche delta, Mississippi River delta plain, Louisiana. *South-Eastern Section of the Geological Society of America: Decade of North American Geology, Centennial Field Guide Volume* 6, 6, 447.

Penland, S., & Ramsey, K. E. (1990). Relative sea-level rise in Louisiana and the Gulf of Mexico: 1908-1988. *Journal of Coastal Research*, 323-342.

Rabalais, N. N., Turner, R. E., & Scavia, D. (2002). Beyond Science into Policy: Gulf of Mexico Hypoxia and the Mississippi River: Nutrient policy development for the Mississippi River watershed reflects the accumulated scientific evidence that the increase in nitrogen loading is the primary factor in the worsening of hypoxia in the northern Gulf of Mexico. *AIBS Bulletin*, *52*(2), 129-142.

Reed, D. J. (1989). Patterns of sediment deposition in subsiding coastal salt marshes, Terrebonne Bay, Louisiana: the role of winter storms. *Estuaries*, 12(4), 222-227.

Reed, D. J. (1992). Effect of weirs on sediment deposition in Louisiana coastal marshes. *Environmental Management*, 16(1), 55-65.

Reed, D. J. (1995). The response of coastal marshes to sea-level rise: Survival or submergence?. Earth Surface Processes and Landforms, 20(1), 39-48.

Ritchie, J. C., Hawks, P. H., & McHenry, J. R. (1975). Deposition rates in valleys determined using fallout cesium-137. *Geological Society of America Bulletin*, 86(8), 1128-1130.

Ritchie, J. C., & McHenry, J. R. (1990). Application of radioactive fallout cesium-137 for measuring soil erosion and sediment accumulation rates and patterns: a review. *Journal of environmental quality*, *19*(2), 215-233.

Roberts, H. H. (1997). Dynamic changes of the Holocene Mississippi River delta plain: the delta cycle. *Journal of Coastal Research*, 605-627.

Sadler, P. M. (1981). Sediment accumulation rates and the completeness of stratigraphic sections. *The Journal of Geology*, 89(5), 569-584.

Sanchez-Cabeza, J., & Ruiz-Fernández, A. (2012). 210Pb sediment radiochronology: An integrated formulation and classification of dating models. *Geochimica et Cosmochimica Acta*, 82, 183-200. doi:10.1016/j.gca.2010.12.024

Shen, Z., Törnqvist, T.E., Mauz, B., Chamberlain, E.L., Nijhuis, A.G., and Sandoval, L. Episodic overbank deposition as a dominant mechanism of floodplain and delta-plain aggradation. *Geology* 43.10 (2015): 875-78. Web.

Shinkle, K. D., & Dokka, R. K. (2004). *Rates of vertical displacement at benchmarks in the lower Mississippi Valley and the northern Gulf Coast* (Vol. 50). US Department of Commerce, National Oceanic and Atmospheric Administration, National Ocean Service, National Geodetic Survey.

Smith, J. E., Bentley, S. J., Snedden, G. A., & White, C. (2015). What role do hurricanes play in sediment delivery to subsiding river deltas?. *Scientific Reports*, 5.

Smith, J. N., & Walton, A. (1980). Sediment accumulation rates and geochronologies measured in the Saguenay Fjord using the Pb-210 dating method. *Geochimica et Cosmochimica Acta*, 44(2), 225-240.

Steyer, G.D., 2010, Coastwide Reference Monitoring System (CRMS): *U.S. Geological Survey Fact Sheet 2010-3018*, 2 p. (Revised August 2010)

Stone, G. W., Grymes III, J. M., Dingler, J. R., & Pepper, D. A. (1997). Overview and significance of hurricanes on the Louisiana coast, USA. *Journal of Coastal Research*, 656-669.

Stone, G. W., & McBride, R. A. (1998). Louisiana barrier islands and their importance in wetland protection: forecasting shoreline change and subsequent response of wave climate. *Journal of Coastal Research*, 900-915.

Swarzenski, P. W. (2014). ^{210}Pb Dating. *Encyclopedia of Scientific Dating Methods* (pp. 1-11). Springer Netherlands.

Törnqvist, T. E., Kidder, T. R., Autin, W. J., van der Borg, K., de Jong, A. F., Klerks, C. J., ... & Wiemann, M. C. (1996). A revised chronology for Mississippi River subdeltas. *Science*, 273(5282), 1693-1696.

Törnqvist, T. E., Bick, S. J., van der Borg, K., & de Jong, A. F. (2006). How stable is the Mississippi Delta?. *Geology* 34(8), 697-700.

Turner, R. E. Wetland loss in the northern Gulf of Mexico: multiple working hypotheses. *Estuaries and Coasts* 20.1 (1997): 1-13.

Turner, R. E., Baustian, J. J., Swenson, E. M., & Spicer, J. S. (2006). Wetland sedimentation from hurricanes Katrina and Rita. *Science*, *314*(5798), 449-452.

Twilley, R. R., Bentley, S. J., Chen, Q., Edmonds, D. A., Hagen, S. C., Lam, N. S. N., ... & McCall, A. (2016). Co-evolution of wetland landscapes, flooding, and human settlement in the Mississippi River Delta Plain. *Sustainability Science*, 11(4), 711-731.

Visser, J. M., Sasser, C. E., Chabreck, R. H., & Linscombe, R. G. (2002). The impact of a severe drought on the vegetation of a subtropical estuary. *Estuaries*, 25(6), 1184-1195.

Walker, H. J., Coleman, J. M., Roberts, H. H., & Tye, R. S. (1987). Wetland loss in Louisiana. *Geografiska Annaler*. Series A. *Physical Geography*, 189-200.

Walker, N. D., & Hammack, A. B. (2000). Impacts of winter storms on circulation and sediment transport: Atchafalaya-Vermilion Bay region, Louisiana, USA. *Journal of Coastal Research*, 996-1010.

Walling, D. E., & He, Q. (1997). Use of fallout ^{137}Cs in investigations of overbank sediment deposition on river floodplains. *Catena*, *29*(3), 263-282.

Wilson, C. A., & Allison, M. A. (2008). An equilibrium profile model for retreating marsh shorelines in southeast Louisiana. *Estuarine, Coastal and Shelf Science*, *80*(4), 483-494.

Wise, S. M. (1980). Caesium-137 and lead-210: a review of the techniques and some applications in geomorphology. *Timescales in geomorphology*, *9*, 109-127.

Wright, L. D., & Nittrouer, C. A. (1995). Dispersal of river sediments in coastal seas: six contrasting cases. *Estuaries and Coasts* 18(3), 494-508.

Xu, K., Bentley, S. J., Robichaux, P., Sha, X., & Yang, H. (2016). Implications of texture and erodibility for sediment retention in receiving basins of coastal Louisiana diversions. *Water*, *8*(1), 26.

Appendix A: Site Location and Other Associated Information

Table A-1

Site ID	Date extracted	Latitude	Longitude	Observed depth (cm)	# of intervals	% compaction
171	6/28/2016	29.3238	-89.796	44.55	21	14.00
172	6/21/2016	29.3165	-89.7343	38.55	23	5.51
173	6/21/2016	29.4543	-89.7299	30.05	18	36.13
175	5/31/2016	29.2874	-90.1379	38.55	22	24.11
189	5/11/2016	29.8099	-90.2605	37.384375	20	20.97
192	5/25/2016	29.8535	-90.5417	45.3	22	9.04
209	4/21/2016	29.4906	-89.7917	46.05	24	13.52
211	5/25/2016	29.7809	-90.4792	28.8	18	27.64
224	4/20/2016	29.49899156	-89.91573695	48.1	22	9.93
225	4/21/2016	29.5632	-90.0105	46.975	20	15.21
237	4/20/2016	29.47589459	-89.94727167	51.8	23	4.52
253	4/20/2016	29.5559	-90.073	47.8	21	12.05
261	6/22/2016	29.5994	-90.1042	47.05	27	11.31
273	5/11/2016	29.8172	-90.323	40.1625	20	20.57
287	6/22/2016	29.6865	-90.0105	12.75	8	73.44
3054	5/25/2016	29.7228	-90.3542	45.3	25	7.17
3166	5/11/2016	29.8585	-90.2887	39.05125	20	25.57
3169	5/11/2016	29.8889	-90.2723	47.226875	26	12.37
3565	4/20/2016	29.49816801	-90.10238365	48.5	24	10.68
3985	3/30/2016	29.5486	-89.9167	39.45	18	20.20
4218	4/20/2016	29.7175	-90.149	50.05	24	21.57
4245	3/30/2016	29.5632	-90.1667	51.9	23	6.54
4529	4/21/2016	29.672	-90.1355	48.25	25	10.21
4690	4/20/2016	29.46956918	-89.82193237	45.875	24	10.23
3617	10/14/2016	29.49857696	-90.04045319	36.55	21	10.49
Average		**29.60 ± 0.18**	**-90.08 ± 0.22**	**42.24 ± 8.7**	**21.6 ± 3.7**	**14.98 ± 14.04**

Table A-2

CRMS Site	total wet weight (g)	total dry weight (g)	Total dry mineral mass (g)	Total dry organic matter mass (g)
171	3527.68	1340.75	1180.03	160.72
172	3420.44	1084.68	920.69	163.99
173	2409.61	441.82	307.06	134.76
175	3280.73	1258.6	1077.44	181.16
189	2399.5	199.28	167.79	31.49
192	3646.41	1129.93	867.75	262.18
209	3460.85	788.41	551.75	236.66
211	2376.38	280.79	158.44	122.35
224	3947.5	1076.82	839.28	237.54
225	3226.77	545.55	339.51	206.04
237	3922.09	851.41	634.86	216.55
253	3165.51	719.04	537.33	181.71
261	3768.04	908.34	618.68	289.66
273	2513.03	218.11	46.68	171.43
287	1097.16	75.97	24.49	51.48
3054	3308.19	897.97	649.12	248.85
3166	2401.94	257.2	97.96	159.24
3169	3471.72	908.53	668.60	239.93
3565	3345.36	565.96	353.89	212.07
3617	4004.09	1573.71	1380.03	196.68
3985	2689.41	335.65	137.28	198.37
4218	2887.52	442.64	281.38	161.26
4245	3734.78	668.22	429.26	239.06
4529	4058.42	1014.6	668.08	179.72
4690	3611.28	847.81	668.08	179.73

Appendix B: ^{137}Cs and ^{210}Pb Data

CRMS 171

Bottom Depth (cm)	Cs Activity (dpm/g)	Supported ^{210}Pb (dpm/g)	Excess ^{210}Pb (dpm/g)
1.7	0.321159973	1.641572026	34.17122912
3.5	0.216813987	1.495836689	30.59687374
5.5	0.00672954	1.455059651	18.98384265
7.4	0.143061919	1.561539488	24.7141732
9.5	0.051535072	1.457712169	28.11727021
11.35	0.128503222	1.632895774	25.39946063
13.35	0.146562883	1.588050637	21.62128939
15.25	0.130620111	1.486842398	24.92086538
17.35	0.298639904	1.562556222	26.88723941
19.15	0.283217141	1.344117329	23.03249288
20.75	0.32906098	1.177653188	18.12081707
22.55	0.309232531	0.949383705	24.84169965
24.25	0.296573933	1.178263573	16.78310815
26.15	0.341467929	1.355253858	26.49703197
28.05	0.340660364	1.288702158	26.43728292
29.65	0.282417364	1.176803479	17.81673747
31.45	0.357976897	1.046326173	24.16110449
33.45	0.349302299	1.264871774	21.68514053
35.35	0.485786897	1.249799599	21.82996113
36.95	0.490092596	1.075887992	17.71525907
38.75	0.310718084	1.241949866	24.48023542

CRMS 172

Bottom Depth (cm)	Cs Activity (dpm/g)	Supported ^{210}Pb (dpm/g)	Excess ^{210}Pb (dpm/g)
1.5	0.247332389	1.513315809	46.84494404
3.3	0.257026501	1.23395977	34.90507709
4.95	0.330809235	1.421377089	40.32724978
6.6	0.293157654	1.456161986	35.67345991
8.3	0.335682793	1.446692144	28.79661084
10.05	0.27937813	1.318219196	28.30497434
11.7	0.311672319	1.668697493	24.57675834
13.25	0.232558681	1.563201733	20.8898333
14.8	0.219687282	1.430401234	27.92179798
16.5	0.121955732	1.235195471	27.69415179
18.15	0.418237451	1.260590362	20.67092852
19.85	0.378146639	1.103506602	30.27477967
21.5	0.304906956	1.171337791	31.68258914
23.25	0.426638145	1.075051242	28.17066093

25	0.373047217	1.263651367	28.91823828
26.7	0.379004057	1.271377254	28.34033664
28.45	0.457837909	1.349161547	19.99326648
30.15	0.30071382	1.31592187	27.75951255
31.75	0.45735599	1.632145022	26.31336536
33.55	0.440377104	1.130071578	29.00077028
35.3	0.389850291	1.394155504	26.91195352
36.95	0.387365369	1.208878801	18.72195947
39.45	0.367613797	1.25522235	17.27942342

CRMS 173

Bottom Depth (cm)	**Cs Activity (dpm/g)**	**Supported ^{210}Pb (dpm/g)**	**Excess ^{210}Pb (dpm/g)**
1.65	0.195193189	1.287292087	13.34711028
3.25	0.040421743	1.12121301	11.16981058
4.95	0.258944172	1.048415501	11.16099052
6.7	0.228019004	1.090339906	11.37386774
8.3	0.043161938	1.038958206	9.512125071
10	0.239332578	1.043078129	6.856163286
11.7	0.133533873	1.180764489	4.845734638
13.45	0.242474771	1.064779989	5.483755341
15.3	0.035777455	1.079167751	4.75995518
17	0.506917751	0.842831128	6.299057348
18.85	0.935080791	1.013913472	7.302685311
20.65	1.122414659	0.91594278	7.042724416
22.25	1.292090873	0.659548469	6.891743429
23.9	1.38924809	0.625459026	7.495560983
25.6	2.019979707	1.301207776	3.81805229
27.4	2.694531959	0.316233183	5.297077443
29.3	2.614692054	0.802424069	6.677124693

CRMS 175

Bottom Depth (cm)	**Cs Activity (dpm/g)**	**Supported ^{210}Pb (dpm/g)**	**Excess ^{210}Pb (dpm/g)**
1.7	0.343871226	1.67289492	34.75253554
3.35	0.209341967	1.768081659	33.60394303
5.2	0.285644456	1.732359481	33.28793698
7	0.219370499	1.583767447	19.45807856
8.6	0.248393348	1.769252991	22.69487278
10.35	0.222460971	1.984601392	28.10103257
12.1	0.210756668	1.879944057	17.74864239
13.8	0.106986323	1.752795442	17.75392134
15.6	0.240628178	1.648280056	19.11250556
17.35	0.393534351	2.004192618	21.24376394

18.9	0.264525667	1.661246531	30.75627908
20.5	0.172225418	1.815627898	20.87910655
22.25	0.373618755	1.646340318	28.04655095
23.9	0.298927488	1.551161684	28.25226845
25.75	0.169838406	1.622392395	21.98316986
27.45	0.36040195	1.793792691	27.63506398
29.15	0.367914637	1.705563332	29.17443595
30.9	0.497586143	1.803021207	22.14432161
32.6	0.519944314	1.694870909	19.79058138
34.35	0.538890416	1.984428482	25.97886571
35.95	0.593122323	1.820973857	30.6793201
38.05	0.552183254	1.819196672	28.63406633

CRMS 189

Bottom Depth (cm)	**Cs Activity (dpm/g)**	**Supported ^{210}Pb (dpm/g)**	**Excess ^{210}Pb (dpm/g)**
2.2	0.156378822	0.428723486	16.49040161
4	0.16227768	0.607750175	16.12709115
6	0.385810592	0.728653728	16.43759836
7.7	0.190249397	0.44311494	16.27539689
9.2	0.052305083	0.865590445	4.050396122
11.1	0.306230752	0.509660903	10.10889458
13.3	0.067324396	0.714610376	8.62719005
15.3	0.399631008	0.325235848	14.69243753
17.4	0.577356661	0.804666943	7.223761913
19.3	0.124600219	0.712288429	8.355939674
21.4	0.175909487	0.40411069	13.47493096
23.3	0.49983494	0.536689959	15.62941984
25.4	0.825887727	0.379678121	11.19491649
27.5	2.225309271	0.444270417	2.156989948
29.3	4.914167924	0.255129135	8.943190292
31.1	8.557406076	0.703699537	8.819699683
33	5.609102219	0.189968013	6.102751192
35	6.390018661	0.36378106	6.256305718
36.6	5.978377435	0.251048316	5.267517415
38.3	3.712554451	0.52134853	3.023573748

CRMS 192

Bottom Depth (cm)	**Cs Activity (dpm/g)**	**Supported ^{210}Pb (dpm/g)**	**Excess ^{210}Pb (dpm/g)**
2.2	0.156378822	0.428723486	16.49040161
4	0.16227768	0.607750175	16.12709115
6	0.385810592	0.728653728	16.43759836
7.7	0.190249397	0.44311494	16.27539689
9.2	0.052305083	0.865590445	4.050396122

11.1	0.306230752	0.509660903	10.10889458
13.3	0.067324396	0.714610376	8.62719005
15.3	0.399631008	0.325235848	14.69243753
17.4	0.577356661	0.804666943	7.223761913
19.3	0.124600219	0.712288429	8.355939674
21.4	0.175909487	0.40411069	13.47493096
23.3	0.49983494	0.536689959	15.62941984
25.4	0.825887727	0.379678121	11.19491649
27.5	2.225309271	0.444270417	2.156989948
29.3	4.914167924	0.255129135	8.943190292
31.1	8.557406076	0.703699537	8.819699683
33	5.609102219	0.189968013	6.102751192
35	6.390018661	0.36378106	6.256305718
36.6	5.978377435	0.251048316	5.267517415
38.3	3.712554451	0.52134853	3.023573748

CRMS 209

Bottom Depth (cm)	**Cs Activity (dpm/g)**	**Supported ^{210}Pb (dpm/g)**	**Excess ^{210}Pb (dpm/g)**
1.9	0.07616536	1.06837581	12.32256459
3.75	0.109098723	1.404634912	9.828141985
5.7	0.086154306	1.487361551	11.60589357
7.45	0.145336763	1.130110399	10.34365632
9.35	0.130500082	1.365198625	15.72776018
11.3	0.374431966	1.233411434	7.35246084
13.15	0.13355934	1.087077509	5.484892572
15.05	0.220288592	1.266729728	6.561268466
16.9	0.173364596	1.237377633	6.655690326
18.8	0.314551175	0.99410383	8.674419974
20.65	0.279478878	0.882419159	10.4154446
22.35	0.44508821	0.771469629	10.71752304
24.1	0.420010026	0.859726677	10.41726998
25.95	0.411397137	0.586116301	11.14069505
27.65	0.435697261	0.757366755	10.78871069
29.45	0.50169894	0.72614807	9.929424305
31.25	0.731904011	0.81883321	7.298976506
33.05	0.590307642	0.939603247	5.850482222
35.05	0.612694784	0.753765091	6.717468375
36.9	0.915816276	0.69928574	7.610599707
38.9	1.225430223	0.90239628	7.14427827
40.85	1.517211159	0.620300316	7.580311308
42.9	1.949683621	1.115838079	3.975633865
45.55	3.662193142	0.874710272	4.664955739

CRMS 211

Bottom Depth (cm)	Cs Activity (dpm/g)	Supported ^{210}Pb (dpm/g)	Excess ^{210}Pb (dpm/g)
1.55	0.098669423	1.407622985	11.23549857
3.15	0.515850382	1.573585163	13.44591826
4.8	0.610288	1.459522593	12.41757656
6.5	0.415550766	1.296930578	11.29606031
8.15	0.434843298	1.237059117	12.75709224
9.9	0.475040141	1.219041105	12.81173112
11.55	0.557696403	1.417869633	12.30600101
13.15	0.325800433	1.040945318	12.24290043
14.85	0.49728556	0.887826103	9.796177359
16.6	0.51332231	1.035727674	8.307394844
18.3	0.884869248	1.090143541	8.658685291
19.7	0.811050933	1.152447698	6.737486617
21.3	1.895286145	1.349682977	6.186338383
23.05	3.082079437	1.312273448	6.964525115
24.95	4.30435606	1.695361936	6.953134247
26.9	5.148160775	1.062002326	4.964889734
28.9	5.042918592	0.902427081	6.361233657
30.8	5.437661158	0.760798888	6.388695111

CRMS 224

Bottom Depth (cm)	Cs Activity (dpm/g)	Supported ^{210}Pb (dpm/g)	Excess ^{210}Pb (dpm/g)
2	0.220660993	21.99601675	0.930829357
3.85	0.236314477	8.366562589	0.380835586
5.8	0.146267256	5.644082627	0.313878386
7.85	0.137274561	4.537207476	0.289942447
9.9	0.259368427	6.04034284	0.361139584
12	0.157869829	6.611125234	0.352686329
13.95	0.279164056	8.494950933	0.424516392
15.95	0.441639155	8.7490722	0.455572256
17.95	0.358610054	9.452007717	0.481240725
19.9	0.526558583	10.56500807	0.523884698
22.05	0.658519085	9.931232467	0.508411389
24	0.816491389	5.962885491	0.389314261
25.9	1.192517481	7.013881471	0.374010233
27.9	1.402120693	6.3579329	0.358022266
29.85	0.436261232	2.36745955	0.214970391
31.95	0.403116106	2.043288036	0.188602373
33.7	1.931280452	4.337393001	0.351810766
35.7	1.346652741	4.054417987	0.335449741
37.7	0.503847109	4.185810704	0.37527958
39.45	2.992211264	3.723791232	0.34994927

41.2	0.700738627	4.055598721	0.344386037
43.7	0.409851311	2.545260304	0.296268299

CRMS 225

Bottom Depth (cm)	Cs Activity (dpm/g)	Supported ^{210}Pb (dpm/g)	Excess ^{210}Pb (dpm/g)
1.9	0.309434382	1.2476495	7.572478712
3.8	0.338270174	1.331561928	7.975190131
5.7	0.204669148	1.377188615	3.586504694
7.6	0.389243531	1.244299047	6.021870896
9.45	0.513442123	1.12062428	6.985354887
11.45	0.553937068	1.046346885	8.266203297
13.2	0.658730123	1.017509169	8.970080176
15.2	0.705106691	1.006477921	8.42102775
17	0.791368738	1.069205354	10.45636233
18.6	0.782760798	1.045736118	10.53301385
20.45	0.897647794	0.983676155	9.026134999
22.1	0.903232229	1.069489355	8.278937513
24.2	1.081247842	1.066102459	7.446025419
25.95	1.06466659	0.961980993	8.11579834
27.95	1.563252372	1.200474147	9.228140178
29.95	1.462721487	0.856209695	6.989368259
32.05	3.45100195	0.836918824	6.497310477
33.8	5.774337391	0.799271501	6.504551531
35.7	1.06357212	0.78538694	3.617409711
38.45	2.209184856	0.783445492	5.778771965

CRMS 237

Bottom Depth (cm)	Cs Activity (dpm/g)	Supported ^{210}Pb (dpm/g)	Excess ^{210}Pb (dpm/g)
2	0.027190111	0.971940119	8.806286563
3.7	0.130180026	1.202801873	5.756902505
5.3	0.0560835	1.065603837	7.357185111
6.3	0.220482963	1.109775776	6.496452247
8.3	0.33139951	1.125853521	7.944017186
10	0.156506318	0.662837678	9.031550761
12.2	0.415926217	0.832759109	7.144671271
14.3	0.323543154	0.855238786	8.081182585
16.2	0.531655349	0.764208592	8.551726761
18.3	1.019837235	0.881922887	6.151983012
20.6	0.862310134	0.762647346	6.302355712
22.35	0.936707339	0.940925074	5.925046971
24.25	0.678122436	1.037994305	4.351267877

26.05	0.985119229	1.361662608	2.464872075
28.35	3.009664024	0.773822174	4.994480447
30.15	1.121468477	0.689469777	4.13555023
32.15	0.304215247	0.613518254	5.357423858
34.05	0.055823934	0.8322074	10.01130163
36.25	0.043260333	0.605590938	3.466452414
38.4	0.068785007	0.68596963	3.013688103
40.5	0.049539197	1.142903047	1.790588216
42.2	0.020512117	0.839172108	2.125088023
43.8	0.016988169	0.484565677	2.517936441

CRMS 253

Bottom Depth (cm)	**Cs Activity (dpm/g)**	**Supported ^{210}Pb (dpm/g)**	**Excess ^{210}Pb (dpm/g)**
1.85	0.210098405	1.172000206	9.359242232
4.05	0.170476267	1.505717815	6.16766873
6.05	0.274595441	1.501681781	9.528296028
7.95	0.280765423	1.486166931	8.624249569
9.65	0.444228965	1.179292817	8.208999497
11.75	0.342541502	1.248680202	6.729190656
13.95	0.256415229	1.442819069	6.394340416
15.65	0.372734287	1.326538306	8.584720647
17.4	0.395189261	1.155569742	11.62486639
19.25	0.426603461	1.080723524	10.96137409
21.55	0.39991572	1.215205857	8.263149265
23.15	0.349550759	1.014210795	7.512472844
24.85	0.430414693	0.978021632	8.040562888
26.95	0.332780062	1.070319183	6.989246518
29.15	0.512285484	1.225555579	9.956909573
31.15	0.380299636	1.154890901	18.07846063
32.85	0.528894728	1.113495735	9.901157676
34.55	0.740058758	1.135992677	8.281198508
36.55	0.978630661	1.191768841	8.839563885
38.55	1.238179387	1.038501294	8.508496777
40.95	1.701028189	1.277440122	7.439599862

CRMS 261

Bottom Depth (cm)	**Cs Activity (dpm/g)**	**Supported ^{210}Pb (dpm/g)**	**Excess ^{210}Pb (dpm/g)**
1.85	0.575794921	1.264565721	13.03240463
3.75	0.658535721	1.39936092	12.85571127
5.6	0.508901542	1.154906922	11.75902406
7.4	0.557193786	1.227650884	13.22114057
9.15	0.643453448	1.227289165	9.908964602

11	0.539867378	1.494693584	9.087064174
12.8	0.482337534	1.569280715	8.516954049
14.55	0.589781184	1.502809739	9.436321557
16.45	0.605780884	1.683157002	13.33167547
18.1	0.735918606	1.700803277	13.93825456
19.95	0.579018061	1.717392548	10.79813754
21.75	0.729002013	1.817893188	12.13960261
23.6	0.923248342	2.095457231	9.08694792
25.25	1.006649656	2.308234385	8.97895941
27.1	0.807379973	2.338499488	8.223640571
28.75	0.882687302	2.267370552	7.788179482
30.6	0.886133036	2.424652237	6.503866542
32.4	1.178891489	2.28785861	6.722575614
34.2	1.106995162	2.377698356	5.744063341
35.9	1.16137551	2.212964206	4.530451713
37.65	1.104064753	2.281464336	5.146136544
39.4	1.279867771	2.323812154	4.820789774
41.1	0.176604154	0.270758503	0.620228119
42.85	2.076998034	2.259463947	6.084346001
44.5	1.962544799	2.391152233	6.263367774
46.2	2.655257798	2.232562415	6.230157889
47.5	2.388054624	2.312916953	4.31954054

CRMS 273

Bottom Depth (cm)	**Cs Activity (dpm/g)**	**Supported ^{210}Pb (dpm/g)**	**Excess ^{210}Pb (dpm/g)**
2	0.694024536	1.547911737	71.16556535
3.9	0.860608118	1.124756987	109.9136111
5.8	0.266637921	1.574797876	75.90443037
7.7	0.735647282	1.095908154	60.42330918
9.5	0.943894922	1.142882239	76.11288655
11	0.055780757	1.671482319	83.71104268
12.7	1.004364199	1.487402781	109.8486526
14.6	0.072349309	1.072148452	74.2803965
16.7	0.059030295	0.832082584	68.91006084
18.5	1.137513708	1.10135883	64.91316302
20.5	1.348460783	1.272479528	105.6253471
22.2	1.250647297	0.825612183	73.46112506
24	0.521676972	1.451610803	83.57501989
25.8	1.18724865	1.288953168	84.04681514
27.3	1.296372374	0.815083989	96.00438326
29.5	1.714806776	1.481132683	107.8837422
31.2	1.699442363	1.668393471	88.43106121
33.2	3.367912811	1.498730992	82.11231479
35.3	3.266605924	1.406661715	64.29732607

37.6	4.247504164	0.681129042	91.68460746

CRMS 287

Bottom Depth (cm)	Cs Activity (dpm/g)	Supported ^{210}Pb (dpm/g)	Excess ^{210}Pb (dpm/g)
1.7	0.864265365	17.20480879	1.425605809
3.35	0.147942728	14.90576448	1.262331929
5.05	0	20.4542024	1.215869536
6.85	0.489194007	24.91088822	1.06803087
8.85	0.319716124	20.01471792	0.965665859
10.85	0.547077237	10.81920527	0.781155868
12.45	0.4092381	14.1908453	0.858879139
16.25	0.628483645	15.39827861	0.785923085

CRMS 3054

Bottom Depth (cm)	Cs Activity (dpm/g)	Supported ^{210}Pb (dpm/g)	Excess ^{210}Pb (dpm/g)
1.4	0.177270726	1.267854101	9.807446637
3	0.003951243	1.318337932	12.19342106
4.7	0.183013683	1.361552832	12.40556612
6.45	0.161195321	1.040909779	11.40941318
8.1	0.145515649	0.821485684	11.60323828
9.7	0.095399351	1.079488602	10.3421887
11.3	0.002093307	1.488499317	8.315229769
12.9	0.073361728	1.287483622	8.792269215
14.6	0.238977965	1.224581729	11.64272763
16.25	0.225626116	1.009341185	14.99735673
18.05	0.398580124	1.143862209	13.20286331
19.75	0.234250078	1.132733814	11.74940371
21.4	0.821277721	1.723848434	8.018763109
23.05	1.043000755	1.656942774	7.642644785
24.9	1.508403148	1.55774381	3.684725207
26.7	2.764310497	2.010052812	3.289276222
28.35	1.76562386	2.095467085	2.181506802
29.85	2.017805941	1.948225034	4.70219042
31.6	1.089290744	2.147773414	0.826916077
33.15	0.521123586	1.992328781	1.833486887
34.85	0.265075353	2.150776422	0.805353633
36.6	0.041112118	2.178104476	0.61022156
38.3	0.031711625	2.319392927	0.722728783
39.85	0.055631688	2.349183762	1.215893716
41.5	0	2.16017304	2.161626133

CRMS 3166

Bottom Depth (cm)	Cs Activity (dpm/g)	Supported ^{210}Pb (dpm/g)	Excess ^{210}Pb (dpm/g)
1.7	0.703106285	1.5565274	62.08941079
3.6	0.835999436	1.273637673	62.06046957
5.5	0.829108226	1.516186821	31.65219749
7.2	0.7621676	1.166625242	57.30037871
9	0.824166716	1.176762097	42.53008286
10.9	0.810725793	0.930597753	44.41522438
12.65	0.803259656	1.077100216	40.57679976
14.55	1.029365514	1.062517904	38.98711459
16.45	0.863278684	1.210715164	79.66437154
18.35	0.542444503	0.70677761	53.09861254
20.25	0.850707518	0.900721958	88.50386555
22.15	0.95947477	0.88257571	75.05482099
23.95	0.677995352	0.882324527	69.89403624
25.7	0.980044022	0.766946984	75.94193558
27.4	1.825836883	0.329213414	48.97240084
29.25	2.985519835	0.757473698	69.40224429
31.15	4.436297621	0.827673512	67.79908293
33.05	5.883789229	0.787360019	71.18407223
34.95	6.948921004	0.878331082	73.22507382
36.55	5.16848013	0.737486755	74.4472825

CRMS 3169

Bottom Depth (cm)	Cs Activity (dpm/g)	Supported ^{210}Pb (dpm/g)	Excess ^{210}Pb (dpm/g)
0.9	0.233075797	1.165518496	13.03121069
2.4	0.392756173	1.813553651	11.33507181
4.05	0.461903369	1.677214727	11.06515169
5.9	0.475270012	2.195739414	9.369164881
7.15	0.420041258	1.79661467	10.37287282
8.85	0.17652799	2.297395525	6.68474296
10.2	0.307276652	2.273360454	5.065840986
11.8	0.145289265	2.203363791	6.180110469
13.4	1.24050135	0.25607205	4.846986307
15.05	0.277389847	2.030968866	6.372890405
16.7	0.313616971	2.296180698	6.336945054
18.35	0.291234052	2.443173947	6.276201457
19.9	0.235787832	2.626992021	6.616904018

21.5	0.23817282	2.244089468	8.670821255
23	0.362926036	1.654372935	13.94906094
24.9	0.449721781	1.193948088	11.74786527
26.5	0.522818342	1.181941487	15.32166388
28.15	0.187210747	0.457663144	7.846165564
29.75	0.148983532	0.602658484	20.16220618
31.5	0.640894109	0.797249989	23.54597329
33	0.520556419	0.91750266	20.21165411
34.65	1.387721273	0.778128213	16.53228336
36.25	3.275204603	0.964501034	16.00742656
38.1	3.646728917	1.023285315	16.64542171
40.05	5.232140006	1.058945234	18.55916262
42.55	4.919870425	1.028702951	16.80033029

CRMS 3565

Bottom Depth (cm)	**Cs Activity (dpm/g)**	**Supported ^{210}Pb (dpm/g)**	**Excess ^{210}Pb (dpm/g)**
1.7	0.379822411	1.210455404	11.77280481
3.6	0.425158919	1.270777067	7.30631127
5.5	0.199997417	1.462349713	5.178165439
6.65	0.500705523	1.122126098	8.43560221
8.15	0.196252963	1.225869071	8.149983494
9.85	0.329686151	1.255818261	9.034566572
11.35	0.644005028	0.681576088	12.1791312
12.85	0.775019475	0.819191654	12.0920489
14.55	0.892985745	0.799426482	11.5046415
16.55	0.983825435	0.993826708	10.72431925
18.75	1.034823336	0.963507663	8.992620713
20.75	1.700127692	1.122645243	9.294685192
22.25	2.561463403	0.839341651	6.386587522
24.25	3.472611821	1.125496789	8.401650282
26	4.37420286	1.130949549	7.691835909
28.1	4.215281061	1.079042729	6.18475846
29.85	6.875289781	0.950964975	7.337711464
31.85	4.983962061	1.004797886	6.210135619
33.95	2.60222296	1.074723802	5.179010995
35.95	1.073224797	1.121441227	5.432063677
37.45	0.425590673	0.895863032	5.058212002
39.35	0.127664131	0.861487652	4.98293187
41.15	0.177856377	0.897976848	4.36337615
43.15	0.220080179	0.78635313	4.408065027

CRMS 3617

Bottom Depth (cm)	Cs Activity (dpm/g)	Supported ^{210}Pb (dpm/g)	Excess ^{210}Pb (dpm/g)
1.8	0.595873393	0.648506221	13.5631946
3.55	0.602153012	0.78922199	12.45351172
5.4	0.745518391	1.011307326	10.59395652
7.15	0.866784977	0.643210238	9.075951889
8.95	1.014415349	0.723487028	9.900316446
10.8	1.77526568	1.123585501	6.531894327
12.85	1.687409942	1.428639788	2.454396512
14.85	2.007866399	1.484464746	1.66021197
16.85	2.938634303	1.438437364	2.379307968
18.75	1.063090443	1.70571446	1.151817248
20.8	0.2735278	1.617295828	1.127890775
22.6	0.117561575	1.715130851	0.763079474
24.45	0.039698249	1.660492164	0.190476137
26.55	0.038054603	1.599426877	0.504661462
28.4	0.055730681	1.729189292	0.262884594
30.35	0.010997206	1.53387389	0.270027066
32.45	0.008371191	1.760384258	0.382342295
34.5	0.01018347	1.875755895	0.228804509
36.8	0.022102597	1.697518174	0.908300672
38.95	0.013523386	1.704537392	0.246845767
41.05	0.004020605	1.584808338	0.715660836

CRMS 3985

Bottom Depth (cm)	Cs Activity (dpm/g)	Supported ^{210}Pb (dpm/g)	Excess ^{210}Pb (dpm/g)
1.9	0	0.743603651	18.74713027
3.9	0.195960649	0.365681646	9.647759179
5.9	0.101779329	0.455538913	12.7319405
7.9	0.112227982	1.1681011	15.77259682
9.9	0.072330022	0.770322121	15.88783897
12.1	0.115706419	0.636422963	15.0859513
14	0.715941128	1.233233917	12.36033293
15.05	0.722704708	1.565371404	9.368235809
17.05	1.095799337	1.646311492	8.368988131
19.05	1.795179771	2.571628959	6.467469457
20.95	3.573040686	2.530410714	6.715603986
22.85	5.343901294	2.690177839	6.822771394
24.55	5.390457989	2.237086061	7.193364376
26.45	8.20107726	1.845239737	6.25504775
28.65	5.38827315	1.562549218	5.102111721
30.35	1.365797816	1.097576729	4.674862291
32.15	0.045412056	0.50419633	5.617622069

34.15	0.995478611	0.92063046	5.878318339

CRMS 4218

Bottom Depth (cm)	Cs Activity (dpm/g)	Supported ^{210}Pb (dpm/g)	Excess ^{210}Pb (dpm/g)
1.65	0.405463818	1.435499366	10.9591726
3.4	0.325538064	1.281316904	8.159641129
5.2	0.310143204	1.834067927	12.87242623
7	0.246985632	1.403880158	9.688694489
8.65	0.316721185	1.669685272	11.09370403
10.5	0.317075623	1.789290561	9.410886474
12.35	0.359835683	1.6731768	10.10780957
14	0.594316814	1.56147908	10.74553308
15.7	0.719666419	1.225871793	12.72545639
17.4	0.677871266	1.34716292	10.54145496
19.05	0.449817578	1.530114232	10.88651313
20.75	0.258103487	1.265395094	10.46232256
22.15	0.439962775	1.498729652	13.7060899
23.8	0.616257904	1.285558387	15.91106489
25.3	0.798025066	1.635466978	16.27173147
26.95	0.767321062	1.286486112	14.87336061
28.65	0.941992307	1.741034386	15.42303521
30.25	1.047393495	1.479708315	12.58340368
31.95	1.937238574	1.997803032	11.70989775
33.6	2.166690257	1.395798924	7.865503707
35.2	2.101634791	1.778339047	6.772392367
36.85	2.07669324	1.47960814	8.593289149
38.5	2.289677962	1.502306521	5.756853883
40.1	2.0911233	1.576469374	5.27590534

CRMS 4245

Bottom Depth (cm)	Cs Activity (dpm/g)	Supported ^{210}Pb (dpm/g)	Excess ^{210}Pb (dpm/g)
2.25	0.131908578	1.031198488	12.06778962
4.5	0.182540553	1.092330587	9.796216894
6.6	0.206583755	1.091635885	9.19909142
8.95	0.198189336	1.171990526	12.21944909
11.25	0.200406925	1.343294746	9.752774653
13.3	0.304880139	1.549262349	7.506658415
15.55	0.250424575	1.54665944	8.510083073
17.85	0.37759476	1.278904851	8.937485686
20	0.505105176	1.392672483	11.191149
22.2	0.479923399	1.435124447	11.29265883
24.75	0.428656685	1.434663152	10.62761155
27.25	0.515949107	1.24258483	12.50408733

29.7	0.296413838	1.198166255	9.840851193
31.85	0.488733553	1.464049618	8.389369661
33.95	0.635303304	1.765137229	8.861212069
36	0.688525355	1.54235096	9.180106503
38	1.008050278	2.228819582	7.590383953
40	1.115153974	1.371847174	8.160427356
42.25	1.277781336	1.536366194	9.34510759
44.3	1.556405372	1.317830212	8.629060548
46.55	2.2695876	1.367542948	7.434148163
48.3	2.857542057	1.118495986	8.367321857
50.35	3.528741437	1.241295564	7.775213664

CRMS 4529

Bottom Depth (cm)	**Cs Activity (dpm/g)**	**Supported ^{210}Pb (dpm/g)**	**Excess ^{210}Pb (dpm/g)**
1.4	0.854976864	2.424627616	150.1447081
3.4	0.41196212	1.426799796	45.08332454
5.4	0.236101935	1.80664137	37.95603382
7.55	0.22189914	1.538224141	23.67611927
9.5	0.171992125	1.508594407	25.66582441
11.5	0.220184008	1.679456411	21.09298423
13.7	0.292699022	1.655948733	26.25328996
15.6	0.437666513	1.315278164	27.0820415
17.5	0.507152466	1.229751003	21.02573649
19.4	0.819456935	1.346052493	28.92099129
21.25	0.863802733	1.278317606	34.05395398
23.4	0.901454051	1.327800237	23.8154554
25.45	1.135838941	1.326008999	31.77059685
27.55	0.565263896	1.706486599	17.01885806
29.55	0.479036942	1.532071063	21.82628603
31.45	3.911774425	1.188698042	25.339926
33.3	3.346361758	1.041867796	51.66661754
35.1	1.012322522	0.65830018	31.37302898
37.05	0.576342504	0.788823874	32.71656871
39.05	0.313544382	1.043760213	35.40412114
41.05	0.043180352	1.432958077	35.58964969
43.15	0.395180312	1.087488667	28.97173064
45.3	0.440136859	0.881618117	37.73945379
47.2	0.534636802	0.857170742	29.03611963
49.7	0.214835885	0.704418603	29.08091774

CRMS 4690

Bottom Depth (cm)	Cs Activity (dpm/g)	Supported ^{210}Pb (dpm/g)	Excess ^{210}Pb (dpm/g)
1.8	0	0.774484427	2.507472907
3.55	0.100051254	1.394105256	7.968881812
5.25	0.051787429	1.644788067	2.783333694
7.15	0.077540778	1.486404858	3.552997789
9.15	0.271153494	1.595785178	0.668478523
11.05	0.173922086	1.41918616	4.46836236
12.95	0.158376412	1.393704128	3.384091364
14.7	0.345868545	1.431965547	2.678103597
16.4	0.236269437	1.270368798	7.105423711
18.1	0.252735842	1.291412492	6.437069498
19.8	0.310443438	1.211250636	5.763240957
21.5	0.420525629	1.210221275	5.093953843
23.5	0.397213824	1.152190823	5.866324769
25.45	0.312469159	1.130033564	5.626719466
27.15	0.40148828	1.194686769	4.879562685
29.15	0.515400096	1.165337096	4.873473889
30.95	0.601338643	1.279585551	3.682752126
33.05	0.783921822	1.005055788	3.993365248
35.35	0.925062385	1.161327963	4.008344218
37.15	0.913646264	1.167404141	3.525686294
39.25	1.017648984	1.226446197	4.160629024
41.25	1.075008814	1.215843674	3.496791277
43.35	2.177640784	1.387119716	2.908300233
45.45	3.230323172	1.433260023	1.518136799

Appendix C: Grain Size Data

CRMS 172

Interval	Mean (φ)	Median (φ)	Sorting	Skewness	Kurtosis
0-2cm	6.35177	6.33659	2.19735	0.0366341	0.75306
2-4cm	9.30473	8.11253	6.36777	4.4989	3.53228
4-6cm	6.25258	6.23	2.21165	0.0455429	0.762565
6-8cm	6.05812	5.87193	2.16334	0.14889	0.767974
8-10cm	6.19549	6.06699	2.21985	0.107586	0.733911
10-12cm	5.99521	5.72978	2.17815	0.197119	0.761452
12-14cm	6.38065	6.34176	2.17897	0.0502259	0.771773
14-16cm	5.30657	4.69905	2.03797	0.456657	0.884548
16-18cm	4.71448	4.08225	1.84117	0.566248	1.27685
18-20cm	6.77626	6.84986	2.09	-0.020572	0.753733
20-22cm	5.98076	5.70433	2.30509	0.196574	0.681609
22-24cm	6.44708	6.43683	2.19032	0.0426817	0.721796
24-26cm	7.47411	7.58748	1.79044	-0.0804515	0.834895
26-28cm	7.3171	7.4209	1.85918	-0.0744847	0.842848

28-30cm	7.06551	7.1633	1.95908	-0.0475184	0.788103
30-32cm	6.72593	6.72836	2.0338	0.0211686	0.790286
32-34cm	6.95537	6.95301	1.92291	0.0207464	0.809002
34-36cm	6.55211	6.56739	2.14528	0.0220123	0.750008
36-38cm	6.11805	5.9752	2.32716	0.118683	0.68748
38-40cm	6.38965	6.43628	2.29525	0.00684878	0.707846
40-42cm	5.57762	5.0861	2.35107	0.310026	0.722105
42-44cm	6.48664	6.58941	2.2556	-0.0199725	0.729652
44-46cm	5.04058	4.03913	2.26094	0.616623	0.749776
Avg	**6.411581304**	**6.21775913**	**2.312275652**	**0.31392033**	**0.904937043**
Std Dev	**0.920089322**	**1.022282505**	**0.898625938**	**0.932461387**	**0.584680677**

CRMS 175

Interval	Mean (φ)	Median (φ)	Sorting	Skewness	Kurtosis
0-2cm	6.4726	6.22557	1.86912	0.186458	0.908629
2-4cm	6.2038	5.89124	1.91787	0.246464	0.879816
4-6cm	5.97919	5.63969	1.93116	0.272561	0.91231
6-8cm	5.42601	4.9566	1.96186	0.385727	0.909674
8-10cm	5.79115	5.52067	1.8921	0.246753	0.962269
10-12cm	6.28977	6.0097	1.96702	0.216348	0.841658
12-14cm	4.72454	4.1375	1.65133	0.616409	1.40006
14-16cm	5.16351	4.51209	1.8606	0.54789	0.990077
16-18cm	5.49767	4.95243	1.91744	0.445151	0.906224
18-20cm	5.8588	5.42403	1.88144	0.3565	0.901287
20-22cm	5.47714	4.96033	1.84136	0.445633	0.98611
22-24cm	5.90685	5.52336	1.88848	0.321878	0.931811
24-26cm	6.06465	5.73423	1.85789	0.276514	0.959969
26-28cm	5.932	5.59224	1.80384	0.305806	0.998534
28-30cm	5.89858	5.58588	1.85089	0.283308	0.962441
30-32cm	6.04351	5.69867	1.87185	0.287153	0.927511
32-34cm	6.19455	5.86398	1.86837	0.26969	0.905614
34-36cm	6.13647	5.79087	1.82346	0.293676	0.959753
36-38cm	6.0014	5.76706	1.67719	0.253416	1.07622
38-40cm	6.23484	5.98428	1.6947	0.248725	1.0267
40-42cm	5.87086	5.59394	1.82343	0.264349	0.925016
42-44cm	5.81881	5.6787	1.55018	0.208102	1.17653
Average	5.863031818	5.501957273	1.836435455	0.317205045	0.974918773

CRMS 192

Interval	Mean (φ)	Median (φ)	Deviation	Skewness	Kurtosis
0-2cm	5.14081	4.78926	2.48826	0.238325	0.790382
2-4cm	3.9807	3.69114	2.58198	0.224728	0.989585
4-6cm	5.23541	4.85737	2.33805	0.271745	0.791104
6-8cm	5.25749	4.94129	2.30344	0.243527	0.87819
8-10cm	5.86397	5.54074	2.1292	0.226315	0.877356
10-12cm	6.03613	5.80522	2.17133	0.170492	0.821787
12-14cm	6.14311	5.95207	2.1931	0.139752	0.804606
14-16cm	6.49894	6.3558	2.07964	0.10723	0.783904

16-18cm	6.6014	6.4511	2.07263	0.113367	0.758579
18-20cm	6.59094	6.41428	2.10298	0.12493	0.751438
20-22cm	6.49665	6.2871	2.08509	0.147995	0.771714
22-24cm	6.66669	6.50531	2.13675	0.112278	0.730888
24-26cm	6.48977	6.29744	2.10003	0.136582	0.790596
26-28cm	6.46238	6.30632	2.17157	0.114793	0.765813
28-30cm	7.40641	7.45536	1.88111	-0.0159676	0.748985
30-32cm	8.21264	8.50896	1.71244	-0.233119	0.861458
32-34cm	8.34823	8.52218	1.56758	-0.150153	0.812099
34-36cm	8.25622	8.42833	1.59888	-0.14011	0.804729
36-38cm	7.55543	7.6845	1.83088	-0.0891875	0.817642
38-40cm	7.45434	7.53621	1.84647	-0.0404608	0.769907
40-42cm	7.75095	7.86442	1.71053	-0.0938683	0.870334
42-44cm	7.56728	7.65882	1.78798	-0.06372	0.818094
Average	6.637085909	6.538782727	2.040450909	0.070248764	0.809508636

CRMS 209

Interval	Mean	Median	Deviation	Skewness	Kurtosis
0-2cm	5.6717	5.58456	1.98736	0.115467	0.897932
2-4cm	5.87075	5.54293	2.04627	0.251766	0.828164
4-6cm	5.66678	5.18761	2.01981	0.354579	0.856457
6-8cm	6.36465	6.18047	1.71862	0.186509	0.983786
8-10cm	5.99834	5.77215	1.81451	0.224012	0.933597
10-12cm	5.83389	5.5345	1.90305	0.270939	0.898511
12-14cm	5.72961	5.41006	1.82933	0.27977	1.05138
14-16cm	5.551	5.15246	1.87987	0.339276	0.939643
16-18cm	5.56764	5.12646	1.85283	0.377278	0.922605
18-20cm	6.2518	5.98695	1.92945	0.215663	0.857426
20-22cm	5.81676	5.60956	1.70227	0.245245	0.954689
22-24cm	5.69399	5.58337	1.27476	0.19223	1.09739
24-26cm	5.8547	5.74112	1.34633	0.192141	1.11785
26-28cm	5.87555	5.74874	1.46758	0.19891	1.109
28-30cm	6.66914	6.51007	1.91897	0.129508	0.837425
30-32cm	6.13437	5.90681	1.66395	0.242494	1.01528
32-34cm	6.57369	6.34688	1.81627	0.191444	0.885013
34-36cm	5.98058	5.60572	1.97217	0.289017	0.872326
36-38cm	6.66607	6.61	1.98741	0.0608019	0.829903
38-40cm	6.28205	6.08154	1.86326	0.175069	0.932759
40-42cm	5.93484	5.71436	1.78797	0.217304	1.01042
42-44cm	6.23186	6.02173	1.95782	0.173011	0.861366
44-46cm	6.32327	6.08983	1.58508	0.254243	0.995818
46-48cm	2.50151	1.64144	2.0804	0.679675	1.38757
Avg	5.876855833	5.612055	1.808555833	0.244014663	0.961512917
Std Dev	0.792394594	0.933133073	0.212629703	0.118220222	0.126676069

CRMS 3054

Interval	Mean (φ)	Median (φ)	Sorting	Skewness	Kurtosis
0-2cm	7.47	7.49	1.67	-0.02	0.9
2-4cm	7.14	7.23	1.88	-0.057	0.87
4-6cm	6.96	6.99	1.96	-0.009	0.81
6-8cm	7.16	7.25	1.91	-0.057	0.84
8-10cm	7.16	7.25	1.93	-0.052	0.8
10-12cm	6.99	7.07	2.01	-0.038	0.75
12-14cm	6.78	6.7	2.05	0.075	0.7
14-16cm	6.59	6.35	2.01	0.17	0.75
16-18cm	6.12	5.91	2.22	0.156	0.77
18-20cm	5.62	5.22	2.29	0.27	0.79
20-22cm	6.41	6.16	2.18	0.177	0.73
22-24cm	6.19	5.92	2.11	0.189	0.81
24-26cm	5.91	5.49	2.16	0.29	0.8
26-28cm	6.88	6.83	1.97	0.049	0.78
28-30cm	6.6	6.4	2.04	0.15	0.75
30-32cm	6.07	5.54	1.95	0.399	0.83
32-34cm	6.72	6.52	1.91	0.17	0.79
34-36cm	5.72	5.08	1.96	0.48	0.91
36-38cm	6.47	6.2	2	0.199	0.8
38-40cm	6.56	6.32	1.99	0.17	0.82
40-42cm	6.55	6.34	1.99	0.16	0.82
42-44cm	6.41	6.18	2	0.17	0.85
44-46cm	6.49	6.24	1.97	0.19	0.83
46-48cm	6.43	6.16	1.996	0.199	0.83
48-50cm	6.55	6.33	1.94	0.17	0.84
Average	6.558	6.3668	2.00384	0.144	0.8068
Std dev	0.459419924	0.639020866	0.122856176	0.136418779	0.049642052

CRMS 3565

Interval	Mean (φ)	Median (φ)	Deviation	Skewness	Kurtosis
0-2cm	7.13127	7.21427	1.95924	-0.0428919	0.765686
2-4cm	5.94305	5.3831	1.7772	0.462899	0.956446
4-6cm	5.7686	5.18542	1.8449	0.469959	0.916147
6-8cm	6.58283	6.37299	1.63519	0.211752	0.987922
8-10cm	6.532	6.27586	1.97265	0.196695	0.77378
10-12cm	6.35664	6.01144	1.98681	0.25401	0.764818
12-14cm	6.7834	6.7767	2.06447	0.0221452	0.740834
14-16cm	7.32846	7.44271	1.85989	-0.0631139	0.785443
16-18cm	7.06718	7.05634	1.89984	0.0129861	0.82815

18-20cm	7.6191	7.67751	1.6914	-0.0561699	0.877951
20-22cm	7.30323	7.25438	1.72203	0.0304448	0.883847
22-24cm	7.61307	7.69099	1.70432	-0.0662838	0.869308
24-26cm					
26-28cm	7.44444	7.52855	1.75656	-0.0620049	0.845087
28-30cm	7.5204	7.59133	1.73131	-0.0574931	0.861869
30-32cm					
32-34cm	7.78812	7.84553	1.49802	-0.0786661	0.964028
34-36cm	7.65302	7.73923	1.66938	-0.0836673	0.914612
36-38cm	7.70198	7.769	1.653	-0.0701809	0.907038
38-40cm					
40-42cm	7.13389	7.14314	1.84052	-0.00481127	0.864935
42-44cm	7.11887	7.10146	1.82672	0.0193853	0.85492
44-46cm	6.86808	6.78398	1.93993	0.0653561	0.824537
46-48cm	6.68964	6.54259	1.79059	0.135509	0.898175
Avg	7.045108095	6.970786667	1.801141429	0.061707544	0.861215857
Std Dev	0.573577861	0.769691612	0.139419152	0.168296802	0.06889669

CRMS 4218

Interval	Median (φ)	Mean (φ)	Sorting	Skewness	Kurtosis
0-2cm	5.46	5.97	1.77	0.43	1.06
2-4cm	5.95	6.36	1.8	0.33	0.91
4-6cm	5.63	6.15	1.8	0.43	0.91
6-8cm	5.29	5.78	1.84	0.39	1.08
8-10cm	5.2	5.75	1.77	0.48	1.09
10-12cm	5.28	5.81	1.83	0.42	1.07
12-14cm	5.25	5.79	1.79	0.45	1.06
14-16cm	5.88	6.26	1.92	0.28	0.89
16-18cm	6.38	6.62	1.9	0.18	0.84
18-20cm	6.8	6.93	1.79	0.11	0.85
20-22cm	6.88	7	1.82	0.097	0.84
22-24cm	6.64	6.82	1.88	0.14	0.82
24-26cm	6.5	6.69	1.94	0.13	0.84
26-28cm	6.746	6.87	1.896	0.098	0.81
28-30cm	6.78	6.899	1.92	0.085	0.82
30-32cm	6.52	6.71	1.93	0.14	0.83
32-34cm	6.85	6.95	1.85	0.085	0.82
34-36cm	6.62	6.8	1.88	0.14	0.81
36-38cm	6.75	6.85	1.94	0.075	0.82
38-40cm	6.63	6.74	1.9	0.086	0.87
40-42cm	6.86	6.93	1.82	0.069	0.85
42-44cm	7.25	7.25	1.85	0.009	0.79
44-46cm	6.23	6.53	1.81	0.23	0.9
46-48cm	6.63	6.79	1.9	0.12	0.84
Average	6.291916667	6.552041667	1.856083333	0.2085	0.8925

Std Dev	0.628910301	0.452514759	0.055883354	0.14949073	0.099269068

Appendix D: Bulk Density, Organic Matter %, and MMPA Data

CRMS 171

Depth (cm)	Bulk Density (g/cm^3)	Organic Matter Fraction	Mineral Mass per Area (kg/m^2year)
1.7	0.316664807	0.14	4.630404022
3.5	0.394949267	0.13	6.184919977
5.5	0.420913874	0.11	7.492284469
7.4	0.46638982	0.12	7.798056026
9.5	0.541234612	0.09	10.34301761
11.35	0.574836791	0.07	9.890090119
13.35	0.748091488	0.05	14.21377151
15.25	0.483866164	0.1	8.274130746
17.35	0.391755685	0.12	7.239661985
19.15	0.397308623	0.12	6.293383301
20.75	0.440074155	0.12	6.196258597
22.55	0.399653154	0.15	6.114707552
24.25	0.382836067	0.15	5.531994098
26.15	0.337401318	0.15	5.44904403
28.05	0.348870009	0.13	5.766834732
29.65	0.396753143	0.14	5.459336011
31.45	0.333838084	0.13	5.227916624
33.45	0.396998052	0.14	6.828382456
35.35	0.486526472	0.16	7.764980648
36.95	0.329881545	0.11	4.697524184
38.75	0.303744595	0.24	4.155235776

CRMS 172

Depth (cm)	Bulk Density (g/cm^3)	Organic Matter Fraction	Mineral Mass per Area (kg/m^2year)
1.5	0.154017745	0.22	1.802011832
3.3	0.214600642	0.21	3.051628265
4.95	0.276936028	0.18	3.746953219
6.6	0.248834601	0.24	3.120393189
8.3	0.287397877	0.17	4.055193529
10.05	0.316172217	0.16	4.647742457
11.7	0.397078595	0.15	5.569040314
13.25	0.619763943	0.09	8.74179086
14.8	0.410313912	0.1	5.723892459

16.5	0.354446072	0.11	5.362781612
18.15	0.276377643	0.17	3.785000669
19.85	0.326879251	0.17	4.612277021
21.5	0.341637909	0.17	4.678742111
23.25	0.320709264	0.19	4.546064446
25	0.28402485	0.17	4.125470591
26.7	0.316726609	0.15	4.576710207
28.45	0.323706923	0.16	4.758502893
30.15	0.307190011	0.16	4.386683619
31.75	0.381782313	0.15	5.192251599
33.55	0.329866338	0.15	5.046966776
35.3	0.402057166	0.13	6.12133467
36.95	0.422437322	0.13	6.064101935
39.45	0.452754133	0.13	9.847425425

CRMS 173

Depth (cm)	**Bulk Density (g/cm^3)**	**Organic Matter Fraction**	**Mineral Mass per Area (kg/m^2year)**
1.65	0.050447821	0.31	0.574349785
3.25	0.150589192	0.3	1.686602895
4.95	0.170760279	0.27	2.119140022
6.7	0.223488733	0.23	3.011517717
8.3	0.227624319	0.23	2.804338162
10	0.221779675	0.26	2.789994832
11.7	0.212643011	0.25	2.711204736
13.45	0.255525169	0.23	3.4432097
15.3	0.209980711	0.25	2.913489173
17	0.148058604	0.38	1.560541334
18.85	0.136598051	0.39	1.541512612
20.65	0.187848032	0.31	2.333078014
22.25	0.167836356	0.35	1.745502181
23.9	0.176948376	0.37	1.839382665
25.6	0.1621775	0.34	1.819635803
27.4	0.173718257	0.32	2.126316439
29.3	0.141643002	0.44	1.507085068
31.05	0.140112902	0.45	1.348589834

CRMS 175

Depth (cm)	**Bulk Density (g/cm^3)**	**Organic Matter Fraction**	**Mineral Mass per Area (kg/m^2year)**
1.7	0.260961825	0.21	3.504725504
3.35	0.34921099	0.19	4.667215793
5.2	0.312756338	0.19	4.68666468

7	0.337993503	0.18	4.988795763
8.6	0.361575439	0.17	4.801733057
10.35	0.397915904	0.18	5.710106575
12.1	0.675203759	0.07	10.98896687
13.8	0.485790532	0.13	7.184858776
15.6	0.457207163	0.12	7.242178402
17.35	0.399297839	0.16	5.869691964
18.9	0.592197315	0.09	8.352962656
20.5	0.431424833	0.14	5.936419582
22.25	0.354119527	0.15	5.267540279
23.9	0.409604175	0.16	5.677127142
25.75	0.338777927	0.15	5.327295366
27.45	0.332072855	0.18	4.62910642
29.15	0.408435155	0.15	5.901901786
30.9	0.401112407	0.15	5.966561003
32.6	0.376398971	0.18	5.24701393
34.35	0.416452104	0.15	6.194739539
35.95	0.434026054	0.16	5.83332381
38.05	0.456599791	0.07	8.917414763

CRMS 189

Depth (cm)	**Bulk Density (g/cm^3)**	**Organic Matter Fraction**	**Mineral Mass per Area (kg/m^2year)**
2.2	0.051070014	0.21	0.887598914
4	0.045351723	0.87	0.10612328
6	0.054744101	0.93	0.076641921
7.7	0.054807207	0.94	0.055903482
9.2	0.053359712	0.93	0.056027828
11.1	0.041572772	0.93	0.055291916
13.3	0.057613971	0.92	0.101400825
15.3	0.057385409	0.94	0.068862651
17.4	0.057321265	0.93	0.084262457
19.3	0.060044226	0.95	0.057042148
21.4	0.045665568	0.96	0.038359167
23.3	0.072921913	0.94	0.083131175
25.4	0.070528419	0.94	0.088866016
27.5	0.061898439	0.92	0.103989621
29.3	0.079003232	0.91	0.127985535
31.1	0.074464564	0.88	0.160843834
33	0.086099526	0.88	0.196307378
35	0.069088371	0.88	0.165812478
36.6	0.107810337	0.66	0.586489605
38.3	0.096054531	0.52	0.783806806

CRMS 192

Depth (cm)	Bulk Density (g/cm^3)	Organic Matter Fraction	Mineral Mass per Area (kg/m^2year)
1.8	0.013406003	0.53	0.113415053
3.65	0.16273271	0.34	1.986971031
5.45	0.260210842	0.28	3.372340396
7.35	0.229089783	0.29	3.090428405
9.05	0.295323591	0.29	3.564564081
11.05	0.236940773	0.33	3.17501378
13.05	0.261317488	0.32	3.553926147
15.15	0.283816599	0.29	4.231715393
17.25	0.275564535	0.28	4.166545519
19.25	0.278093648	0.31	3.837701323
21.35	0.256243129	0.32	3.659160435
22.95	0.28614321	0.34	3.021679368
24.75	0.304998249	0.35	3.56848786
26.55	0.468026045	0.19	6.823835695
28.3	0.470109221	0.2	6.581544486
30.05	0.513512298	0.15	7.638513294
32.25	0.307575675	0.14	5.819345379
34.05	0.453444864	0.18	6.692861843
35.95	0.43726323	0.18	6.812577062
37.95	0.427385642	0.18	7.009140924
39.95	0.484177704	0.17	8.037368684
42.75	0.436918938	0.16	10.27635745

CRMS 209

Depth (cm)	Bulk Density (g/cm^3)	Organic Matter Fraction	Mineral Mass per Area (kg/m^2year)
1.9	0.123464872	0.35	1.524794737
3.75	0.236025904	0.24	3.318531973
5.7	0.388257892	0.12	6.662521015
7.45	0.245972777	0.28	3.099264239
9.35	0.355325189	0.18	5.535979395
11.3	0.311250854	0.25	4.552054381
13.15	0.271942165	0.3	3.521659271
15.05	0.203248139	0.34	2.548737625
16.9	0.227739339	0.23	3.244154471
18.8	0.212289785	0.3	2.823460737

20.65	0.225377737	0.34	2.751868609
22.35	0.194544787	0.35	2.14972492
24.1	0.188268883	0.38	2.042722161
25.95	0.175484378	0.43	1.850487097
27.65	0.155256574	0.4	1.583620759
29.45	0.157738384	0.38	1.76036448
31.25	0.148751958	0.42	1.552974071
33.05	0.19690732	0.34	2.339264438
35.05	0.176280342	0.35	2.291649806
36.9	0.15438438	0.44	1.599425913
38.9	0.125341213	0.47	1.328619967
40.85	0.143537936	0.43	1.595427891
42.9	0.286151842	0.21	4.634239925
45.55	0.204787794	0.31	3.744553566

CRMS 211

Depth (cm)	**Bulk Density (g/cm^3)**	**Organic Matter Fraction**	**Mineral Mass per Area (kg/m^2year)**
1.55	0.103237698	0.28	1.152135403
3.15	0.09073767	0.32	0.987228154
4.8	0.088455217	0.3	1.021660141
6.5	0.103548194	0.33	1.179416684
8.15	0.138322029	0.36	1.46068404
9.9	0.078757676	0.4	0.826957531
11.55	0.124553549	0.39	1.253634402
13.15	0.075617625	0.52	0.580744718
14.85	0.119890274	0.49	1.039451105
16.6	0.109685052	0.51	0.940551523
18.3	0.102314672	0.52	0.834889677
19.7	0.140185247	0.51	0.961673042
21.3	0.138108388	0.48	1.149064477
23.05	0.153997374	0.37	1.697825022
24.95	0.115868882	0.47	1.166802366
26.9	0.119681014	0.44	1.306919727
28.9	0.098915295	0.57	0.850673523
30.8	0.124132725	0.52	1.132093096

CRMS 224

Depth (cm)	**Bulk Density (g/cm^3)**	**Organic Matter Fraction**	**Mineral Mass per Area (kg/m^2year)**
2	0.185518971	0.24	2.819894948
3.85	0.360960506	0.21	5.275450126
5.8	0.49693753	0.11	8.624370998

7.85	0.57792212	0.09	10.78116235
9.9	0.280060325	0.24	4.363350062
12	0.309547222	0.2	5.20040549
13.95	0.256456745	0.28	3.600661123
15.95	0.234820747	0.28	3.381426667
17.95	0.202778704	0.3	2.838908498
19.9	0.18905614	0.35	2.396292182
22.05	0.210085704	0.33	3.026291641
24	0.194636797	0.37	2.391118647
25.9	0.221697232	0.28	3.032825229
27.9	0.238434177	0.27	3.481147126
29.85	0.65886928	0.11	11.43470309
31.95	0.76631523	0.05	15.28802459
33.7	0.232781496	0.37	2.566421995
35.7	0.14609261	0.42	1.694678235
37.7	0.251986669	0.33	3.376629256
39.45	0.33170503	0.25	4.353638704
41.2	0.196480936	0.45	1.891133431
43.7	0.148062046	0.54	1.702717512

CRMS 225

Depth (cm)	**Bulk Density (g/cm^3)**	**Organic Matter Fraction**	**Mineral Mass per Area (kg/m^2year)**
1.9	0.185984685	0.38	2.190904715
3.8	0.270603394	0.24	3.907522151
5.7	0.283773389	0.26	3.989863179
7.6	0.273249498	0.3	3.634226828
9.45	0.235713517	0.32	2.965282977
11.45	0.205268813	0.35	2.668500814
13.2	0.188901454	0.37	2.082643402
15.2	0.187988646	0.37	2.368662474
17	0.159092976	0.36	1.832755375
18.6	0.171666555	0.36	1.757869636
20.45	0.121195978	0.47	1.188329341
22.1	0.13590845	0.37	1.412771646
24.2	0.174724028	0.37	2.31160429
25.95	0.186106771	0.39	1.986694428
27.95	0.162733201	0.37	2.050443133
29.95	0.129255153	0.48	1.344256737
32.05	0.11278952	0.61	0.923748329
33.8	0.106462445	0.57	0.801131773
35.7	0.130166903	0.48	1.286052008
38.45	0.106732305	0.6	1.174058101

CRMS 237

Depth (cm)	Bulk Density (g/cm^3)	Organic Matter Fraction	Mineral Mass per Area (kg/m^2year)
2	0.194491051	0.22	3.034067497
3.7	0.365728212	0.13	5.409132902
5.3	0.395167886	0.15	5.374295814
6.3	0.640602838	0.18	5.252955556
8.3	0.317208366	0.17	5.265671185
10	0.275261095	0.27	3.415998172
12.2	0.178631645	0.36	2.51513945
14.3	0.168806682	0.33	2.375115566
16.2	0.170760133	0.38	2.011559067
18.3	0.177215729	0.31	2.567861925
20.6	0.160532599	0.32	2.510735712
22.35	0.154441138	0.31	1.864881104
24.25	0.35679597	0.13	5.897851178
26.05	0.532419137	0.13	8.337703178
28.35	0.17241744	0.33	2.656958967
30.15	0.166766542	0.38	1.861118958
32.15	0.133741822	0.45	1.471163487
34.05	0.150989514	0.4	1.72128449
36.25	0.147078506	0.42	1.87672612
38.4	0.228420265	0.31	3.388622562
40.5	0.348477179	0.19	5.927610671
42.2	0.20011199	0.36	2.177223541
43.8	0.161307179	0.46	1.393697282

CRMS 253

Depth (cm)	Bulk Density (g/cm^3)	Organic Matter Fraction	Mineral Mass per Area (kg/m^2year)
1.85	0.129124563	0.31	1.648278905
4.05	0.283919804	0.18	5.121925237
6.05	0.303000241	0.21	4.787415004
7.95	0.262453758	0.25	3.739974802
9.65	0.267172105	0.24	3.451871673
11.75	0.299655636	0.23	4.845442963
13.95	0.232350126	0.21	4.03825463
15.65	0.23111016	0.27	2.868083788
17.4	0.179314698	0.33	2.102469751
19.25	0.215528247	0.29	2.830970141
21.55	0.244847598	0.25	4.223630943
23.15	0.204828443	0.31	2.261311298

24.85	0.189931598	0.32	2.195614408
26.95	0.200076093	0.26	3.109189761
29.15	0.177075107	0.26	2.882789489
31.15	0.190501487	0.26	2.819428599
32.85	0.186467034	0.25	2.377460247
34.55	0.181612935	0.24	2.346444601
36.55	0.186309739	0.28	2.682866518
38.55	0.203144655	0.26	3.006547926
40.95	0.163201611	0.25	2.937635873

CRMS 261

Depth (cm)	**Bulk Density (g/cm^3)**	**Organic Matter Fraction**	**Mineral Mass per Area (kg/m^2year)**
1.85	0.095526705	0.38	1.095693863
3.75	0.158190863	0.34	1.983718065
5.6	0.212252892	0.37	2.47381324
7.4	0.238831964	0.36	2.751350662
9.15	0.283643812	0.31	3.425007033
11	0.222221933	0.39	2.507780376
12.8	0.264637696	0.34	3.143903175
14.55	0.320299094	0.36	3.587358243
16.45	0.173561483	0.4	1.978605538
18.1	0.168051361	0.4	1.663712367
19.95	0.154393082	0.44	1.599516073
21.75	0.149696618	0.46	1.455054534
23.6	0.197680293	0.38	2.267398266
25.25	0.237474777	0.33	2.625289795
27.1	0.214556443	0.35	2.580047266
28.75	0.269713265	0.34	2.937184326
30.6	0.247816932	0.32	3.117544296
32.4	0.258766037	0.31	3.21388169
34.2	0.31463382	0.24	4.304200727
35.9	0.295822084	0.25	3.771740395
37.65	0.295750384	0.24	3.933489303
39.4	0.273593662	0.25	3.590925217
41.1	0.261740961	0.28	3.203716859
42.85	0.254051438	0.27	3.245514707
44.5	0.253134154	0.28	3.007240786
46.2	0.294175324	0.24	3.800754075
47.5	0.30837344	0.24	3.046736717

CRMS 273

Depth (cm)	Bulk Density (g/cm^3)	Organic Matter Fraction	Mineral Mass per Area (kg/m^2year)
2	0.047534742	0.76	0.228167297
3.9	0.060846873	0.71	0.335267053
5.8	0.077816358	0.7	0.443554281
7.7	0.083361809	0.62	0.601873671
9.5	0.086726636	0.64	0.561989913
11	0.071324175	0.8	0.213973026
12.7	0.076082388	0.75	0.323350904
14.6	0.049161378	0.82	0.168132307
16.7	0.066979383	0.85	0.210985551
18.5	0.075049339	0.83	0.229651515
20.5	0.060079012	0.88	0.144189965
22.2	0.071763564	0.84	0.19519735
24	0.055277278	0.87	0.129349132
25.8	0.071417965	0.79	0.26996054
27.3	0.086994197	0.82	0.234884881
29.5	0.077921281	0.8	0.342854438
31.2	0.076961458	0.83	0.222419134
33.2	0.087045918	0.8	0.348184486
35.3	0.083787733	0.83	0.299122907
37.6	0.069036374	0.84	0.25405445

CRMS 3054

Depth (cm)	Bulk Density (g/cm^3)	Organic Matter Fraction	Mineral Mass per Area (kg/m^2year)
1.4	0.078	0.40	0.657866895
3	0.131	0.37	1.321721501
4.7	0.152	0.44	1.448548123
6.45	0.132	0.41	1.366975166
8.1	0.126	0.44	1.167578964
9.7	0.175	0.40	1.684118116
11.3	0.292	0.41	2.760446187
12.9	0.120	0.50	0.95749948
14.6	0.123	0.51	1.022984565
16.25	0.112	0.56	0.811259051
18.05	0.100	0.62	0.682244893
19.75	0.124	0.60	0.843737989
21.4	0.191	0.44	1.768580038
23.05	0.181	0.45	1.643303307
24.9	0.172	0.40	1.912054345
26.7	0.329	0.24	4.502409876

28.35	0.364	0.24	4.567043698
29.85	0.264	0.32	2.696071927
31.6	0.434	0.18	6.223581519
33.15	0.431	0.21	5.280032397
34.85	0.529	0.17	7.463522774
36.6	0.570	0.16	8.384332038
38.3	0.546	0.16	7.79132876
39.85	0.553	0.15	7.286531887
41.5	0.425	0.17	5.822230727

CRMS 3166

Depth (cm)	**Bulk Density (g/cm^3)**	**Organic Matter Fraction**	**Mineral Mass per Area (kg/m^2year)**
1.7	0.087932007	0.36	0.956702468
3.6	0.130971974	0.38	1.542853457
5.5	0.121689995	0.44	1.294784574
7.2	0.173366422	0.42	1.709396922
9	0.114371165	0.43	1.173450902
10.9	0.110122616	0.45	1.150784028
12.65	0.086947425	0.61	0.593417561
14.55	0.113394398	0.63	0.797164483
16.45	0.059296362	0.78	0.247859371
18.35	0.056638894	0.84	0.17218264
20.25	0.068378225	0.8	0.259837863
22.15	0.053592549	0.79	0.213834771
23.95	0.076686127	0.8	0.276070702
25.7	0.077692766	0.74	0.35350291
27.4	0.076405317	0.84	0.207822948
29.25	0.057765439	0.79	0.224419257
31.15	0.056430827	0.79	0.225159527
33.05	0.072599602	0.83	0.234497263
34.95	0.07601036	0.83	0.245514037
36.55	0.070688327	0.82	0.203582858

CRMS 3169

Depth (cm)	**Bulk Density (g/cm^3)**	**Organic Matter Fraction**	**Mineral Mass per Area (kg/m^2year)**
0.9	0.098861672	0.43	0.507161562
2.4	0.218779376	0.3	2.297188816
4.05	0.408905928	0.18	5.53251015

5.9	0.390917013	0.21	5.713265511
7.15	0.504115571	0.17	5.230211285
8.85	0.535011698	0.14	7.82188932
10.2	0.538909371	0.13	6.329505369
11.8	0.508358569	0.12	7.157705383
13.4	0.600980679	0.11	8.557984881
15.05	0.500468309	0.11	7.349394308
16.7	0.479903588	0.13	6.889032109
18.35	0.455154141	0.14	6.458652364
19.9	0.381266628	0.18	4.845910177
21.5	0.16905502	0.26	2.001616116
23	0.113381204	0.62	0.646274372
24.9	0.101244038	0.71	0.557855952
26.5	0.09016681	0.62	0.548215484
28.15	0.060952668	0.71	0.291659197
29.75	0.099248089	0.83	0.269955434
31.5	0.102848852	0.88	0.215983095
33	0.109868555	0.82	0.296645792
34.65	0.107836212	0.77	0.409239382
36.25	0.110497086	0.71	0.512707676
38.1	0.11023018	0.7	0.611778931
40.05	0.114611804	0.68	0.715179329
42.55	0.090422529	0.69	0.70077624

CRMS 3565

Depth (cm)	**Bulk Density (g/cm^3)**	**Organic Matter Fraction**	**Mineral Mass per Area (kg/m^2year)**
1.7	0.139045093	0.36	1.512814154
3.6	0.319369059	0.19	4.915101306
5.5	0.377758231	0.15	6.100809693
6.65	0.237919964	0.31	1.887899326
8.15	0.185360972	0.39	1.696056863
9.85	0.145437078	0.42	1.434012943
11.35	0.129989598	0.53	0.916428811
12.85	0.126446951	0.46	1.024222697
14.55	0.138521445	0.45	1.295178543
16.55	0.141354345	0.39	1.724527037
18.75	0.127602089	0.37	1.768569088
20.75	0.136962761	0.37	1.725734825
22.25	0.173885409	0.37	1.643220954
24.25	0.145186497	0.39	1.771279405
26	0.137038794	0.36	1.534838078
28.1	0.142046685	0.36	1.909111908

29.85	0.143274075	0.37	1.579600376
31.85	0.156391734	0.35	2.033097298
33.95	0.144449025	0.39	1.850396338
35.95	0.136477801	0.52	1.310189952
37.45	0.170491457	0.52	1.227541363
39.35	0.137186871	0.59	1.068688226
41.15	0.121043577	0.55	0.980455266
43.15	0.100080196	0.63	0.740595184

CRMS 3617

Depth (cm)	**Bulk Density (g/cm^3)**	**Organic Matter Fraction**	**Mineral Mass per Area (kg/m^2year)**
1.8	0.108211084	0.55	0.876511828
3.55	0.09429242	0.6	0.66004848
5.4	0.087681301	0.56	0.713727459
7.15	0.114844301	0.5	1.004889987
8.95	0.097869238	0.55	0.792742678
10.8	0.163326244	0.35	1.964002682
12.85	0.362235458	0.17	6.163450736
14.85	0.256280332	0.22	3.997982527
16.85	0.26799007	0.23	4.127056727
18.75	0.658819829	0.08	11.51619754
20.8	0.798509908	0.07	15.22362699
22.6	0.682196324	0.09	11.17440192
24.45	0.774387209	0.09	13.03683915
26.55	0.869429189	0.07	16.97999177
28.4	0.818820255	0.08	13.93635333
30.35	0.93118463	0.07	16.88707276
32.45	0.645940076	0.1	12.20829599
34.5	0.686312828	0.09	12.80319574
36.8	0.524368787	0.12	10.61324907
38.95	0.520990743	0.09	10.19320773
41.05	0.314401401	0.19	5.347980343

CRMS 3985

Depth (cm)	**Bulk Density (g/cm^3)**	**Organic Matter Fraction**	**Mineral Mass per Area (kg/m^2year)**
1.9	0.030685771	0.69	0.180739613
3.9	0.059640982	0.69	0.369774955
5.9	0.110483885	0.58	0.928066807
7.9	0.112573328	0.61	0.878074011
9.9	0.114370672	0.65	0.800596576
12.1	0.076766001	0.8	0.337771194
14	0.107632385	0.62	0.77710764

15.05	0.198080911	0.54	0.956733037
17.05	0.131872353	0.5	1.318726613
19.05	0.19142325	0.36	2.450223324
20.95	0.171234651	0.38	2.017148905
22.85	0.176827199	0.37	2.116626516
24.55	0.180256849	0.61	1.195105702
26.45	0.146994895	0.61	1.089234722
28.65	0.112472194	0.74	0.643342455
30.35	0.091599798	0.87	0.202436028
32.15	0.090964616	0.86	0.22923137
34.15	0.12287723	0.82	0.442359062

CRMS 4218

Depth (cm)	**Bulk Density (g/cm^3)**	**Organic Matter Fraction**	**Mineral Mass per Area (kg/m^2year)**
1.65	0.034	0.28	0.407370899
3.4	0.076	0.28	0.955254525
5.2	0.082	0.32	1.005097686
7	0.075	0.37	0.85298109
8.65	0.128	0.38	1.30608604
10.5	0.165	0.26	2.264193695
12.35	0.134	0.31	1.710535165
14	0.149	0.38	1.519216806
15.7	0.158	0.34	1.774972293
17.4	0.169	0.34	1.892974863
19.05	0.144	0.41	1.400052229
20.75	0.113	0.44	1.071658224
22.15	0.126	0.38	1.096840825
23.8	0.134	0.41	1.303098175
25.3	0.107	0.42	0.928310794
26.95	0.131	0.47	1.14706897
28.65	0.112	0.50	0.952117053
30.25	0.129	0.45	1.133264792
31.95	0.141	0.37	1.50771931
33.6	0.191	0.29	2.236684441
35.2	0.201	0.34	2.12688777
36.85	0.173	0.35	1.855894368
38.5	0.198	0.34	2.156239883
40.1	0.209	0.37	2.102355669

CRMS 4245

Depth (cm)	**Bulk Density (g/cm^3)**	**Organic Matter Fraction**	**Mineral Mass per Area (kg/m^2year)**

2.25	0.057	0.46	0.696734331
4.5	0.158	0.34	2.33951926
6.6	0.173	0.29	2.579275584
8.95	0.086	0.39	1.234864444
11.25	0.139	0.34	2.115386772
13.3	0.244	0.28	3.59420083
15.55	0.167	0.34	2.482875559
17.85	0.198	0.36	2.907717083
20	0.174	0.42	2.165856187
22.2	0.157	0.34	2.283233123
24.75	0.119	0.42	1.754855022
27.25	0.143	0.43	2.043050681
29.7	0.139	0.39	2.084777018
31.85	0.182	0.35	2.538023269
33.95	0.209	0.30	3.069189037
36	0.225	0.28	3.327618228
38	0.207	0.29	2.935052403
40	0.182	0.35	2.362298701
42.25	0.188	0.36	2.713110372
44.3	0.182	0.41	2.196418064
46.55	0.170	0.43	2.178481849
48.3	0.169	0.41	1.743798311
50.35	0.136	0.43	1.58902488

CRMS 4529

Depth (cm)	**Bulk Density (g/cm^3)**	**Organic Matter Fraction**	**Mineral Mass per Area (kg/m^2year)**
1.4	0.012	0.36	0.103611436
3.4	0.111	0.31	1.53453108
5.4	0.226	0.20	3.61041556
7.55	0.245	0.17	4.36505851
9.5	0.301	0.13	5.108874243
11.5	0.404	0.09	7.347575341
13.7	0.359	0.10	7.10542639
15.6	0.316	0.11	5.341649239
17.5	0.254	0.19	3.904999242
19.4	0.256	0.16	4.078509619
21.25	0.286	0.17	4.390846015
23.4	0.233	0.23	3.849510869
25.45	0.316	0.14	5.569583273
27.55	0.636	0.06	12.55809803
29.55	0.667	0.05	12.66572837
31.45	0.251	0.20	3.81979145
33.3	0.146	0.37	1.697307195

35.1	0.177	0.47	1.683949728
37.05	0.143	0.49	1.425395521
39.05	0.151	0.44	1.694077018
41.05	0.157	0.40	1.884869484
43.15	0.165	0.41	2.045297029
45.3	0.135	0.57	1.249164476
47.2	0.145	0.44	1.54645622
49.7	0.131	0.54	1.504018669

CRMS 4690

Depth (cm)	**Bulk Density (g/cm^3)**	**Organic Matter Fraction**	**Mineral Mass per Area (kg/m^2year)**
1.8	0.110913925	0.3	1.397518727
3.55	0.456980502	0.09	7.277431507
5.25	0.308233109	0.19	4.244379832
7.15	0.173550641	0.06	3.099621693
9.15	0.152344375	0.1	2.742205164
11.05	0.218134168	0.2	3.315647113
12.95	0.161763184	0.1	2.766156915
14.7	0.291454637	0.22	3.9783651
16.4	0.235830534	0.26	2.966755051
18.1	0.247729393	0.23	3.242785341
19.8	0.234019233	0.25	2.983752197
21.5	0.195926478	0.3	2.331530538
23.5	0.213330388	0.28	3.071964764
25.45	0.202125376	0.28	2.837846913
27.15	0.246801552	0.26	3.104770784
29.15	0.228881947	0.25	3.433237237
30.95	0.250973823	0.26	3.342979134
33.05	0.211887615	0.24	3.381734249
35.35	0.224448633	0.23	3.974994589
37.15	0.257462361	0.21	3.66112333
39.25	0.21806219	0.22	3.571867028
41.25	0.312927504	0.17	5.194608711
43.35	0.227648022	0.19	3.872301918
45.45	0.180161276	0.31	2.610542999

Appendix E: Hurricane Path Map

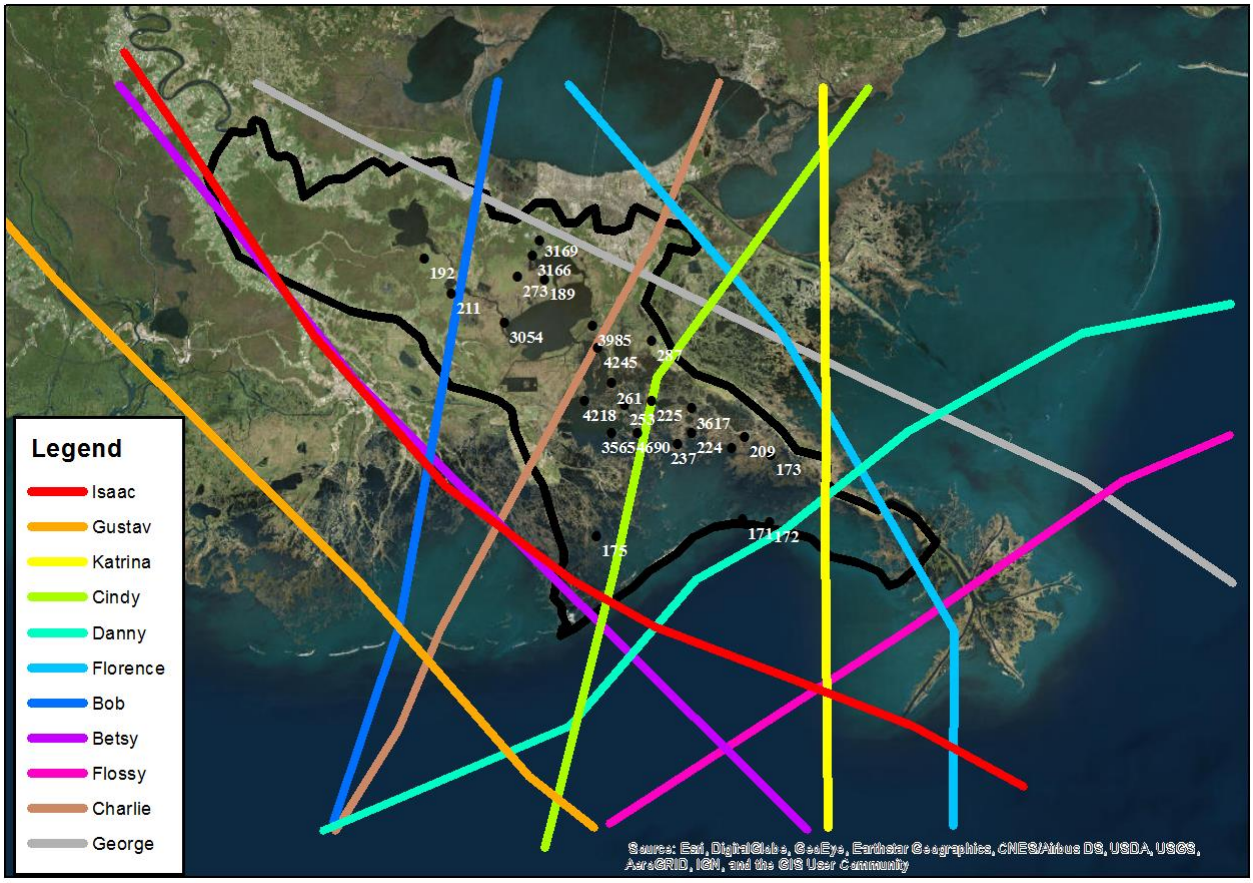

Appendix F: T-Test Results

Fresh to Intermediate VAR

t-Test: Two-Sample Assuming Unequal Variances		
	Fresh	Intermediate
Mean	0.646518422	0.815320914
Variance	0.013825022	0.039110713
Observations	7	4
Hypothesized Mean Difference	0.16	
df	4	
t Stat	-3.032959556	
P(T<=t) one-tail	0.019334066	
t Critical one-tail	2.131846786	
P(T<=t) two-tail	0.038668131	
t Critical two-tail	2.776445105	

Fresh to Brackish VAR

t-Test: Two-Sample Assuming Unequal Variances		
	Fresh	Brackish
Mean	0.646518422	0.619332792
Variance	0.013825022	0.01541654
Observations	7	5
Hypothesized Mean Difference	0.005	
df	8	
t Stat	0.311938502	
P(T<=t) one-tail	0.381531139	
t Critical one-tail	1.859548038	
P(T<=t) two-tail	0.763062277	
t Critical two-tail	2.306004135	

Fresh to Saline VAR

t-Test: Two-Sample Assuming Unequal Variances		
	Fresh	Saline
Mean	0.646518422	0.637156534
Variance	0.013825022	0.009065209
Observations	7	8
Hypothesized Mean Difference	0.02	
df	12	
t Stat	-0.190815333	
P(T<=t) one-tail	0.425930248	
t Critical one-tail	1.782287556	
P(T<=t) two-tail	0.851860496	
t Critical two-tail	2.17881283	

Intermediate to Brackish VAR

t-Test: Two-Sample Assuming Unequal Variances		
	Intermediate	Brackish
Mean	0.815320914	0.619332792
Variance	0.039110713	0.01541654

Observations	4	5
Hypothesized Mean Difference	0.2	
df	5	
t Stat	-0.035376158	
P(T<=t) one-tail	0.486574334	
t Critical one-tail	2.015048373	
P(T<=t) two-tail	0.973148668	
t Critical two-tail	2.570581836	

Intermediate to Saline VAR

t-Test: Two-Sample Assuming Unequal Variances		
	Intermediate	Saline
Mean	0.815320914	0.637156534
Variance	0.039110713	0.009065209
Observations	4	8
Hypothesized Mean Difference	0.18	
df	4	
t Stat	-0.017573324	
P(T<=t) one-tail	0.493410428	
t Critical one-tail	2.131846786	
P(T<=t) two-tail	0.986820855	
t Critical two-tail	2.776445105	
t-Test: Two-Sample Assuming Unequal Variances		

Brackish to Saline VAR

t-Test: Two-Sample Assuming Unequal Variances		
	Brackish	Saline
Mean	0.619332792	0.637156534
Variance	0.01541654	0.009065209
Observations	5	8
Hypothesized Mean Difference	0.02	
df	7	
t Stat	-0.58249276	
P(T<=t) one-tail	0.289253127	
t Critical one-tail	1.894578605	

P(T<=t) two-tail	0.578506254	
t Critical two-tail	2.364624252	

N-S of Lake Salvador MAR comparison

t-Test: Two-Sample Assuming Unequal Variances		
	N of Lake Salvador	S of Lake Salvador
Mean	0.946376396	1.881333333
Variance	0.214006702	0.53548381
Observations	8	15
Hypothesized Mean Difference	0.37	
df	20	
t Stat	-5.221927036	
P(T<=t) one-tail	2.06769E-05	
t Critical one-tail	1.724718243	
P(T<=t) two-tail	4.13538E-05	
t Critical two-tail	2.085963447	

Fresh to Intermediate MMA

t-Test: Two-Sample Assuming Unequal Variances		
	Fresh	Intermediate
Mean	1.017142857	0.8575
Variance	1.448090476	0.073825
Observations	7	4
Hypothesized Mean Difference	0.16	
df	7	
t Stat	-0.000752378	
P(T<=t) one-tail	0.499710341	
t Critical one-tail	1.894578605	
P(T<=t) two-tail	0.999420682	
t Critical two-tail	2.364624252	

Fresh to Brackish MMA

t-Test: Two-Sample Assuming Unequal Variances		

	Fresh	Brackish
Mean	1.017142857	1.144
Variance	1.448090476	0.07333
Observations	7	5
Hypothesized Mean Difference	0.12	
df	7	
t Stat	-0.524473412	
P(T<=t) one-tail	0.30807128	
t Critical one-tail	1.894578605	
P(T<=t) two-tail	0.616142561	
t Critical two-tail	2.364624252	

Fresh to Saline MMA

t-Test: Two-Sample Assuming Unequal Variances		
	Fresh	Saline
Mean	1.017142857	1.715
Variance	1.448090476	0.506857143
Observations	7	8
Hypothesized Mean Difference	0.7	
df	9	
t Stat	-2.689046118	
P(T<=t) one-tail	0.012417646	
t Critical one-tail	1.833112933	
P(T<=t) two-tail	0.024835291	
t Critical two-tail	2.262157163	

Intermediate to Brackish MMA

t-Test: Two-Sample Assuming Unequal Variances		
	Intermediate	Brackish
Mean	0.8575	1.144
Variance	0.073825	0.07333
Observations	4	5
Hypothesized Mean Difference	0.28	
df	7	
t Stat	-3.112719589	
P(T<=t) one-tail	0.008508134	

t Critical one-tail	1.894578605	
P(T<=t) two-tail	0.017016268	
t Critical two-tail	2.364624252	

Intermediate to Saline

t-Test: Two-Sample Assuming Unequal Variances		
	Intermediate	Saline
Mean	0.8575	1.715
Variance	0.073825	0.506857143
Observations	4	8
Hypothesized Mean Difference	0.86	
df	10	
t Stat	-6.004606388	
P(T<=t) one-tail	6.565E-05	
t Critical one-tail	1.812461123	
P(T<=t) two-tail	0.0001313	
t Critical two-tail	2.228138852	

Brackish to Saline MMA

t-Test: Two-Sample Assuming Unequal Variances		
	Variable 1	Variable 2
Mean	1.144	1.715
Variance	0.07333	0.506857143
Observations	5	8
Hypothesized Mean Difference	0.58	
df	10	
t Stat	-4.120629843	
P(T<=t) one-tail	0.001037502	
t Critical one-tail	1.812461123	
P(T<=t) two-tail	0.002075003	
t Critical two-tail	2.228138852	

Appendix G: ^{210}Pb CRS Results

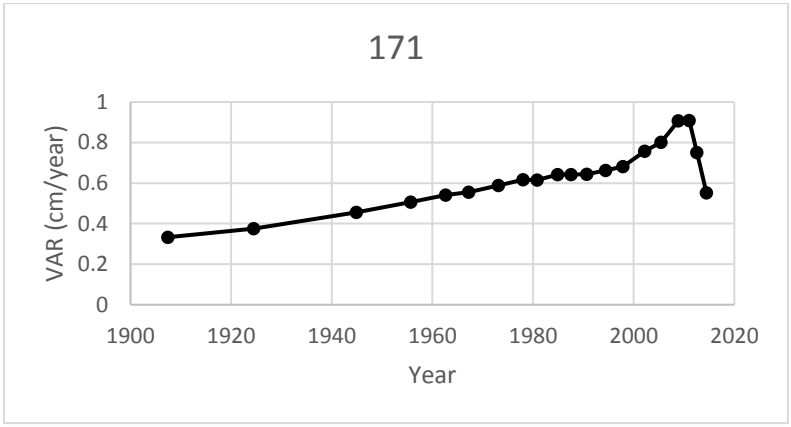

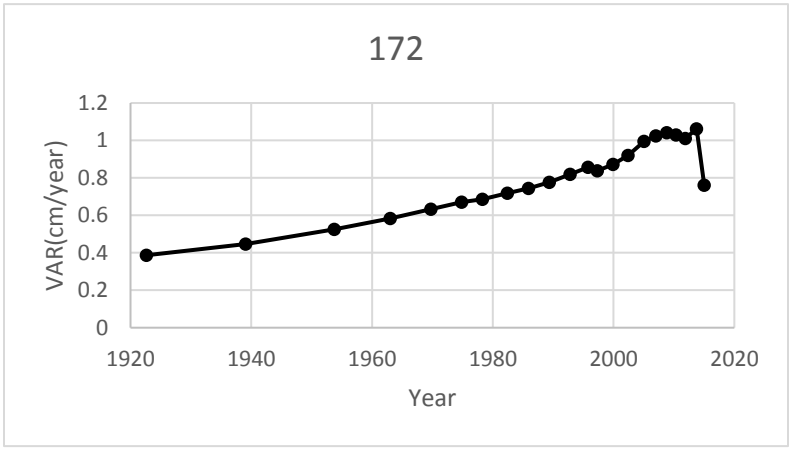

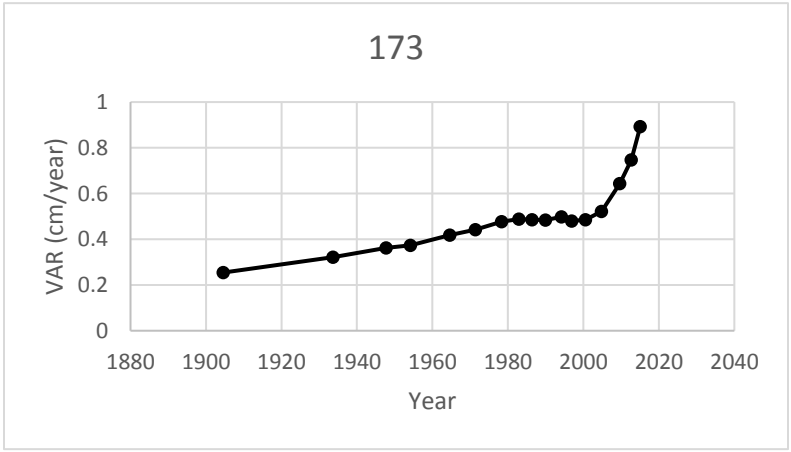

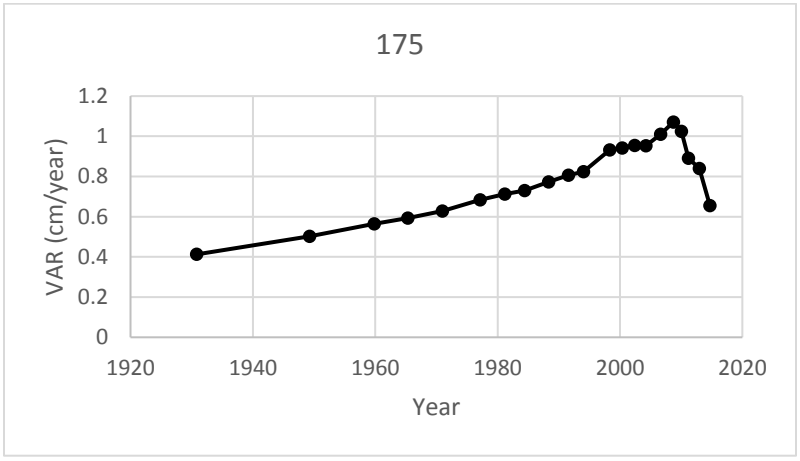
175
VAR (cm/year)
1.2
1
0.8
0.6
0.4
0.2
0
1920
1940
1960
1980
2000
2020
Year

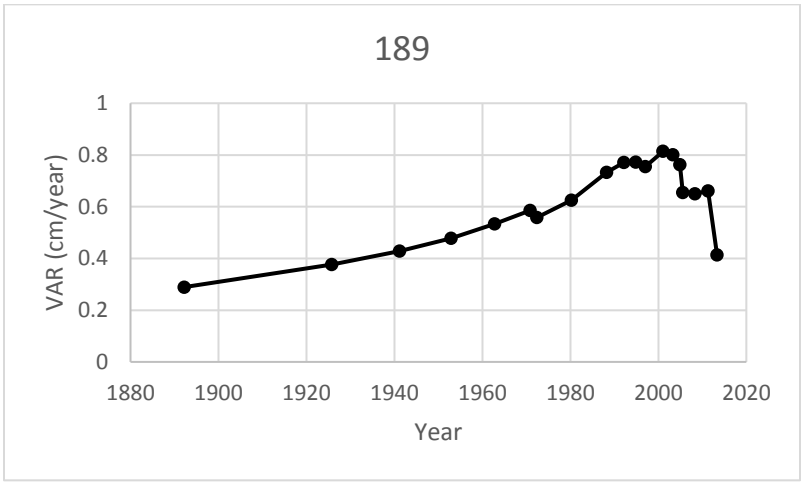
189
VAR (cm/year)
1
0.8
0.6
0.4
0.2
0
1880
1900
1920
1940
1960
1980
2000
2020
Year

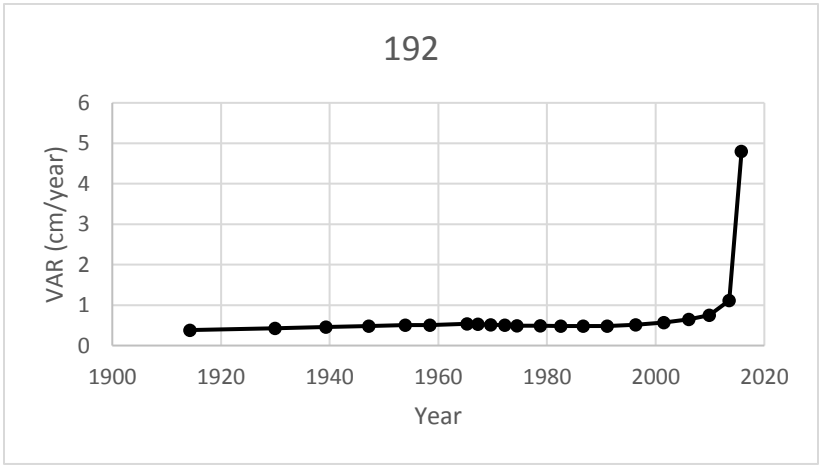
192
VAR (cm/year)
6
5
4
3
2
1
0
1900
1920
1940
1960
1980
2000
2020
Year

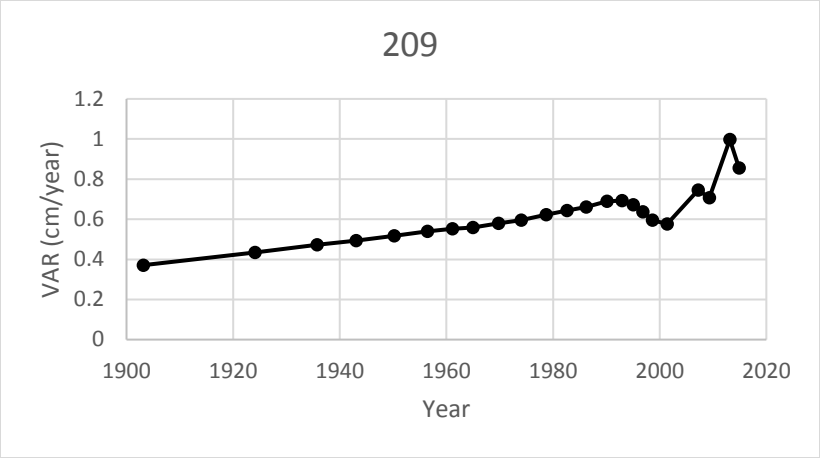
209
1.2
1
0.8
0.6
0.4
0.2
0
VAR (cm/year)
1900
1920
1940
1960
1980
2000
2020
Year

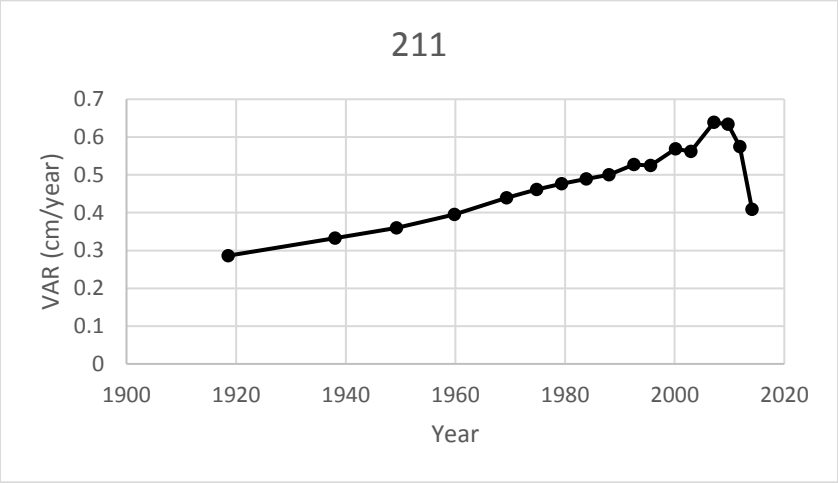
211
0.7
0.6
0.5
0.4
0.3
0.2
0.1
0
VAR (cm/year)
1900
1920
1940
1960
1980
2000
2020
Year

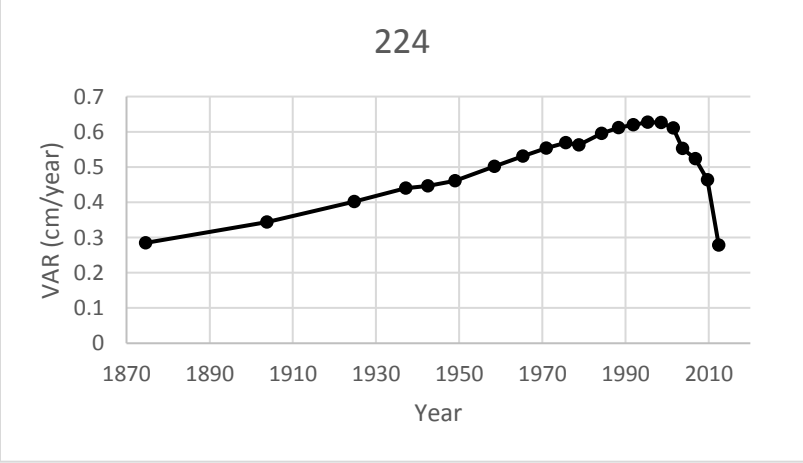
224
0.7
0.6
0.5
0.4
0.3
0.2
0.1
0
VAR (cm/year)
1870
1890
1910
1930
1950
1970
1990
2010
Year

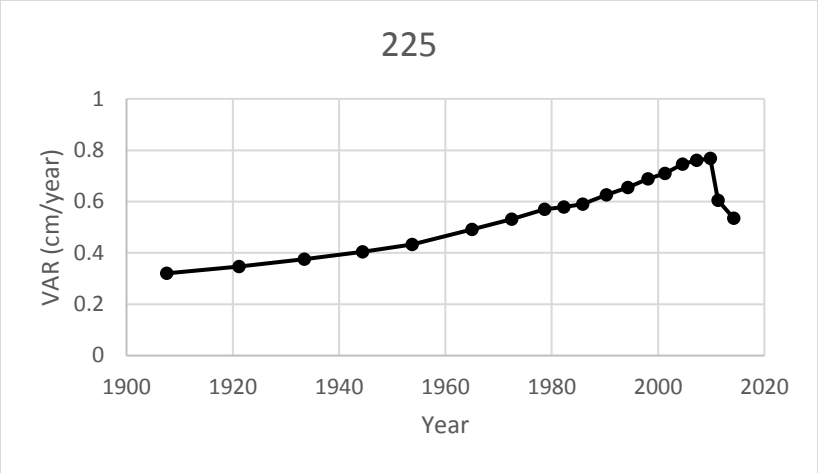
225
VAR (cm/year)
1
0.8
0.6
0.4
0.2
0
1900
1920
1940
1960
1980
2000
2020
Year

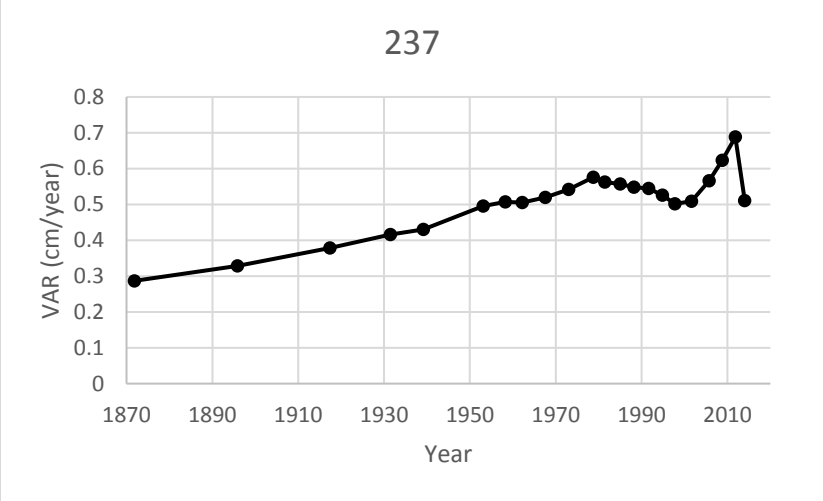
237
VAR (cm/year)
0.8
0.7
0.6
0.5
0.4
0.3
0.2
0.1
0
1870
1890
1910
1930
1950
1970
1990
2010
Year

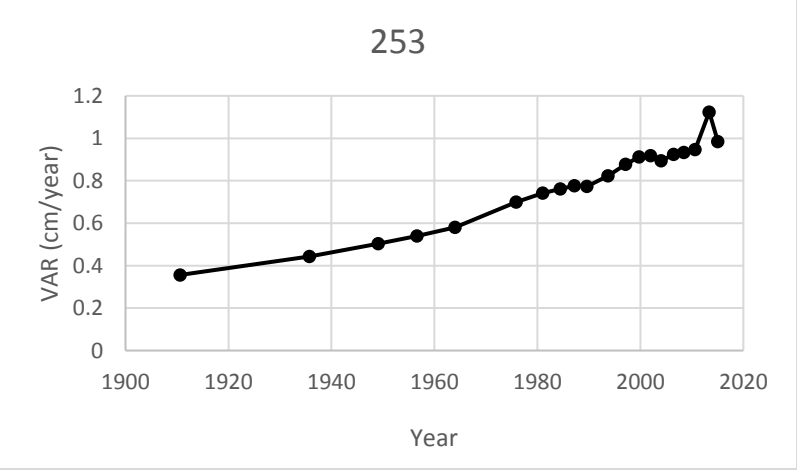
253
VAR (cm/year)
1.2
1
0.8
0.6
0.4
0.2
0
1900
1920
1940
1960
1980
2000
2020
Year

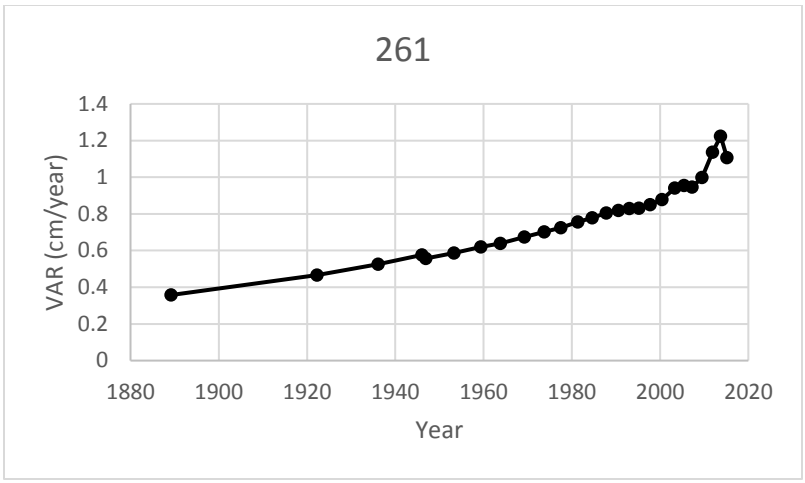
261
VAR (cm/year)
1.4
1.2
1
0.8
0.6
0.4
0.2
0
1880
1900
1920
1940
1960
1980
2000
2020
Year

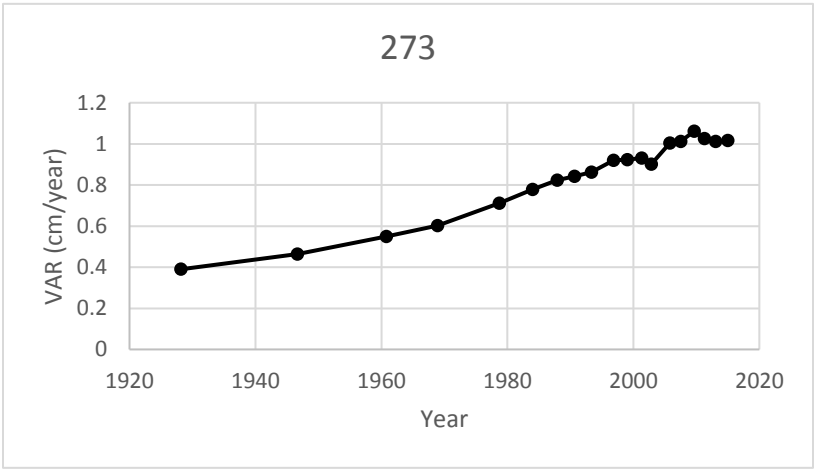
273
VAR (cm/year)
1.2
1
0.8
0.6
0.4
0.2
0
1920
1940
1960
1980
2000
2020
Year

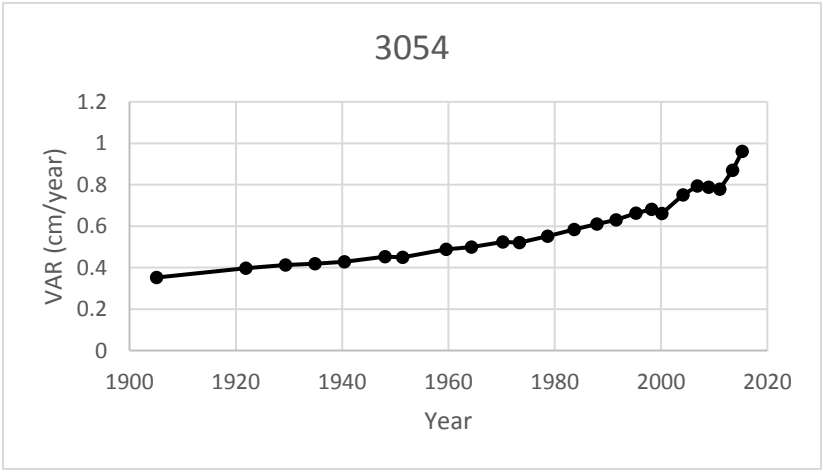
3054
VAR (cm/year)
1.2
1
0.8
0.6
0.4
0.2
0
1900
1920
1940
1960
1980
2000
2020
Year

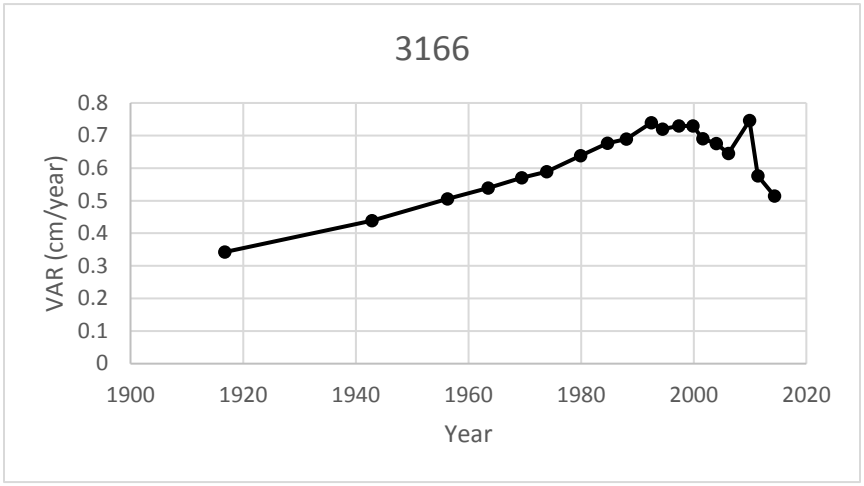
3166
VAR (cm/year)
0.8
0.7
0.6
0.5
0.4
0.3
0.2
0.1
0
1900
1920
1940
1960
1980
2000
2020
Year

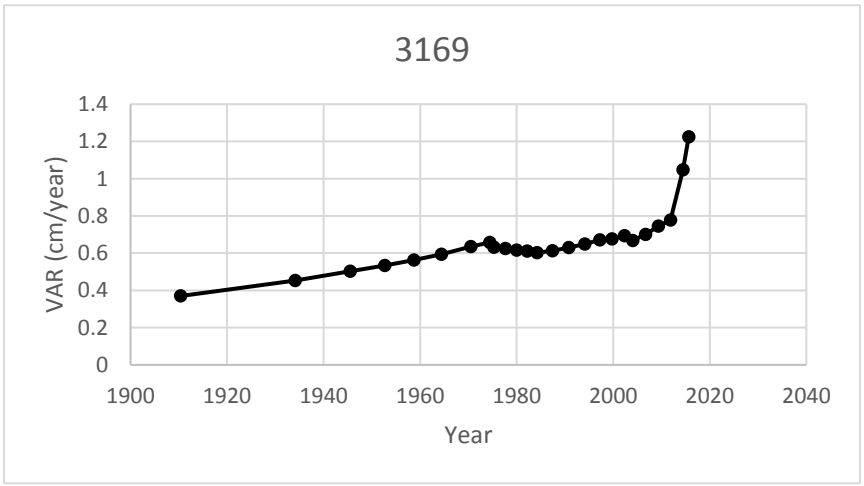
3169
VAR (cm/year)
1.4
1.2
1
0.8
0.6
0.4
0.2
0
1900
1920
1940
1960
1980
2000
2020
2040
Year

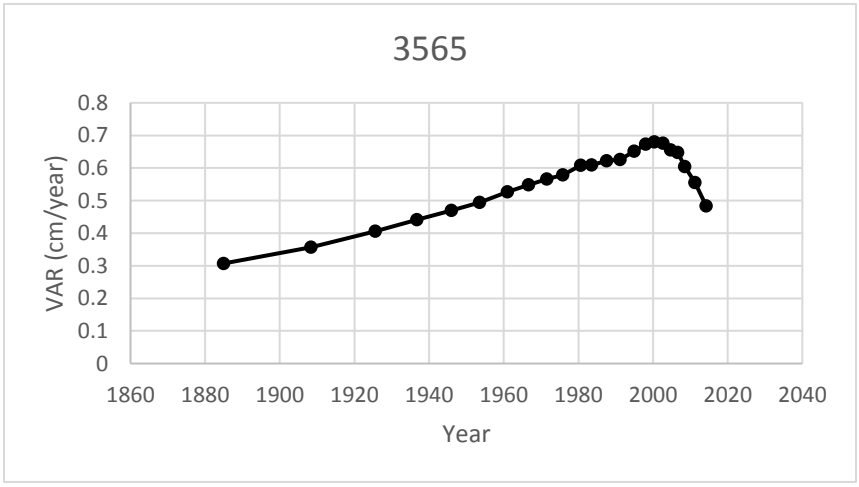
3565
VAR (cm/year)
0.8
0.7
0.6
0.5
0.4
0.3
0.2
0.1
0
1860
1880
1900
1920
1940
1960
1980
2000
2020
2040
Year

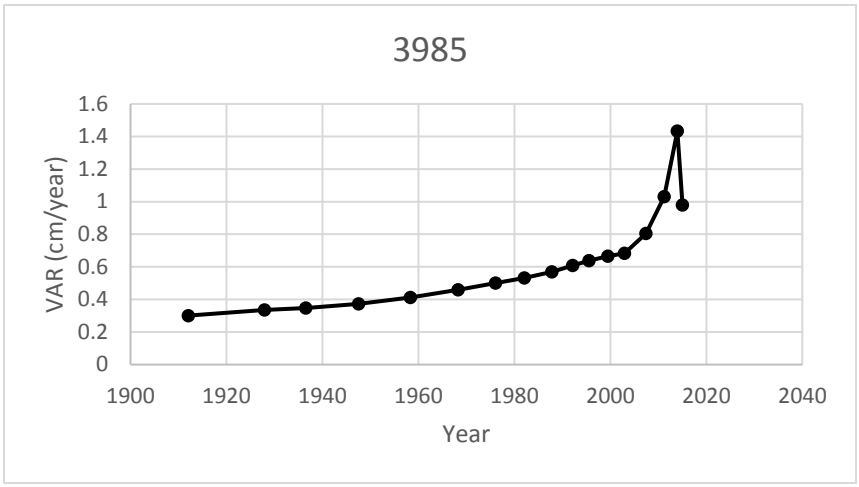
3985
VAR (cm/year)
1.6
1.4
1.2
1
0.8
0.6
0.4
0.2
0
1900
1920
1940
1960
1980
2000
2020
2040
Year

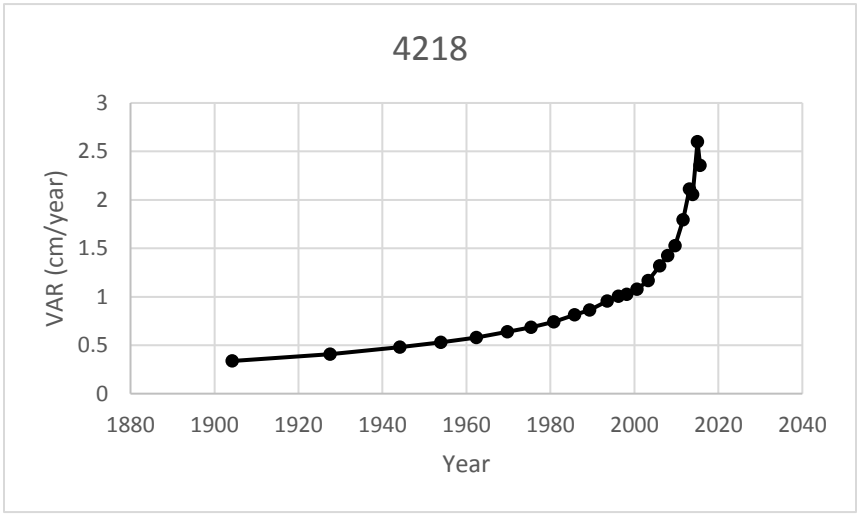
4218
VAR (cm/year)
3
2.5
2
1.5
1
0.5
0
1880
1900
1920
1940
1960
1980
2000
2020
2040
Year

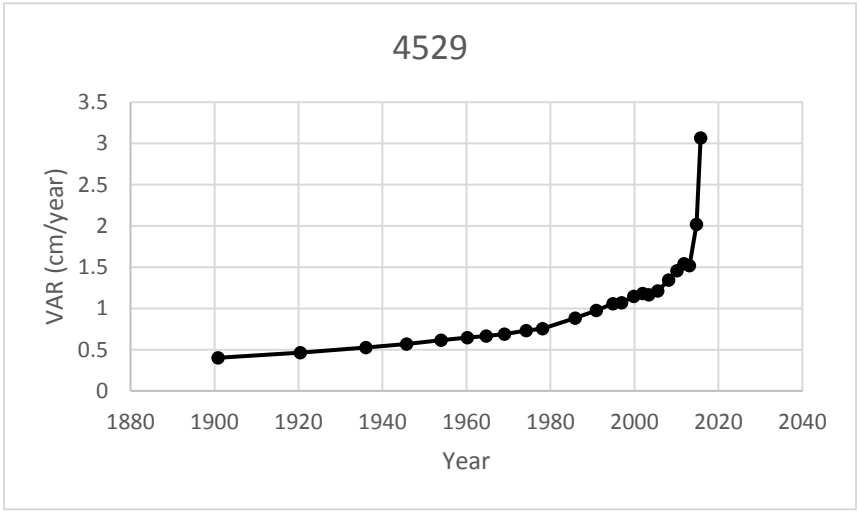
4529
VAR (cm/year)
3.5
3
2.5
2
1.5
1
0.5
0
1880
1900
1920
1940
1960
1980
2000
2020
2040
Year

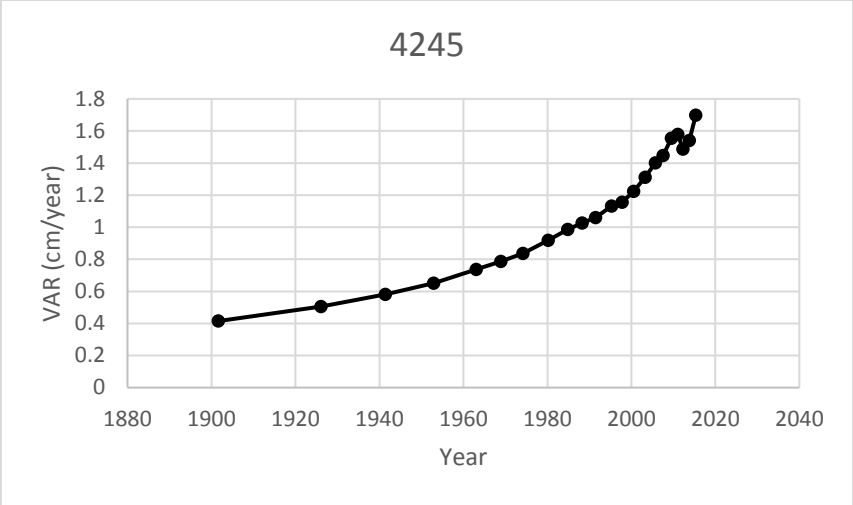
4245
VAR (cm/year)
1.8
1.6
1.4
1.2
1
0.8
0.6
0.4
0.2
0
1880
1900
1920
1940
1960
1980
2000
2020
2040
Year

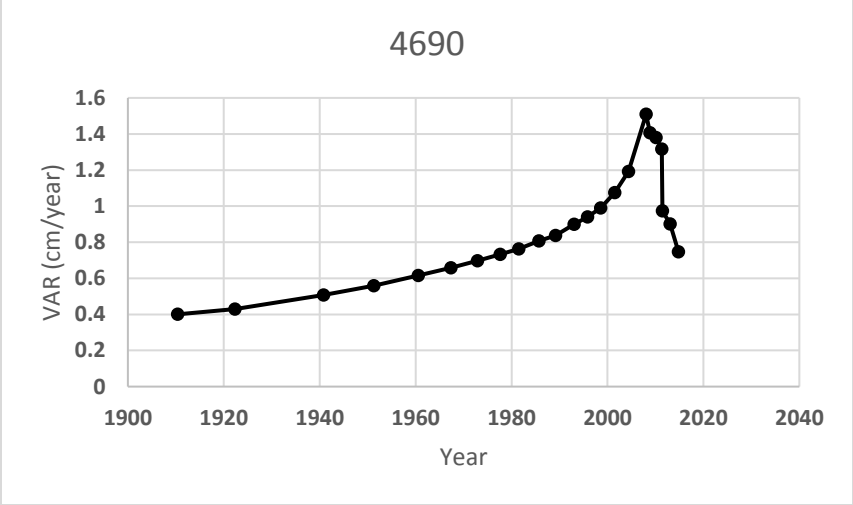
4690
VAR (cm/year)
1.6
1.4
1.2
1
0.8
0.6
0.4
0.2
0
1900
1920
1940
1960
1980
2000
2020
2040
Year

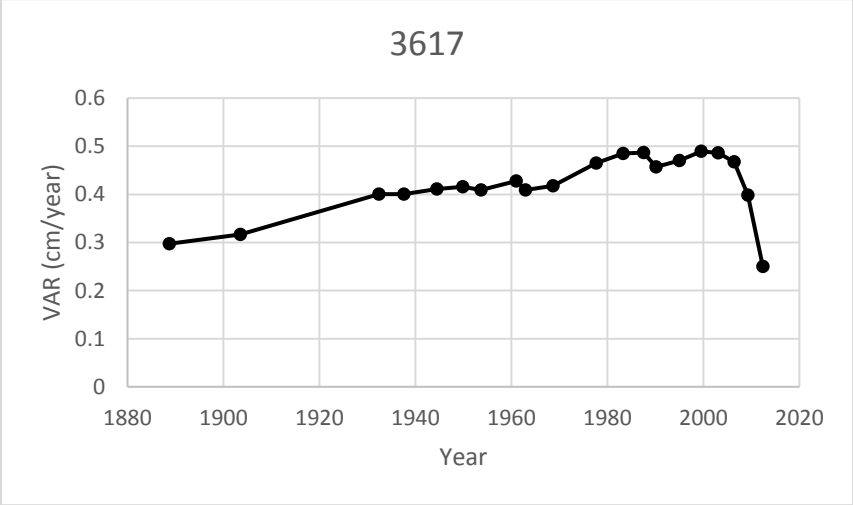
3617
VAR (cm/year)
0.6
0.5
0.4
0.3
0.2
0.1
0
1880
1900
1920
1940
1960
1980
2000
2020
Year

Appendix H: Mineral Mass Accumulation Data

CRMS 171

Mid Point Depth (cm)	Avg VAR t (years)	Dry Mineral Mass (g)	MPA (kg/m2)	Cumulative MPA	MMA (kg/m2year)
0.85	1.30	37.53	4.63	4.63	3.57
2.60	3.97	50.14	6.18	10.82	2.72
4.50	6.88	60.74	7.49	18.31	2.66
6.45	9.86	63.22	7.80	26.11	2.65
8.45	12.91	83.85	10.34	36.45	2.82
10.43	15.93	80.18	9.89	46.34	2.91
12.35	18.87	115.24	14.21	60.55	3.21
14.30	21.85	67.08	8.27	68.83	3.15
16.30	24.91	58.69	7.24	76.07	3.05
18.25	27.88	51.02	6.29	82.36	2.95
19.95	30.48	50.24	6.20	88.56	2.91
21.65	33.08	49.57	6.11	94.67	2.86
23.40	35.75	44.85	5.53	100.20	2.80
25.20	38.50	44.18	5.45	105.65	2.74
27.10	41.41	46.75	5.77	111.42	2.69
28.85	44.08	44.26	5.46	116.88	2.65
30.55	46.68	42.38	5.23	122.11	2.62
32.45	49.58	55.36	6.83	128.93	2.60
34.40	52.56	62.95	7.76	136.70	2.60
36.15	55.23	38.08	4.70	141.40	2.56
37.85	57.83	33.69	4.16	145.55	2.52

CRMS 172

Mid Point Depth (cm)	Avg VAR t (years)	Dry Mineral Mass (g)	MPA (kg/m2)	Cumulative MPA	MMA (kg/m2year)
0.75	1.02	14.61	1.80	1.80	1.77
2.40	3.25	24.74	3.05	4.85	1.49
4.13	5.59	30.38	3.75	8.60	1.54
5.78	7.82	25.30	3.12	11.72	1.50
7.45	10.09	32.88	4.06	15.78	1.56
9.18	12.43	37.68	4.65	20.42	1.64
10.88	14.73	45.15	5.57	25.99	1.76
12.48	16.90	70.87	8.74	34.73	2.06
14.03	19.00	46.41	5.72	40.46	2.13
15.65	21.20	43.48	5.36	45.82	2.16

17.33	23.47	30.69	3.79	49.61	2.11
19.00	25.74	37.39	4.61	54.22	2.11
20.68	28.01	37.93	4.68	58.90	2.10
22.38	30.31	36.86	4.55	63.44	2.09
24.13	32.68	33.45	4.13	67.57	2.07
25.85	35.02	37.10	4.58	72.15	2.06
27.58	37.36	38.58	4.76	76.90	2.06
29.30	39.69	35.56	4.39	81.29	2.05
30.95	41.93	42.10	5.19	86.48	2.06
32.65	44.23	40.92	5.05	91.53	2.07
34.43	46.64	49.63	6.12	97.65	2.09
36.13	48.94	49.16	6.06	103.72	2.12
38.20	51.75	79.84	9.85	113.56	2.19

CRMS 173

Mid Point Depth (cm)	Avg VAR t (years)	Dry Mineral Mass (g)	MPA (kg/m2)	Cumulative MPA	MMA (kg/m2year)
0.83	1.66	4.66	0.57	0.57	0.35
2.45	4.94	13.67	1.69	2.26	0.46
4.10	8.26	17.18	2.12	4.38	0.53
5.83	11.73	24.42	3.01	7.39	0.63
7.50	15.11	22.74	2.80	10.20	0.67
9.15	18.43	22.62	2.79	12.99	0.70
10.85	21.86	21.98	2.71	15.70	0.72
12.58	25.33	27.92	3.44	19.14	0.76
14.38	28.96	23.62	2.91	22.05	0.76
16.15	32.54	12.65	1.56	23.61	0.73
17.93	36.11	12.50	1.54	25.16	0.70
19.75	39.79	18.92	2.33	27.49	0.69
21.45	43.21	14.15	1.75	29.23	0.68
23.08	46.49	14.91	1.84	31.07	0.67
24.75	49.86	14.75	1.82	32.89	0.66
26.50	53.39	17.24	2.13	35.02	0.66
28.35	57.11	12.22	1.51	36.53	0.64
30.18	60.79	10.93	1.35	37.88	0.62

CRMS 175

Mid Point Depth (cm)	Avg VAR t (years)	Dry Mineral Mass (g)	MPA (kg/m2)	Cumulative MPA	MMA (kg/m2year)
0.85	1.17	28.41	3.50	3.50	2.99

2.53	3.48	37.84	4.67	8.17	2.35
4.28	5.90	38.00	4.69	12.86	2.18
6.10	8.42	40.45	4.99	17.85	2.12
7.80	10.76	38.93	4.80	22.65	2.10
9.48	13.07	46.29	5.71	28.36	2.17
11.23	15.49	89.09	10.99	39.35	2.54
12.95	17.87	58.25	7.18	46.53	2.60
14.70	20.29	58.71	7.24	53.78	2.65
16.48	22.73	47.59	5.87	59.64	2.62
18.13	25.01	67.72	8.35	68.00	2.72
19.70	27.18	48.13	5.94	73.93	2.72
21.38	29.50	42.71	5.27	79.20	2.69
23.08	31.84	46.03	5.68	84.88	2.67
24.83	34.26	43.19	5.33	90.21	2.63
26.60	36.71	37.53	4.63	94.84	2.58
28.30	39.05	47.85	5.90	100.74	2.58
30.03	41.43	48.37	5.97	106.70	2.58
31.75	43.81	42.54	5.25	111.95	2.56
33.48	46.19	50.22	6.19	118.15	2.56
35.15	48.50	47.29	5.83	123.98	2.56
37.00	51.06	72.30	8.92	132.90	2.60

CRMS 189

Mid Point Depth (cm)	Avg VAR t (years)	Dry Mineral Mass (g)	MPA (kg/m2)	Cumulative MPA	MMA (kg/m2year)
1.10	1.86	7.20	0.89	0.89	0.48
3.10	5.24	0.86	0.11	0.99	0.19
5.00	8.45	0.62	0.08	1.07	0.13
6.85	11.57	0.45	0.06	1.13	0.10
8.45	14.28	0.45	0.06	1.18	0.08
10.15	17.15	0.45	0.06	1.24	0.07
12.20	20.61	0.82	0.10	1.34	0.06
14.30	24.16	0.56	0.07	1.41	0.06
16.35	27.63	0.68	0.08	1.49	0.05
18.35	31.01	0.46	0.06	1.55	0.05
20.35	34.39	0.31	0.04	1.59	0.05
22.35	37.76	0.67	0.08	1.67	0.04
24.35	41.14	0.72	0.09	1.76	0.04
26.45	44.69	0.84	0.10	1.86	0.04
28.40	47.99	1.04	0.13	1.99	0.04
30.20	51.03	1.30	0.16	2.15	0.04
32.05	54.15	1.59	0.20	2.35	0.04
34.00	57.45	1.34	0.17	2.51	0.04

35.80	60.49	4.75	0.59	3.10	0.05
37.45	63.28	6.35	0.78	3.88	0.06

CRMS 192

Mid Point Depth (cm)	Avg VAR t (years)	Dry Mineral Mass (g)	MPA (kg/m2)	Cumulative MPA	MMA (kg/m2year)
0.90	1.78	0.92	0.11	0.11	0.06
2.73	5.38	16.11	1.99	2.10	0.39
4.55	8.99	27.34	3.37	5.47	0.61
6.40	12.64	25.06	3.09	8.56	0.68
8.20	16.20	28.90	3.56	12.13	0.75
10.05	19.85	25.74	3.18	15.30	0.77
12.05	23.80	28.81	3.55	18.86	0.79
14.10	27.85	34.31	4.23	23.09	0.83
16.20	32.00	33.78	4.17	27.25	0.85
18.25	36.05	31.11	3.84	31.09	0.86
20.30	40.10	29.67	3.66	34.75	0.87
22.15	43.76	24.50	3.02	37.77	0.86
23.85	47.11	28.93	3.57	41.34	0.88
25.65	50.67	55.32	6.82	48.17	0.95
27.43	54.18	53.36	6.58	54.75	1.01
29.18	57.63	61.93	7.64	62.39	1.08
31.15	61.53	47.18	5.82	68.21	1.11
33.15	65.49	54.26	6.69	74.90	1.14
35.00	69.14	55.23	6.81	81.71	1.18
36.95	72.99	56.83	7.01	88.72	1.22
38.95	76.94	65.16	8.04	96.76	1.26
41.35	81.68	83.31	10.28	107.03	1.31

CRMS 209

Mid Point Depth (cm)	Avg VAR t (years)	Dry Mineral Mass (g)	MPA (kg/m2)	Cumulative MPA	MMA (kg/m2year)
0.95	1.31	12.36	1.52	1.52	1.17
2.83	3.89	26.90	3.32	4.84	1.24
4.73	6.51	54.02	6.66	11.51	1.77
6.58	9.05	25.13	3.10	14.61	1.61
8.40	11.57	44.88	5.54	20.14	1.74

10.33	14.22	36.90	4.55	24.69	1.74
12.23	16.84	28.55	3.52	28.21	1.68
14.10	19.42	20.66	2.55	30.76	1.58
15.98	22.00	26.30	3.24	34.01	1.55
17.85	24.58	22.89	2.82	36.83	1.50
19.73	27.16	22.31	2.75	39.58	1.46
21.50	29.61	17.43	2.15	41.73	1.41
23.23	31.98	16.56	2.04	43.78	1.37
25.03	34.46	15.00	1.85	45.63	1.32
26.80	36.91	12.84	1.58	47.21	1.28
28.55	39.32	14.27	1.76	48.97	1.25
30.35	41.80	12.59	1.55	50.52	1.21
32.15	44.27	18.97	2.34	52.86	1.19
34.05	46.89	18.58	2.29	55.15	1.18
35.98	49.54	12.97	1.60	56.75	1.15
37.90	52.19	10.77	1.33	58.08	1.11
39.88	54.91	12.93	1.60	59.68	1.09
41.88	57.67	37.57	4.63	64.31	1.12
44.23	60.90	30.36	3.74	68.06	1.12

CRMS 211

Mid Point Depth (cm)	Avg VAR t (years)	Dry Mineral Mass (g)	MPA (kg/m2)	Cumulative MPA	MMA (kg/m2year)
0.78	1.48	9.34	1.15	1.15	0.78
2.35	4.50	8.00	0.99	0.99	0.22
3.98	7.61	8.28	1.02	1.02	0.13
5.65	10.82	9.56	1.18	1.18	0.11
7.33	14.03	11.84	1.46	1.46	0.10
9.03	17.28	6.70	0.83	0.83	0.05
10.73	20.54	10.16	1.25	1.25	0.06
12.35	23.65	4.71	0.58	0.58	0.02
14.00	26.81	8.43	1.04	1.04	0.04
15.73	30.12	7.63	0.94	0.94	0.03
17.45	33.42	6.77	0.83	0.83	0.02
19.00	36.39	7.80	0.96	0.96	0.03
20.50	39.26	9.32	1.15	1.15	0.03
22.18	42.47	13.76	1.70	1.70	0.04
24.00	45.96	9.46	1.17	1.17	0.03
25.93	49.65	10.60	1.31	1.31	0.03
27.90	53.43	6.90	0.85	0.85	0.02
29.85	57.17	9.18	1.13	1.13	0.02

CRMS 224

Mid Point Depth (cm)	Avg VAR t (years)	Dry Mineral Mass (g)	MPA (kg/m2)	Cumulative MPA	MMA (kg/m2year)
1.00	1.62	22.86	2.82	2.82	1.74
2.93	4.75	42.77	5.28	8.10	1.71
4.83	7.83	69.92	8.62	16.72	2.14
6.83	11.07	87.41	10.78	27.50	2.48
8.88	14.40	35.38	4.36	31.86	2.21
10.95	17.76	42.16	5.20	37.06	2.09
12.98	21.05	29.19	3.60	40.67	1.93
14.95	24.25	27.41	3.38	44.05	1.82
16.95	27.50	23.02	2.84	46.89	1.71
18.93	30.70	19.43	2.40	49.28	1.61
20.98	34.03	24.54	3.03	52.31	1.54
23.03	37.35	19.39	2.39	54.70	1.46
24.95	40.48	24.59	3.03	57.73	1.43
26.90	43.64	28.22	3.48	61.21	1.40
28.88	46.85	92.70	11.43	72.65	1.55
30.90	50.13	123.94	15.29	87.94	1.75
32.83	53.25	20.81	2.57	90.50	1.70
34.70	56.30	13.74	1.69	92.20	1.64
36.70	59.54	27.38	3.38	95.57	1.61
38.58	62.58	35.30	4.35	99.93	1.60
40.33	65.42	15.33	1.89	101.82	1.56
42.45	68.87	13.80	1.70	103.52	1.50

CRMS 225

Mid Point Depth (cm)	Avg VAR t (years)	Dry Mineral Mass (g)	MPA (kg/m2)	Cumulative MPA	MMA (kg/m2year)
0.95	1.60	28.65	2.19	2.19	1.37
2.85	4.81	41.68	3.91	6.10	1.27
4.75	8.01	43.71	3.99	10.09	1.26
6.65	11.21	42.09	3.63	13.72	1.22
8.53	14.37	35.35	2.97	16.69	1.16
10.45	17.62	33.28	2.67	19.36	1.10
12.33	20.78	26.80	2.08	21.44	1.03
14.20	23.94	30.48	2.37	23.81	0.99
16.10	27.15	23.22	1.83	25.64	0.94
17.80	30.01	22.27	1.76	27.40	0.91

19.53	32.92	18.18	1.19	28.59	0.87
21.28	35.87	18.18	1.41	30.00	0.84
23.15	39.03	29.75	2.31	32.31	0.83
25.08	42.28	26.40	1.99	34.30	0.81
26.95	45.44	26.39	2.05	36.35	0.80
28.95	48.81	20.96	1.34	37.69	0.77
31.00	52.27	19.20	0.92	38.62	0.74
32.93	55.51	15.10	0.80	39.42	0.71
34.75	58.59	20.05	1.29	40.70	0.69
37.08	62.51	23.80	1.17	41.88	0.67

CRMS 237

Mid Point Depth (cm)	Avg VAR t (years)	Dry Mineral Mass (g)	MPA (kg/m2)	Cumulative MPA	MMA (kg/m2year)
1.00	1.96	24.60	3.03	3.03	1.55
2.85	5.60	43.85	5.41	8.44	1.51
4.50	8.84	43.57	5.37	13.82	1.56
5.80	11.39	42.59	5.25	19.07	1.67
7.30	14.33	42.69	5.27	24.34	1.70
9.15	17.97	27.69	3.42	27.75	1.54
11.10	21.79	20.39	2.52	30.27	1.39
13.25	26.02	19.26	2.38	32.64	1.25
15.25	29.94	16.31	2.01	34.65	1.16
17.25	33.87	20.82	2.57	37.22	1.10
19.45	38.19	20.36	2.51	39.73	1.04
21.48	42.16	15.12	1.86	41.60	0.99
23.30	45.75	47.82	5.90	47.50	1.04
25.15	49.38	67.60	8.34	55.83	1.13
27.20	53.40	21.54	2.66	58.49	1.10
29.25	57.43	15.09	1.86	60.35	1.05
31.15	61.16	11.93	1.47	61.82	1.01
33.10	64.99	13.96	1.72	63.54	0.98
35.15	69.01	15.22	1.88	65.42	0.95
37.33	73.28	27.47	3.39	68.81	0.94
39.45	77.46	48.06	5.93	74.74	0.96
41.35	81.19	17.65	2.18	76.91	0.95
43.00	84.43	11.30	1.39	78.31	0.93

CRMS 253

Mid Point Depth (cm)	Avg VAR t (years)	Dry Mineral Mass (g)	MPA (kg/m2)	Cumulative MPA	MMA (kg/m2year)
0.93	1.21	19.37	1.65	1.65	1.36
2.95	3.87	50.64	5.12	6.77	1.75
5.05	6.62	49.13	4.79	11.56	1.75
7.00	9.18	40.43	3.74	15.30	1.67
8.80	11.54	36.82	3.45	18.75	1.63
10.70	14.03	51.02	4.85	23.59	1.68
12.85	16.85	41.44	4.04	27.63	1.64
14.80	19.40	31.85	2.87	30.50	1.57
16.53	21.66	25.44	2.10	32.60	1.51
18.33	24.02	32.33	2.83	35.43	1.48
20.40	26.74	45.66	4.22	39.66	1.48
22.35	29.30	26.57	2.26	41.92	1.43
24.00	31.46	26.18	2.20	44.12	1.40
25.90	33.95	34.06	3.11	47.22	1.39
28.05	36.77	31.58	2.88	50.11	1.36
30.15	39.52	30.89	2.82	52.93	1.34
32.00	41.95	25.70	2.38	55.30	1.32
33.70	44.18	25.03	2.35	57.65	1.30
35.55	46.60	30.21	2.68	60.33	1.29
37.55	49.22	32.94	3.01	63.34	1.29
39.75	52.11	31.76	2.94	66.28	1.27

CRMS 261

Mid Point Depth (cm)	Avg VAR t (years)	Dry Mineral Mass (g)	MPA (kg/m2)	Cumulative MPA	MMA (kg/m2year)
0.93	1.13	8.88	1.10	1.10	0.97
2.80	3.42	16.08	1.98	3.08	0.90
4.68	5.72	20.06	2.47	5.55	0.97
6.50	7.95	22.31	2.75	8.30	1.05
8.28	10.12	27.77	3.43	11.73	1.16
10.08	12.32	20.33	2.51	14.24	1.16
11.90	14.55	25.49	3.14	17.38	1.19
13.68	16.72	29.08	3.59	20.97	1.25
15.50	18.95	16.04	1.98	22.95	1.21
17.28	21.12	13.49	1.66	24.61	1.17
19.03	23.26	12.97	1.60	26.21	1.13
20.85	25.49	11.80	1.46	27.67	1.09
22.68	27.72	18.38	2.27	29.93	1.08

24.43	29.86	21.28	2.63	32.56	1.09
26.18	32.00	20.92	2.58	35.14	1.10
27.93	34.14	23.81	2.94	38.08	1.12
29.68	36.28	25.27	3.12	41.19	1.14
31.50	38.51	26.06	3.21	44.41	1.15
33.30	40.71	34.90	4.30	48.71	1.20
35.05	42.85	30.58	3.77	52.48	1.22
36.78	44.96	31.89	3.93	56.42	1.25
38.53	47.10	29.11	3.59	60.01	1.27
40.25	49.20	25.97	3.20	63.21	1.28
41.98	51.31	26.31	3.25	66.46	1.30
43.68	53.39	24.38	3.01	69.46	1.30
45.35	55.44	30.81	3.80	73.26	1.32
46.85	57.27	24.70	3.05	76.31	1.33

CRMS 273

Mid Point Depth (cm)	Avg VAR t (years)	Dry Mineral Mass (g)	MPA (kg/m2)	Cumulative MPA	MMA (kg/m2year)
1.00	1.32	1.85	0.23	0.23	0.17
2.95	3.88	2.72	0.34	0.56	0.15
4.85	6.38	3.60	0.44	1.01	0.16
6.75	8.88	4.88	0.60	1.61	0.18
8.60	11.31	4.56	0.56	2.17	0.19
10.25	13.48	1.73	0.21	2.38	0.18
11.85	15.58	2.62	0.32	2.71	0.17
13.65	17.95	1.36	0.17	2.88	0.16
15.65	20.58	1.71	0.21	3.09	0.15
17.60	23.14	1.86	0.23	3.32	0.14
19.50	25.64	1.17	0.14	3.46	0.13
21.35	28.08	1.58	0.20	3.66	0.13
23.10	30.38	1.05	0.13	3.79	0.12
24.90	32.74	2.19	0.27	4.06	0.12
26.55	34.91	1.90	0.23	4.29	0.12
28.40	37.35	2.78	0.34	4.63	0.12
30.35	39.91	1.80	0.22	4.86	0.12
32.20	42.34	2.82	0.35	5.20	0.12
34.25	45.04	2.43	0.30	5.50	0.12
36.45	47.93	2.06	0.25	5.76	0.12

CRMS 3054

Mid Point Depth (cm)	Avg VAR t (years)	Dry Mineral Mass (g)	MPA (kg/m2)	Cumulative MPA	MMA (kg/m2year)
0.70	1.29	5.33	0.66	0.66	0.51
2.20	4.07	10.72	1.32	1.98	0.49
3.85	7.12	11.74	1.45	3.43	0.48
5.58	10.31	11.08	1.37	4.80	0.47
7.28	13.46	9.47	1.17	5.96	0.44
8.90	16.46	13.65	1.68	7.65	0.46
10.50	19.42	22.38	2.76	10.41	0.54
12.10	22.38	7.76	0.96	11.36	0.51
13.75	25.43	8.29	1.02	12.39	0.49
15.43	28.53	6.58	0.81	13.20	0.46
17.15	31.72	5.53	0.68	13.88	0.44
18.90	34.96	6.84	0.84	14.72	0.42
20.58	38.05	14.34	1.77	16.49	0.43
22.23	41.10	13.32	1.64	18.14	0.44
23.98	44.34	15.50	1.91	20.05	0.45
25.80	47.72	36.50	4.50	24.55	0.51
27.53	50.91	37.03	4.57	29.12	0.57
29.10	53.82	21.86	2.70	31.81	0.59
30.73	56.83	50.46	6.22	38.04	0.67
32.38	59.88	42.81	5.28	43.32	0.72
34.00	62.88	60.51	7.46	50.78	0.81
35.73	66.07	67.97	8.38	59.17	0.90
37.45	69.26	63.17	7.79	66.96	0.97
39.08	72.27	59.07	7.29	74.24	1.03
40.68	75.23	47.20	5.82	80.07	1.06

CRMS 3166

Mid Point Depth (cm)	Avg VAR t (years)	Dry Mineral Mass (g)	MPA (kg/m2)	Cumulative MPA	MMA (kg/m2year)
0.85	1.35	7.76	0.96	0.96	0.71
2.65	4.21	12.51	1.54	2.50	0.59
4.55	7.22	10.50	1.29	3.79	0.53
6.35	10.08	13.86	1.71	5.50	0.55
8.10	12.85	9.51	1.17	6.68	0.52
9.95	15.79	9.33	1.15	7.83	0.50
11.78	18.69	4.81	0.59	8.42	0.45
13.60	21.58	6.46	0.80	9.22	0.43
15.50	24.60	2.01	0.25	9.47	0.38

17.40	27.61	1.40	0.17	9.64	0.35
19.30	30.63	2.11	0.26	9.90	0.32
21.20	33.64	1.73	0.21	10.11	0.30
23.05	36.58	2.24	0.28	10.39	0.28
24.83	39.40	2.87	0.35	10.74	0.27
26.55	42.13	1.68	0.21	10.95	0.26
28.33	44.95	1.82	0.22	11.17	0.25
30.20	47.93	1.83	0.23	11.40	0.24
32.10	50.94	1.90	0.23	11.63	0.23
34.00	53.96	1.99	0.25	11.88	0.22
35.75	56.73	1.65	0.20	12.08	0.21

CRMS 3169

Mid Point Depth (cm)	Avg VAR t (years)	Dry Mineral Mass (g)	MPA (kg/m2)	Cumulative MPA	MMA (kg/m2year)
0.45	0.64	4.11	0.51	0.51	0.79
1.65	2.36	18.62	2.30	2.80	1.19
3.23	4.62	44.85	5.53	8.34	1.81
4.98	7.12	46.32	5.71	14.05	1.97
6.53	9.34	42.40	5.23	19.28	2.06
8.00	11.45	63.41	7.82	27.10	2.37
9.53	13.64	51.32	6.33	33.43	2.45
11.00	15.75	58.03	7.16	40.59	2.58
12.60	18.04	69.38	8.56	49.15	2.72
14.23	20.37	59.58	7.35	56.50	2.77
15.88	22.73	55.85	6.89	63.39	2.79
17.53	25.09	52.36	6.46	69.84	2.78
19.13	27.38	39.29	4.85	74.69	2.73
20.70	29.64	16.23	2.00	76.69	2.59
22.25	31.86	5.24	0.65	77.34	2.43
23.95	34.29	4.52	0.56	77.90	2.27
25.70	36.80	4.44	0.55	78.44	2.13
27.33	39.12	2.36	0.29	78.74	2.01
28.95	41.45	2.19	0.27	79.01	1.91
30.63	43.85	1.75	0.22	79.22	1.81
32.25	46.17	2.41	0.30	79.52	1.72
33.83	48.43	3.32	0.41	79.93	1.65
35.45	50.75	4.16	0.51	80.44	1.58
37.18	53.22	4.96	0.61	81.05	1.52
39.08	55.94	5.80	0.72	81.77	1.46
41.30	59.13	5.68	0.70	82.47	1.39

CRMS 3565

Mid Point Depth (cm)	Avg VAR t (years)	Dry Mineral Mass (g)	MPA (kg/m2)	Cumulative MPA	MMA (kg/m2year)
0.85	1.54	12.26	1.51	1.51	0.98
2.65	4.81	39.85	4.92	6.43	1.34
4.55	8.25	49.46	6.10	12.53	1.52
6.08	11.02	15.31	1.89	14.42	1.31
7.40	13.42	13.75	1.70	16.11	1.20
9.00	16.33	11.63	1.43	17.55	1.07
10.60	19.23	7.43	0.92	18.46	0.96
12.10	21.95	8.30	1.02	19.49	0.89
13.70	24.85	10.50	1.30	20.78	0.84
15.55	28.21	13.98	1.72	22.51	0.80
17.65	32.02	14.34	1.77	24.28	0.76
19.75	35.82	13.99	1.73	26.00	0.73
21.50	39.00	13.32	1.64	27.64	0.71
23.25	42.17	14.36	1.77	29.42	0.70
25.13	45.57	12.44	1.53	30.95	0.68
27.05	49.07	15.48	1.91	32.86	0.67
28.98	52.56	12.81	1.58	34.44	0.66
30.85	55.96	16.48	2.03	36.47	0.65
32.90	59.68	15.00	1.85	38.32	0.64
34.95	63.40	10.62	1.31	39.63	0.63
36.70	66.57	9.95	1.23	40.86	0.61
38.40	69.65	8.66	1.07	41.93	0.60
40.25	73.01	7.95	0.98	42.91	0.59
42.15	76.46	6.00	0.74	43.65	0.57

CRMS 3985

Mid Point Depth (cm)	Avg VAR t (years)	Dry Mineral Mass (g)	MPA (kg/m2)	Cumulative MPA	MMA (kg/m2year)
0.95	1.16	1.47	0.18	0.18	0.16
2.90	3.55	3.00	0.37	0.55	0.15
4.90	6.00	7.52	0.93	1.48	0.25
6.90	8.45	7.12	0.88	2.36	0.28
8.90	10.90	6.49	0.80	3.16	0.29
11.00	13.47	2.74	0.34	3.50	0.26
13.05	15.98	6.30	0.78	4.27	0.27
14.53	17.79	7.76	0.96	5.23	0.29
16.05	19.66	10.69	1.32	6.55	0.33
18.05	22.11	19.86	2.45	9.00	0.41

20.00	24.50	16.35	2.02	11.01	0.45
21.90	26.82	17.16	2.12	13.13	0.49
23.70	29.03	9.69	1.20	14.33	0.49
25.50	31.23	8.83	1.09	15.42	0.49
27.55	33.75	5.22	0.64	16.06	0.48
29.50	36.13	1.64	0.20	16.26	0.45
31.25	38.28	1.86	0.23	16.49	0.43
33.15	40.60	3.59	0.44	16.93	0.42

CRMS 4218

Mid Point Depth (cm)	Avg VAR t (years)	Dry Mineral Mass (g)	MPA (kg/m2)	Cumulative MPA	MMA (kg/m2year)
0.83	0.91	3.30	0.41	0.41	0.45
2.53	2.80	7.74	0.96	1.36	0.49
4.30	4.77	8.15	1.01	2.37	0.50
6.10	6.77	6.92	0.85	3.22	0.48
7.83	8.68	10.59	1.31	4.53	0.52
9.58	10.62	18.36	2.26	6.79	0.64
11.43	12.67	13.87	1.71	8.50	0.67
13.18	14.61	12.32	1.52	10.02	0.69
14.85	16.47	14.39	1.77	11.80	0.72
16.55	18.35	15.35	1.89	13.69	0.75
18.23	20.21	11.35	1.40	15.09	0.75
19.90	22.07	8.69	1.07	16.16	0.73
21.45	23.79	8.89	1.10	17.26	0.73
22.98	25.48	10.56	1.30	18.56	0.73
24.55	27.23	7.53	0.93	19.49	0.72
26.13	28.97	9.30	1.15	20.64	0.71
27.80	30.83	7.72	0.95	21.59	0.70
29.45	32.66	9.19	1.13	22.72	0.70
31.10	34.49	12.22	1.51	24.23	0.70
32.78	36.35	18.13	2.24	26.47	0.73
34.40	38.15	17.24	2.13	28.59	0.75
36.03	39.95	15.05	1.86	30.45	0.76
37.68	41.78	17.48	2.16	32.60	0.78
39.30	43.59	17.04	2.10	34.71	0.80

CRMS 4529

Mid Point Depth (cm)	Avg VAR t (years)	Dry Mineral Mass (g)	MPA (kg/m2)	Cumulative MPA	MMA (kg/m2year)

0.70	0.96	0.84	0.10	0.10	0.11
2.40	3.29	12.44	1.53	1.64	0.50
4.40	6.03	29.27	3.61	5.25	0.87
6.48	8.87	35.39	4.37	9.61	1.08
8.53	11.68	41.42	5.11	14.72	1.26
10.50	14.38	59.57	7.35	22.07	1.53
12.60	17.26	57.61	7.11	29.18	1.69
14.65	20.07	43.31	5.34	34.52	1.72
16.55	22.67	31.66	3.90	38.42	1.69
18.45	25.27	33.07	4.08	42.50	1.68
20.33	27.84	35.60	4.39	46.89	1.68
22.33	30.58	31.21	3.85	50.74	1.66
24.43	33.46	45.15	5.57	56.31	1.68
26.50	36.30	101.81	12.56	68.87	1.90
28.55	39.11	102.69	12.67	81.53	2.08
30.50	41.78	30.97	3.82	85.35	2.04
32.38	44.35	13.76	1.70	87.05	1.96
34.20	46.85	13.65	1.68	88.74	1.89
36.08	49.42	11.56	1.43	90.16	1.82
38.05	52.12	13.73	1.69	91.85	1.76
40.05	54.86	15.28	1.88	93.74	1.71
42.10	57.67	16.58	2.05	95.79	1.66
44.23	60.58	10.13	1.25	97.03	1.60
46.25	63.36	12.54	1.55	98.58	1.56
48.45	66.37	12.19	1.50	100.08	1.51

CRMS 4690

Mid Point Depth (cm)	Avg VAR t (years)	Dry Mineral Mass (g)	MPA (kg/m2)	Cumulative MPA	MMA (kg/m2year)
0.90	1.43	11.33	1.40	1.40	0.97
2.68	4.26	59.00	7.28	8.67	2.04
4.40	7.01	34.41	4.24	12.92	1.84
6.20	9.87	25.13	3.10	16.02	1.62
8.15	12.98	22.23	2.74	18.76	1.45
10.10	16.09	26.88	3.32	22.08	1.37
12.00	19.11	22.43	2.77	24.84	1.30
13.83	22.02	32.25	3.98	28.82	1.31
15.55	24.77	24.05	2.97	31.79	1.28
17.25	27.47	26.29	3.24	35.03	1.28
18.95	30.18	24.19	2.98	38.01	1.26
20.65	32.89	18.90	2.33	40.35	1.23

22.50	35.84	24.91	3.07	43.42	1.21
24.48	38.98	23.01	2.84	46.26	1.19
26.30	41.89	25.17	3.10	49.36	1.18
28.15	44.84	27.83	3.43	52.79	1.18
30.05	47.86	27.10	3.34	56.14	1.17
32.00	50.97	27.42	3.38	59.52	1.17
34.20	54.47	32.23	3.97	63.49	1.17
36.25	57.74	29.68	3.66	67.15	1.16
38.20	60.84	28.96	3.57	70.73	1.16
40.25	64.11	42.11	5.19	75.92	1.18
42.30	67.37	31.39	3.87	79.79	1.18
44.40	70.72	21.16	2.61	82.40	1.17

CRMS 3617

Mid Point Depth (cm)	Avg VAR t (years)	Dry Mineral Mass (g)	MPA (kg/m2)	Cumulative MPA	MMA (kg/m2year)
0.90	1.94	7.11	0.88	0.88	0.45
2.68	5.77	5.35	0.66	1.54	0.27
4.48	9.66	5.79	0.71	2.25	0.23
6.28	13.54	8.15	1.00	3.26	0.24
8.05	17.38	6.43	0.79	4.05	0.23
9.88	21.31	15.92	1.96	6.01	0.28
11.83	25.52	49.97	6.16	12.18	0.48
13.85	29.89	32.41	4.00	16.17	0.54
15.85	34.21	33.46	4.13	20.30	0.59
17.80	38.42	93.37	11.52	31.82	0.83
19.78	42.68	123.42	15.22	47.04	1.10
21.70	46.84	90.59	11.17	58.21	1.24
23.53	50.78	105.69	13.04	71.25	1.40
25.50	55.04	137.66	16.98	88.23	1.60
27.48	59.30	112.99	13.94	102.17	1.72
29.38	63.40	136.91	16.89	119.05	1.88
31.40	67.78	98.98	12.21	131.26	1.94
33.48	72.25	103.80	12.80	144.07	1.99
35.65	76.95	86.05	10.61	154.68	2.01
37.88	81.75	82.64	10.19	164.87	2.02
40.00	86.34	43.36	5.35	170.22	1.97

Vita

Samuel Shrull is a native of Sugar Land, Texas. He graduated in May 2016 with a Bachelor of Science in Geological Sciences from the University of Texas at Austin. He plans to start a career in the oil industry in Texas after graduation at LSU.